CAPE PENINSULA
UNIVERSITY OF TECHNOLOGY

9000447

CPT ARC 621.3821 WIC

OFDM MODULATION TECHNIQUES FOR DOMESTIC POWER LINE COMMUNICATION

by

Lindsay Paul Wicomb

A dissertation submitted in fulfillment of
the requirements for the degree of

Masters Degree of Technology

(Electrical Engineering)

at the

Cape Peninsula University of Technology

December 2005

DECLARATION

I, the undersigned, hereby declare that the dissertation presented here is my own work and the opinions contained herein are my own and do not necessarily reflect those of the Cape Peninsula University of Technology. All references used have been accurately reported.

Name: Lindsay Paul Wicomb

Signature: LWicomb

Date: 22/02/2006

DECLARATION

I, the undersigned, hereby declare that the dissertation presented here is my own work and the opinions contained herein are my own and do not necessarily reflect those of the Cape Peninsula University of Technology. All references used have been accurately reported.

Name: Lindsay Paul Wiscomb

Signature: LWiscomb

Date: 22/02/2006

© Copyright by Lindsay Paul Wicomb December 2005

All Rights Reserved

ABSTRACT

With the growth of the personal computer industry, a number of households now contain two or more personal computers. The need to share resources such as printers, scanners and other PC peripherals has become evident. Communication between personal computers and other smart devices in the home is also required. This brings the emergence of home networking together with home automation. Home networking is the collection of elements to enable the connection and integration of multiple computing, control and communication devices. There are various options at this stage for home networking. One of the broadband options is indoor power line communication.

The aim of the project was to evaluate a communication system capable of performing efficiently in South African Home Power line environment. In designing a communication system capable of performing in the harsh conditions which are presented in the home environment (noise, attenuation, phase distortion, etc.), a mathematical model that is representative of a typical suburban South African home power line is required. To aid the modeling process, an experimental network was constructed so measurements could be taken in a controlled environment. In conjunction with simulation, the model of the home power line network has aided the design of the data communication system.

The project has involved:

- Determining optimal specifications for the communication system.
- Development of a home power line model representative of a typical South African suburban home environment.

- Construction and measurement of an experimental power grid
- Development of methods, algorithms and programs for the design of an OFDM PLC modem (in software) to optimal specifications.
- Simulation development in MATLAB of the OFDM Modem.
- Comparison of different OFDM sub-modulation schemes for enhancing the communication system performance.

In conclusion, the simulation model of the PLC modem correlates well with typical practical systems. Optimising throughput of the communication system and hardware development of the modem will form the basis for further research.

ACKNOWLEDGMENTS

The author wishes to acknowledge the dedication, patience and understanding of his research promoter, Robert Van Zyl, without who's assistance, this dissertation would not have been possible. Also the author would like to thank Tony Abrahams and Shaheen Behardien for their initial contribution and assistance in this research endeavour.

The author would also like to personally thank the staff at the Department of Electrical Engineering, CPUT, Bellville Campus, for making the environment conducive for the completion of my dissertation. A special word of thanks to Nathan Momsen and the rest of the staff at BDS for their constant support and encouragement.

And finally, but most importantly, I would like to thank my family and friends for their support and encouragement throughout my academic career.

The author wishes to dedicate this dissertation to his Mother and Father, who have instilled the importance of education and perseverance.

TABLE OF CONTENTS

Page

ABSTRACT 1

LIST OF TABLES 8

LIST OF FIGURES 9

NOMENCLATURE 14

1 Introduction 17

1.1 Domestic Power line communication 18
1.1.1 Overview 18
1.1.2 Channel characteristics of Domestic power line 20
1.1.3 Modulation schemes for Domestic Power line communication 21
1.2 Objectives of the Research Project 24
1.2.1 Modeling an experimental domestic power network 24
1.2.2 Development of an OFDM simulation 25
1.2.3 Analysis of various encoding methods for optimal OFDM performance . . 25
1.3 Scope and limitations of the project 25
1.3.1 Modeling an experimental network 26
1.3.2 Limited Noise sources 26
1.3.3 Simulation scope and limitations 27
1.4 Thesis Layout / Chapter Description 27

2 Digital Modulation theory for High Bit rate applications 29

2.1 Chapter Description 29
2.2 Parallel Data Transmission 29
2.2.1 Frequency Division Multiplexing 30
2.2.2 Parallel Data transmission using FDM 31
2.3 Orthogonal Frequency Division Multiplexing 32
2.3.1 Advantages of OFDM 32
2.3.2 Drawbacks of Practical OFDM systems 33

Page

2.4 Theory of Operation . . . 35
2.4.1 *Orthogonality of DFT Sinusoids* . . . 37
2.4.2 Importance of Orthogonality in OFDM . . . 39
2.5 Description of a conventional OFDM Transmitter . . . 39
2.5.1 Description of stages in an OFDM Transmitter . . . 42
2.6 Description of a conventional OFDM Receiver . . . 47
2.6.1 Importance of synchronisation . . . 49
2.6.2 Channel Estimation . . . 51
2.6.3 Description of stages in a typical OFDM Receiver . . . 51
2.7 Conclusion . . . 54

3 Domestic power network modeling . . . 55

3.1 Chapter Description . . . 56
3.2 Literature review on relevant channel models . . . 58
3.3 Proposed Transfer Function approximation Methodology . . . 59
3.3.1 Theory of Scattering matrix parameters . . . 60
3.3.2 Complex transfer function approximation using S-Parameters . . . 62
3.3.3 Compensation for Coupling effects . . . 63
3.4 Practical Setup and implementation . . . 65
3.4.1 Coupling circuit design and construction . . . 65
3.4.2 VNA (Vector Network Analyser) Calibration . . . 66
3.4.3 Construction of an experimental power network . . . 68
3.4.4 Load impedances . . . 70
3.4.5 Measurement procedure for transfer function approximation . . . 71
3.5 Post-processing . . . 72
3.5.1 Post-processing Procedure . . . 72
3.5.2 *MATLAB Script Design* . . . 73
3.6 Analysis of Results . . . 76
3.7 Conclusion . . . 76

4 OFDM Communication System Simulation in MATLAB . . . 80

4.1 Chapter Description . . . 80
4.2 OFDM Simulation Concepts . . . 81
4.2.1 Overall Description . . . 81
4.3 OFDM Transmitter Simulation . . . 83
4.3.1 OFDM Transmitter Algorithm . . . 83
4.3.2 MATLAB OFDM Transmitter Implementation . . . 86
4.4 Domestic Power network simulation . . . 86

Page

4.4.1 Domestic Power network Algorithm and implementation 89
4.5 OFDM Receiver Simulation 92
4.5.1 OFDM Receiver Algorithm 92
4.5.2 MATLAB OFDM Receiver Implementation 97
4.6 Algorithm verification 101
4.6.1 Process of Algorithm verification 101
4.6.2 Results of Algorithm verification 102
4.7 Conclusion 103

5 Results of simulated communication scenarios 109

5.1 Chapter Description 109
5.2 Simulation Criteria 109
5.3 Simulation Results 113
5.3.1 PSK 113
5.3.2 DPSK 121
5.3.3 QAM 128
5.3.4 Comparative analysis and recommendations 136
5.4 Conclusion 138

6 Conclusion 144

6.1 Overview and Achievements 144
6.2 Future Work 146
6.2.1 Simulation Software 146
6.2.2 Hardware Implementation 146

LIST OF REFERENCES 148

APPENDICES

Appendix A: Orthogonal functions in Digital Communication 152
Appendix B: GUI Development 162
Appendix C: MATLAB scripts for Domestic Power Network Modeling 171
Appendix D: MATLAB script for the experimental power line model function 175
Appendix E: MATLAB scripts for OFDM-PLC Simulation 177
Appendix F: MATLAB scripts for PSK, DPSK and QAM modulation and demodulation 213
Appendix G: Miscellaneous MATLAB scripts used in the OFDM simulation scripts . 233

LIST OF TABLES

Table Page

3.1 Two-Port S-parameter definitions 62

4.1 Verification Results - BPSK 104

4.2 Verification Results - QPSK 104

4.3 Verification Results - DBPSK 104

4.4 Verification Results - DQPSK 104

4.5 Verification Results - 8QAM 105

4.6 Verification Results - 16QAM 105

Appendix
Table

DISCARD THIS PAGE

LIST OF FIGURES

Figure Page

1.1 A Typical Domestic power line networking setup 19

1.2 Noise scenario in domestic powerline channel (Dostert & Zimmerman 2000) 21

1.3 Illustration of Narrow-band modulation techniques (Downey & Sutterlin 1999) 23

1.4 Illustration of Spread Spectrum techniques (Downey & Sutterlin, 1999) 23

1.5 Illustration of the experimental, domestic power network employed in the project . . . 26

2.1 Comparison of the bandwidth utilisation for FDM and OFDM 31

2.2 Sub-carriers spectral overlap 33

2.3 Attenuation threshold of sub-bands 34

2.4 Channel distortion on individual sub-bands having a relatively flat response on each sub-band 34

2.5 The effect of a frequency offset (Δf) on sub-carrier f_2 leading to spectral leakage into adjacent sub-carrier (f_1 and f_2). 36

2.6 Conceptual OFDM Transmitter Structure where d represents the complex data symbol and S(t) represents the output waveform. 40

2.7 Conceptual OFDM Receiver Structure where $R(t)$ is the received vector and $\tilde{d}$ is the estimated complex symbol. 40

2.8 Block Diagram of a conventional OFDM Transmitter 41

2.9 Example of a typical resultant OFDM spectrum 43

2.10 The use of the IFFT and FFT for Multiplexing (Litwin & Pugel 2001) 45

Figure Page

4.4 Spectrum usage for OFDM Transmission and Reception 87

4.5 Flowchart for MATLAB OFDM Transmitter 88

4.6 Block Diagram of Domestic power line model 89

4.7 Flowchart for determination of E_b/N_o for a selected communciation scenario 93

4.8 Block Diagram of OFDM Receiver 94

4.9 Pilot data is used to estimate the amount of fading during transmission, and compensate the information data appropriately (Harada & Prasad 2002) 96

4.10 Flowchart for MATLAB OFDM Receiver 100

4.11 Results of Verification for OFDM-BPSK Simulation 105

4.12 Results of Verification for OFDM-QPSK Simulation 106

4.13 Results of Verification for OFDM-DBPSK Simulation 106

4.14 Results of Verification for OFDM-DQPSK Simulation 107

4.15 Results of Verification for OFDM-8QAM Simulation 107

4.16 Results of Verification for OFDM-16QAM Simulation 108

5.1 Transfer function (Magnitude) - Path AB with PC at C 110

5.2 Transfer function (Magnitude) - Path AC with Vacuum-cleaner at C 111

5.3 Transfer function (Magnitude) - Path BC with Mixer at C 111

5.4 Transfer function (Magnitude) - Path BD with Television at A 112

5.5 Transfer function (Magnitude) - Path CD with Hair-dryer at A 112

5.6 Results (PSK) - Scenario 1 114

5.7 Results (PSK) - Scenario 2 115

5.8 Results (PSK) - Scenario 3 116

Figure Page

5.9 Results (PSK) - Scenario 4 117

5.10 Results (PSK) - Scenario 5 118

5.11 Results (DPSK) - Scenario 1 122

5.12 Results (DPSK) - Scenario 2 123

5.13 Results (DPSK) - Scenario 3 124

5.14 Results (DPSK) - Scenario 4 125

5.15 Results (DPSK) - Scenario 5 126

5.16 Results (QAM) - Scenario 1 129

5.17 Results (QAM) - Scenario 2 130

5.18 Results (QAM) - Scenario 3 131

5.19 Results (QAM) - Scenario 4 132

5.20 Results (QAM) - Scenario 5 133

5.21 Scenario 1 - Comparative Results 139

5.22 Scenario 2 - Comparative Results 140

5.23 Scenario 3 - Comparative Results 141

5.24 Scenario 4 - Comparative Results 142

5.25 Scenario 5 - Comparative Results 143

6.1 OFDM Simulation Diagram with FEC 147

Appendix
Figure

A.1 Vectors x and y 154

A.2 Scheme for generating S(t) 158

Figure Page

A.3 Correlator Receiver 159

A.4 QAM Modulator 160

A.5 QAM Correlator Receiver 161

B.1 Screen-shot of the GUIDE Environment used for GUI Development 164

B.2 An example of a TF plot displayed on the GUI 165

B.3 Screen-shot of the initial user screen when the GUI is launched 166

B.4 An example of a BER plot given after a simulated scenario 167

B.5 Flowchart for BER Calculation 169

B.6 Multiple BER Plots for a given scenario 170

NOMENCLATURE

Abbreviations and Definitions

AC —→ Alternating Current

ADSL —→ Asymmetric Digital Subscriber Line

AWGN —→ Additive White Gaussian Noise

BER —→ Bit Error Rate

BPSK —→ Binary Phase Shift Keying

CE —→ Channel Estimation

DAB —→ Digital Audio Broadcasting

DBPSK —→ Differential Binary Phase Shift Keying

DFT —→ Digital Fourier Transform

DMT —→ Discrete Multi-tone Modulation

DPSK —→ Differential Phase Shift Keying

DQPSK —→ Differential Quadrature Phase Shift Keying

DSP —→ Digital Signal Processing

EMC —→ Electro-magnetic compatibility

FDM —→ Frequency Division Multiplexing

FEC —→ Forward Error Correction

FFT —→ Fast Fourier Transform

ICI —→ Inter-carrier Interference

IEEE —→ Institute of Electrical and Electronics Engineers

IFFT —→ Inverse Fast Fourier Transform

ISI —→ Inter-symbol Interference

MATLAB $\longrightarrow$ **Matrix Laboratory**

OFDM $\longrightarrow$ **Orthogonal Frequency Division Multiplexing**

OFDM-PSK $\longrightarrow$ ***OFDM using PSK-based encoding***

OFDM-DPSK $\longrightarrow$ **OFDM using DPSK-based encoding**

OFDM-QAM $\longrightarrow$ **OFDM using QAM-based encoding**

OFDM-BPSK $\longrightarrow$ **OFDM using BPSK encoding**

OFDM-QPSK $\longrightarrow$ **OFDM using QPSK encoding**

OFDM-DBPSK $\longrightarrow$ **OFDM using DBPSK encoding**

OFDM-DQPSK $\longrightarrow$ **OFDM using DQPSK encoding**

OFDM-8QAM $\longrightarrow$ **OFDM using 8QAM encoding**

OFDM-16QAM $\longrightarrow$ **OFDM using 16QAM encoding**

OFDM-PLC $\longrightarrow$ **OFDM in Power-line communication**

PAPR $\longrightarrow$ **Peak Average Power Ratio**

PLC $\longrightarrow$ **Power line Communication**

PSD $\longrightarrow$ **Power Spectral Density**

PSK $\longrightarrow$ **Phase Shift Keying**

QAM $\longrightarrow$ **Quadrature Amplitude Modulation**

QPSK $\longrightarrow$ **Quadrature Phase Shift Keying**

SOLT $\longrightarrow$ **Short, Open, Load and Thru standards used for calibrating a network analyser**

TCM $\longrightarrow$ ***Trellis-Coded Modulation***

VLSI $\longrightarrow$ **Very Large Scale Integration**

Symbols

A $\longrightarrow$ **Amplitude**

a $\longrightarrow$ **Roll-off factor**

d_n $\longrightarrow$ **Serial data sequence**

E_b $\longrightarrow$ **Energy per Bit**

$\mathfrak{F}$ $\longrightarrow$ **Fourier Transform**

f_n ⟶ **Discrete sub-carrier frequency**

F_m ⟶ **Nyquist Bandwidth**

H ⟶ **Transfer Function**

N ⟶ **Number of Channels**

$R(t)$ ⟶ **Received Signal (Time)**

$S(t)$ ⟶ **Transmitted Signal (Time)**

S_{11} ⟶ **Reflection coefficient of the input**

S_{22} ⟶ **Reflection coefficient of the output**

S_{21} ⟶ **Forward transmission gain**

S_{12} ⟶ **Reverse transmission gain**

S_k ⟶ **Complex DFT Sinusoid**

S_l ⟶ **Complex DFT Sinusoid**

T_g ⟶ **Guard Interval**

$X(k)$ ⟶ **Discrete Fourier Transform output signal**

$x(n)$ ⟶ **Discrete input sequence**

Z_L ⟶ **Load impedance**

Z_O ⟶ **Characteristic impedance**

Z_S ⟶ **Source impedance**

α_i ⟶ **Attenuation factor**

φ_i ⟶ **Phase distortion**

Chapter 1

Introduction

With the growth of the personal computer industry, a number of households now contain two or more personal computers. The need to share resources such as printers, scanners and other PC peripherals has become evident. Communication between personal computers and other smart devices in the home is also required. This has brought about the need for home networking together with Home Automation. Home networking is the collection of elements to enable the connection and integration of multiple computing, control and communication devices. There are various options at this stage for home networking. The option should provide a simplistic and reliable solution to facilitate any home networking application.

In terms of home networking technologies, the options are either to use wireless based technology or existing wired solutions. The most common and popular form of home networking technologies is Ethernet networking, with wireless standards IEEE 802.11g, IEEE 802.16 (WiMAX) and IEEE 802.11a, WiFi (Wireless Networking) becoming popular choices for use in home networking.

Another option for home networking, which is explored in this dissertation, is the use of domestic power line networking.

1.1 Domestic Power line communication

1.1.1 Overview

Domestic power line communication involves the use of the existing domestic wiring for data communication purposes. Simply translated, this means that the same line that supplies electrical power to an appliance or another electrical device, can also provide a medium for communication, i.e. data communication. The domestic power line offers an ideal medium for data communications considering it is a ubiquitous medium that is available in all areas of a typical suburban home. And unlike Ethernet or telephony-based networking technologies, no additional wiring is required. Domestic power line communication can thus be categorised among the "no new wires" networking solutions that aims to provide transparent networking to home users.

In the words of Dostert, (Dostert 2001), 'Connecting to the Internet may some day be as easy as plugging into the same wall socket outlet that serves your stereo.', which with current Homeplug technology (Dostert 2001) is becoming a reality. Figure 1.1 illustrates a typical domestic power line based network.

The idea of sending information on power lines has been proposed and researched for quite some time and have been limited, until recently, to low bit rate PLC (Power line communication) systems. These low bit-rate PLC systems such as the popular X10 technology, are designed for home automation applications. With advances in DSP (Digital Signal Processing) technology, however, the use of complex modulation techniques can now provide broadband networking applications on a domestic power line.

Modulation refers to the process of transmitting information by converting the digital information into a suitable signal that can be transmitted over a specific medium. Most of the common modulation schemes, were developed for the specific purpose of transmission through air or any other guided medium, of which the characteristics (noise, impedance, attenuation, etc.) are known.

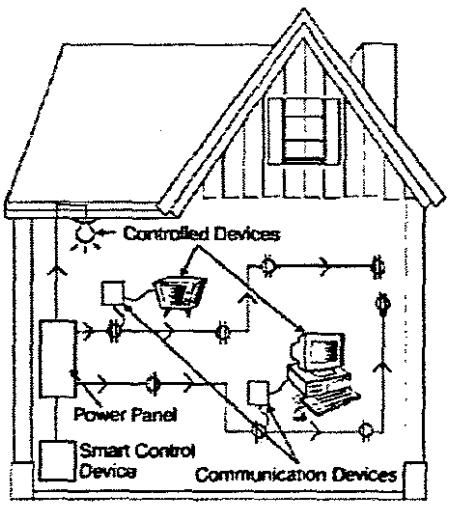

Figure 1.1: A Typical Domestic power line networking setup

1.1.2 Channel characteristics of Domestic power line

The domestic power line presents a practically hostile communication medium and thus presents a difficult challenge for communication engineers. Electrical wiring was never intended to serve as a communication medium. It therefore presents a number of unfavourable characteristics - such as varying impedance, signal attenuation and noise - which adversely affect reliable information transfer. These characteristics are dynamic and can be attributed to appliances and other devices which inject significant noise onto the power line network (Van-Der-Gracht & Donaldson 1985), (O'Neal 1986), (Chan & Donaldson 1989), (Sutterlin & Downey 1999).

The power line channel thus does not represent an AWGN (additive white Gaussian noise) environment (Dostert & Zimmerman 2000), in contrast to other wireless or other wired mediums, for which most communication systems are designed.

Noise sources present on the domestic power line channel include (Dostert 2001):

- Coloured background noise with a relatively low PSD (power spectral density) and varying frequency.
- Narrow-band noise, which consists mainly of sinusoidal signals with modulated amplitudes caused by commercial broadcasts (television and radio).
- Periodic impulsive noise, which is asynchronous and synchronous to the AC (Alternating Current) power frequency, induced by either the AC frequency (asynchronous) or by switching power supplies (synchronous).
- Asynchronous impulsive noise (on/off switching), which is undoubtedly a significant problem since switching events are completely random and thus unpredictable sources.

The occurrence of impulsive noise events causes a significantly high noise PSD, which could lead to bit or burst errors in data transmission (Dostert & Zimmerman 2000).

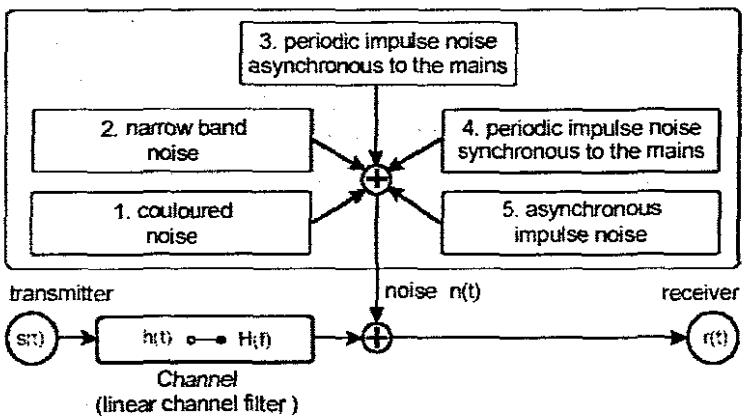

Figure 1.2: Noise scenario in domestic powerline channel (Dostert & Zimmerman 2000)

Loads (appliances) on the power network affect the impedance behaviour of the domestic power channel (Krishnan, et al. 2002) as well as the the attenuation characteristics of the channel. A study conducted by C.J. Kim and M.F. Chouikha (Kim & Chouikha 2002) on the attenuation characteristics of domestic and office power networks, concluded that the attenuation factor of the power network is influenced by the number of loads present on the network.

The domestic power line channel provides a design challenge in using complex digital communication methods for dealing with the dynamic and harsh effects of this particular medium.

1.1.3 Modulation schemes for Domestic Power line communication

Typical modulation schemes used in power line communication can be divided into two types of modulation schemes, namely *Narrow-band modulation schemes* and *Spread Spectrum modulation schemes*.

Narrow band modulation schemes for domestic power communication are shown in Figure 1.3. Modulation is achieved by varying either amplitude, frequency or phase information of the carrier frequency according to the input binary data. These techniques can be implemented in relatively low cost hardware and are only sufficient for low bit rate applications, as relatively basic digital

modulation methods are utilised in these applications.

Spread Spectrum modulation offers resistance against a variety of interferences and can operate effectively in hostile channel environments such as the domestic power line. This is accomplished by subjecting the modulated signal to a second modulation step using a wide-band signal, other than data transmitted, as a source for modulation (Sutterlin & Downey 1999). This technique is currently used in the CeBUS protocol for domestic PLC (Radford 1996). The main disadvantage of this technique, is that it requires a large band for modulation.

With recent developments by the Homeplug Alliance(Homeplug-Alliance 2005), the Homeplug 1.0 standard has proven that a multi-carrier approach can be used for reliable high-bit rate domestic PLC. The standard is based on Orthogonal Frequency Division Multiplexing (OFDM) which is a spectrally-efficient technique. OFDM exhibits robustness against various types of interference (Dostert 2001), especially in fading environments, where attenuation varies with changes in the network.

Comparative studies have shown that OFDM is the underlying approach for reliable and effective networking applications. (Lin, et al. 2003) (Raphaeli & Bassin 1999).

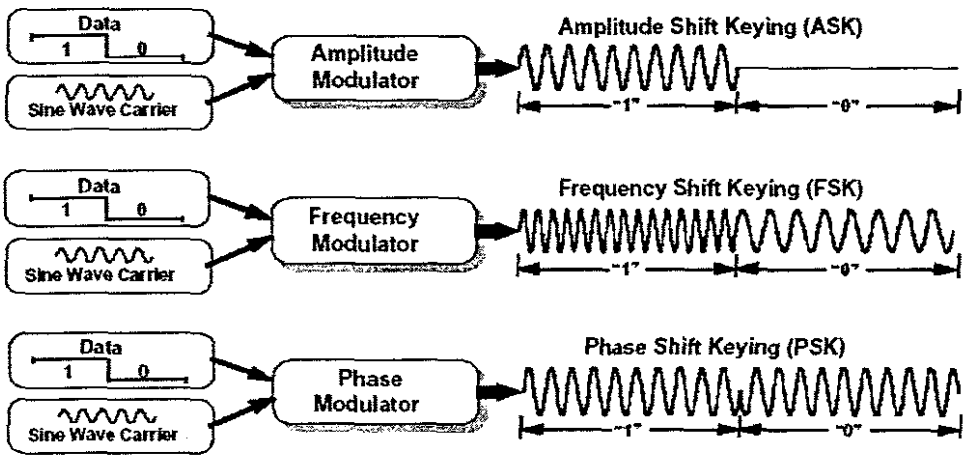

Figure 1.3: Illustration of Narrow-band modulation techniques (Downey & Sutterlin 1999)

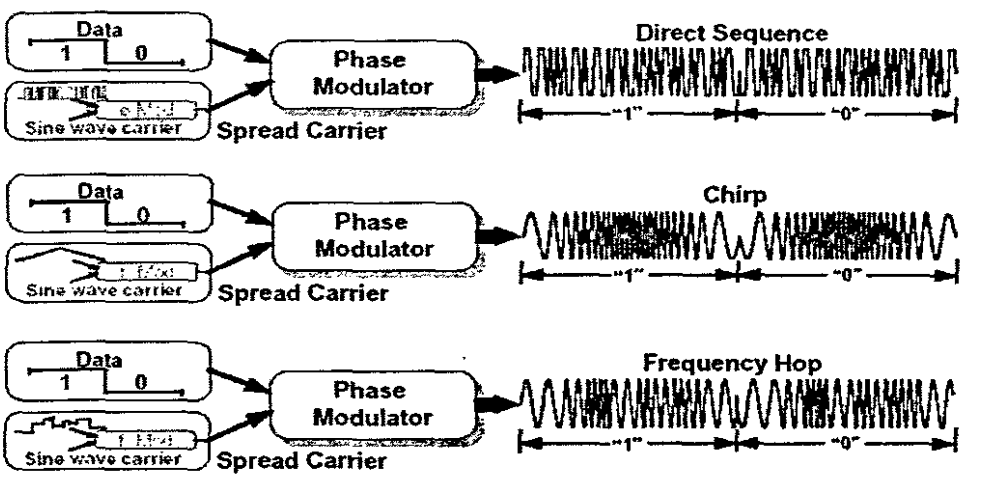

Figure 1.4: Illustration of Spread Spectrum techniques (Downey & Sutterlin, 1999)

1.2 Objectives of the Research Project

The aim of the research project was to study the performance of various modulation techniques for an OFDM-based domestic power line modem. The study consisted of:

- Modeling an experimental network which is representative of a typical South African domestic power network.
- Implementing and simulating an OFDM-based communication system for domestic power line communication.
- Evaluation of various modulation methods for the OFDM-based Modem.

1.2.1 Modeling an experimental domestic power network

A number of approaches can be employed for modeling a domestic power line. Commonly, these techniques aim to characterise the physical influences of the power cable itself. The influence of the cable can thus be quantified in terms of a *transfer function*.

The transfer function can then be used to describe the input/output relationship of the domestic power network, allowing the selection of a communication strategy to mitigate the influence of this medium on the transmitted signal. Methods of determining the transfer function for South African domestic power lines were investigated.

To produce a relatively good estimate of this unique channel, the loading effect of typical noise sources, present on this particular channel, is introduced into the overall measured model. Typical noise sources found on this channel are discussed in Dostert (Dostert 2001).

The aim of this portion of the project is to have a general domestic power network model which includes the prominent sources of degradation on this particular communication medium, which is

limited to the loading effect of these sources on the network.

1.2.2 Development of an OFDM simulation

In order to verify or predict the performance of any communication system today, the process of simulation is employed. The aim of this portion of the study is to have a fully simulated OFDM communication system in software. This will allow the system parameters to be easily varied for optimal performance and stability. The inclusion of the domestic power line model will provide for a complete analysis of the communication system.

The simulation software will be critical in understanding how certain parameters can be modified to allow for improved performance under the harsh channel conditions. An assessment can then be made of modulation techniques to enhance the reliability of the data that is transferred.

1.2.3 Analysis of various encoding methods for optimal OFDM performance

The analysis of various sub-modulation methods (e.g. BPSK, QAM, DPSK, etc.) is a crucial component of this study. Results obtained from the simulated scenarios will aid in the analysis and selection of an optimal and robust modulation method for domestic power line communication.

1.3 Scope and limitations of the project

As with any research endeavor, the scope and limitations of the research has to be clearly defined. The scope and limitations apply to two crucial areas of the project which will now be discussed.

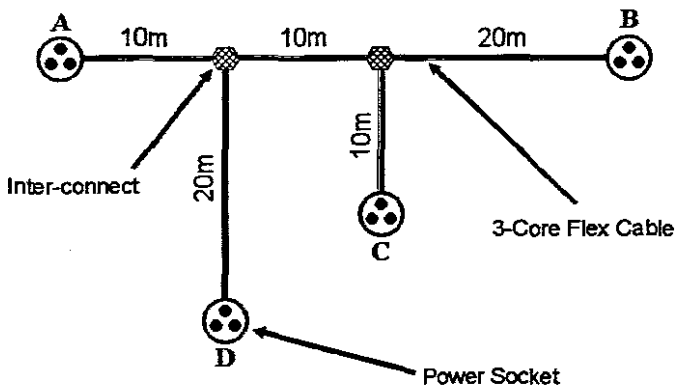

Figure 1.5: Illustration of the experimental, domestic power network employed in the project

1.3.1 Modeling an experimental network

The task of modeling a typical domestic power network can become quite daunting. It was therefore essential to limit the modeling to physically measuring an experimental power network. The experimental network provided a well-defined system (where all dimensions were known to the author), ensuring that mathematical techniques can be applied to predict the attenuation and phase response along a transmission path. In the same token, measuring parameters on an experimental network ensures that results remain static for numerous measurements.

The experimental network constructed for this purpose was based on an experimental set-up for characterisation employed by D. Anastasiadou and T. Atonakopoulos (2002). The experimental set-up is depicted in Figure 1.5

1.3.2 Limited Noise sources

The amount of appliances / noise sources used for this particular study was limited to several typical household appliances. Certain of these appliances have been identified as contributing substantially to the distortion of transmitted signals, i.e. light dimmers and universal motors. The loading effect of these appliances formed part of the overall measurement along a particular transmission path. This will be discussed in detail in Chapter 3 (Domestic power network modeling).

1.3.3 Simulation scope and limitations

When simulating a digital communication system, one is faced with the task of deciding on which areas to include into the simulation (e.g. error correction, synchronisation, etc.). With the scope of this particular research project, the author was only interested in the effects of different encoding / modulation techniques in a simulated domestic environment.

Therefore the scope of this project has been limited to a basic OFDM Transmitter / Receiver system, which includes channel estimation and equalisation as a basic measure against simulated interference. The simulation will not include some of the associated issues related to Digital Communication or OFDM such as:

- Synchronisation
- Error Correction / Detection (Convolutional encoding / Viterbi Decoding, Forward Error Correction, etc.)
- Carrier recovery

1.4 Thesis Layout / Chapter Description

Some background to digital modulation theory, as well as a description of the Multiplexing Technique OFDM will be given in Chapter 2. Following a review of the theory, Chapter 3 then presents a summary of the power network modeling procedure.

The design and simulation of an OFDM communication system in Matrix Laboratory (MATLAB), is discussed in Chapter 4. Chapter 4 will include the algorithm design for the OFDM transmitter and receiver as well as integration of the domestic power network model into the final simulation.

The performance analysis of various encoding techniques for an OFDM-based power line communication system will be dealt with in Chapter 5. Selected communication scenarios e.g. noise sources and transmission paths will be simulated and discussed to provide an overall analysis of particular encoding strategies (coherent and non-coherent).

The final chapter (Chapter 6) will reveal the author's conclusions and discuss the achievements of the research. Future research on this topic will be discussed as well.

Chapter 2

Digital Modulation theory for High Bit rate applications

2.1 Chapter Description

This chapter serves as an introduction into the theory of parallel data transmission, focusing specifically on OFDM (Orthogonal Frequency Division Multiplexing).

The chapter will therefore focus on:

- Parallel data transmission.
- Orthogonal Frequency Division Multiplexing (OFDM)
- The theory of operation for OFDM
- Description of a typical OFDM system (Transmitter and Receiver)

2.2 Parallel Data Transmission

A parallel, or multiplexed, data system offers possibilities for mitigating problems that occur in traditional high-speed serial systems (Cimini 1985). Parallel data transmission is the process of transmitting N number of parallel data streams simultaneously. Even though the separate parallel data streams are transmitted at a much lower bit rate, their accumulative sum yields an overall high data rate. This results in high-speed data transmission.

In such a system, each parallel stream only occupies a small portion of the available bandwidth. With a classical parallel data system, the total bandwidth is divided into *N non-overlapping frequency sub-channels* (Cimini 1985).

Bandwidth efficiency can be increased if the sub-channels are allowed to *overlap*, whilst remaining *orthogonal* to each other. Orthogonality between sub-channels ensures that sub-carriers can be separated at the receiver. This is in essence the arrangement presented in *Orthogonal Frequency Division Multiplexing*, a *parallel data transmission scheme.*

To begin the discussion on this particular parallel data transmission scheme, an examination of Frequency Division Multiplexing will precede.

2.2.1 Frequency Division Multiplexing

Frequency Division Multiplexing (FDM) is the process of splitting the available channel's bandwidth in *N* number of sub-bands, for either parallel data transmission or multiple user access of the channel. In FDM for multiple access, individual sub-bands are allocated to the various users, allowing simultaneous use of the channel without requiring additional bandwidth for each user. In traditional FDM, a guard band is allocated between sub-bands to prevent spectral interference from adjacent sub-bands.

An important use of Frequency Division Multiplexing is in parallel data transmission.

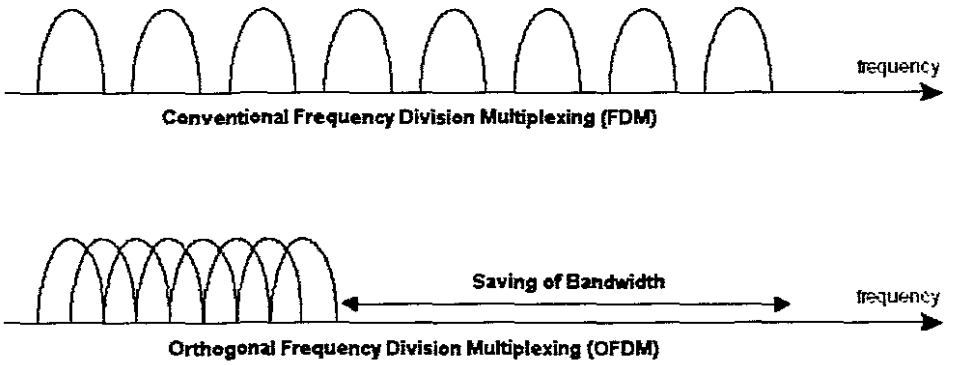

Figure 2.1: Comparison of the bandwidth utilisation for FDM and OFDM

2.2.2 Parallel Data transmission using FDM

Parallel data transmission scheme using *FDM* allows the use of *multiple sub-carriers*, each carrying a *portion of the data stream*. A bank of filters is utilised at the receiver to separate individual sub-bands for processing. In traditional FDM a guard band is used to prevent the spectral interference from adjacent sub-bands. A disadvantage, however, is that the guard bands lower the system's effective information rate when compared to a single carrier system (Litwin & Puegel 2001).

Another disadvantage, when using filters to distinguish between sub-bands, is an increase in the required sub-band's bandwidth. The increase can be defined from F_m (Nyquist Bandwidth) to $(1+a)\cdot F_m$ where a is defined as the filter roll-off factor. Another difficulty with using filters to divide sub-bands, is the construction of a matched filter bank when the number of sub-bands is large (Matic 1998).

Orthogonal Frequency Division Multiplexing thus solves these problems by allowing spectral overall. *Separation* of the *sub-carriers* at the receiver is maintained by the use of *orthogonal sub-carriers*. Efficient bandwidth use is also achieved as depicted in Figure 2.1.

2.3 Orthogonal Frequency Division Multiplexing

OFDM is a multi-carrier scheme for high-speed, parallel data transmission. This parallel data transmission scheme uses an important mathematical property to multiplex and de-multiplex information at the respective transmission and receiver stages. Further analysis of this property will be discussed in an upcoming section.

OFDM was conceptualised in the early 60's as a method for transmitting information simultaneously through a linear band-limited channel, without inter-channel interference (ICI) and Inter-symbol interference (ISI) (Edfors, et al. 1996). A major contribution to OFDM was the paper presented by Weistein (Langfeld & Dostert 2000) who proposed the use of the Discrete Fourier Transform (DFT) to perform base band modulation and demodulation (Edfors et al. 1996). Weistein also added the use of a guard space between OFDM symbols in the time domain as well as raised cosine filtering in the time domain to further protect against frequency-selective attenuation.

Although the concept of OFDM has been around for quite a long time, the complexity issues in terms of implementation can now be dealt with. Advances in DSP and Very Large Scale Integration (VLSI) have made these obstacles no longer relevant.

OFDM is currently used in the European Digital Audio Broadcasting (DAB) standard (Edfors et al. 1996). Another important application of OFDM is in Asymmetric Digital Subscriber Line technology (ADSL). In ADSL, OFDM is referred to as Discrete Multi-tone (DMT) modulation.

2.3.1 Advantages of OFDM

- OFDM offers high spectral efficiency when compared to conventional FDM technology (Figure 2.1). This is accomplished by allowing sub-carrier spectra to overlap while maintaining their orthogonality (shown in Figure 2.2).

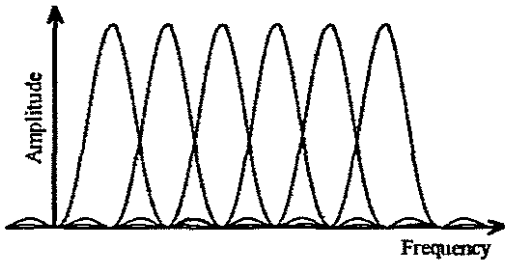

Figure 2.2: Sub-carriers spectral overlap

- One major advantage that OFDM has shown is its ability to accommodate the common channel impairment of ISI in both wireless and wired environments (Edfors et al. 1996).

- OFDM offers robustness against the distortion due to channel conditions. This is due to the narrow sub-channels (an example is portrayed in Figure 2.4) having a relatively flat amplitude distortion. The result is a requirement for simpler equalization (frequency domain equalization) in contrast to wideband equalization (time domain equalization) in the single-carrier case. This is due to the narrow-band nature of the sub-channels, where each sub-channel has a relatively constant attenuation and group delay.

- In certain OFDM systems, only sub-channels, which are above a pre-defined attenuation threshold, are used to transmit information (Figure 2.3). This is accomplished through a periodic OFDM training sequence, which estimates the current channel conditions in order to determine which sub-channels are not suitable for data transmission.

2.3.2 Drawbacks of Practical OFDM systems

OFDM communication systems require the transmitter and receiver to be synchronized to one another. The alignment of the phase and frequency of the receiver oscillator and the transmitter thus becomes critical in order to successfully recover the transmitted information. Synchronization is also used to determine the beginning and the end of each consecutive OFDM symbol.

Inaccurate synchronization can lead to three sources of error (Bingham 1990) namely:

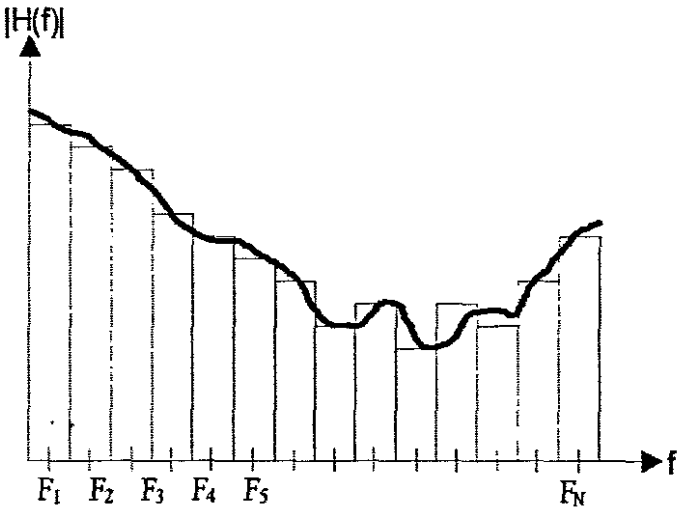

Figure 2.3: Attenuation threshold of sub-bands

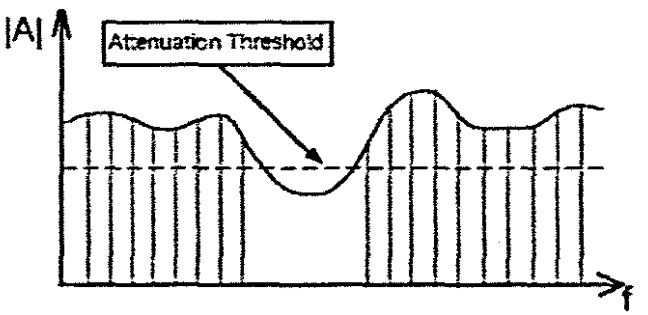

Figure 2.4: Channel distortion on individual sub-bands having a relatively flat response on each sub-band

- Mismatched coarse timing - results in an arbitrary time shift in the demodulation process.
- Frequency Deviation - due to deviation of oscillator frequencies in the transmitter and receiver. (Figure 2.5)
- Sampling error - different sampling periods in the receiver and transmitter leading to offsets in the recovered symbol.

Another consideration for OFDM is the Peak Average Power Ratio (PAPR) (Agilent-Technologies 2002) or "CREST Factor" (Dostert 2001). Practical OFDM systems use quite a number of sub-carriers (e.g. 1526 sub-carriers are used in the case of DAB). This leads to a high peak average power for an OFDM symbol.

A high PAPR can cause inter-modulation distortion between sub-carriers resulting in a higher error rate. Another problem that can occur because of a high PAPR is limiting / saturation in the transmit power amplifier. The power required for the transmit amplifier should be kept as low as possible for both cost and Electromagnetic Compatibility (EMC) reasons (Dostert 2001). Lawrey (1999) discusses this issue further in detail.

2.4 Theory of Operation

The principle operation of an OFDM system is the multiplexing and de-multiplexing of sub-carriers at the respective transmitter and receiver stages. The core element, or process, of OFDM is the Discrete Fourier Transform (DFT), practically implemented using the Fast Fourier Transform (FFT). The DFT is defined as (J. Smith 2003):

$$X(k) = \sum_{n=0}^{N-1} x(n) e^{-j\frac{2\pi km}{N}} \quad k = 0, 1, 2, 3, ..., N-1 \tag{2.1}$$

where k is the discrete frequency index. The Inverse Discrete Fourier Transform is defined as:

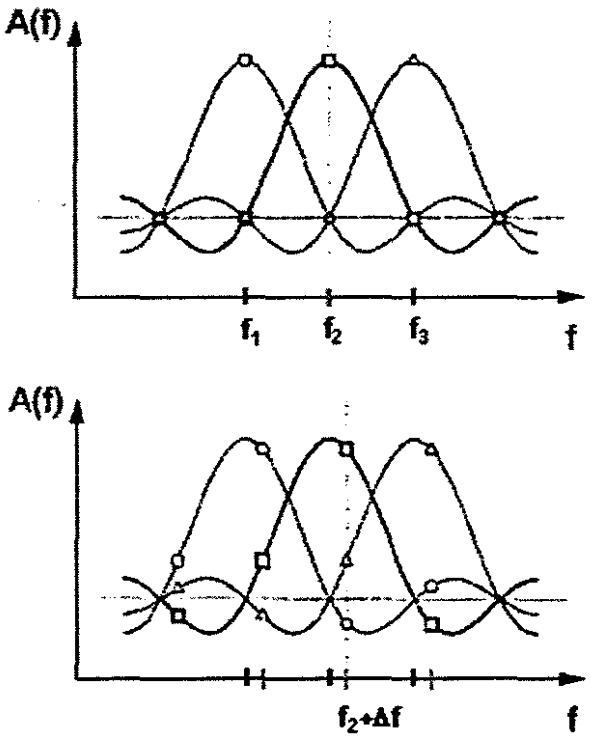

Figure 2.5: The effect of a frequency offset (Δf) on sub-carrier f_2 leading to spectral leakage into adjacent sub-carrier (f_1 and f_2).

$$x(n) = \frac{1}{N}\sum_{k=0}^{N-1} X(k)e^{-j\frac{2\pi km}{N}} \tag{2.2}$$

Analysis of the DFT reveals the mathematical relationship, which allows sub-carriers to be added at the transmitter, and separated at the receiver. This mathematical relationship is Orthogonality. Referring to Appendix A, the importance of orthogonal functions in Digital Communication is described. The *DFT operation* itself can be defined as an *inner product* operation where the *input signal* is correlated with a *set of k complex exponential sinusoids*. It can be proven that the DFT complex exponential sinusoids form an orthonormal basis (orthogonal functions).

2.4.1 Orthogonality of DFT Sinusoids

Proof (Smith 2003): Let:

$S_k = e^{j\frac{2\pi kn}{N}}$ and $S_l = e^{j\frac{2\pi ln}{N}}$ representing the DFT complex sinusoids

Then computing the inner product of S_k and S_l:

$$\langle S_k, S_l \rangle = \sum_{n=0}^{N-1} S_k\overline{S_l} = \sum_{n=0}^{N-1} e^{j\frac{2\pi kn}{N}} e^{j\frac{2\pi ln}{N}} = \sum_{n=0}^{N-1} e^{j\frac{2\pi(k-l)n}{N}} \tag{2.3}$$

$$= \sum_{n=0}^{N-1} e^{j\frac{2\pi(k-l)n}{N}} = \frac{1 - e^{j2\pi(k-l)}}{1 - e^{j\frac{2\pi(k-l)}{N}}}$$

where the last step is derived using close-form expression for the sum of a geometric series. Evaluating the expression, we find that for all $k \neq l$ the denominator is nonzero while the numerator is zero. This proves that $S_k \perp S_l$ and that the DFT complex sinusoids are orthogonal to each other.

For an orthonormal complex sinusoidal set, the norm of the DFT complex sinusoids must also be calculated:

$$\langle S_k, S_l \rangle = \sum_{n=0}^{N-1} S_k \overline{S_l} = \sum_{n=0}^{N-1} e^{j\frac{2\pi(k-k)n}{N}} = N \tag{2.4}$$

which proves that $\| S_k \| = \sqrt{N}$

Normalising the set of complex DFT sinusoids, an orthonormal set can be obtained (Smith 2003):

$$\tilde{S}_k(n) = \frac{S_k(n)}{\sqrt{N}} = \frac{e^{j2\pi kn/N}}{\sqrt{N}} \tag{2.5}$$

The orthonormal complex sinusoidal basis signals satisfy the conditions (Smith 2003):

$$\langle \tilde{S}_k, \tilde{S}_l \rangle = \begin{cases} 1, & k = l \\ 0, & k \neq l \end{cases} \tag{2.6}$$

This forms a normalised set of DFT complex exponential sinusoids.

In OFDM, the *orthonormal basis of complex sinusoids* of the DFT is used as sub-carriers for the purposes of parallel data transmission. The discrete transmitted OFDM signal can thus be stated as:

$$S(n) = \sum_{n=0}^{N-1} d_n e^{j\frac{2\pi kn}{N}} \tag{2.7}$$

where each d_n is a complex number $d_n = a_n + jb_n$ and represents a symbol for either QPSK and QAM.

The transmitted signal when passed through the D/A (Digital to Analog Converter) can also be stated as (continuous time form):

$$S(n) = \sum_{n=0}^{N-1} d_n e^{j2\pi f_n t} \tag{2.8}$$

where f_n refers to the specific sub-carrier component and the serial data sequence is given by d_n.

Using the above derivations, a conceptual structure of an OFDM system is given in Figure 2.6 and the continuous time model in Figure 2.7 (Continuous Time Model). Similarities exist between the OFDM transmitter structure in Figure 2.6 and the diagram presented in Appendix A, for the generation of the transmitted symbol.

Similarities between the diagrams presented in Appendix A for the generation of the transmitted symbol and the correlation receiver can be made to Figure 2.6. The coefficients in the case of OFDM are the complex data symbols and the orthonormal basis functions are complex exponentials provided by the Discrete Fourier transform.

2.4.2 Importance of Orthogonality in OFDM

The importance of Orthogonality in OFDM can now be appreciated, since the entire transmission scheme relies on this fundamental mathematical property. If orthogonality is lost during the process of transmission, then the accurate separation of sub-carriers will be impossible.

Timing and frequency offsets affect the orthogonality of sub-carriers in practical OFDM systems. This is illustrated once again in Figure 2.5.

2.5 Description of a conventional OFDM Transmitter

As with the conceptual description of OFDM, the transmitter operation is quite simple. The serial data stream is converted to a parallel data stream. The conversion from serial to parallel also forms a buffer to allow processing of only one data block at a time. The parallel data stream then feeds the bank of signal mapping / encoding stages. The type of encoding or modulation (e.g. 16 QAM, 32 QAM, QPSK) is determined by the number of bits assigned to each signal mapper. The output of the signal mapper is a complex number $d_n = a_n + jn_n$, representing a constellation point

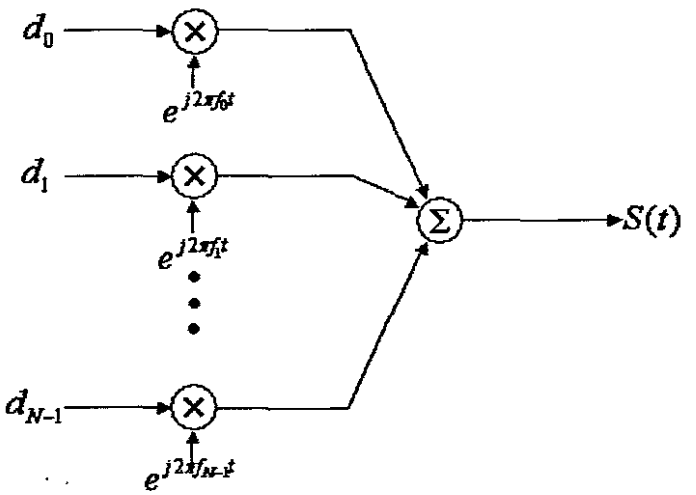

Figure 2.6: Conceptual OFDM Transmitter Structure where *d* represents the complex data symbol and S(t) represents the output waveform.

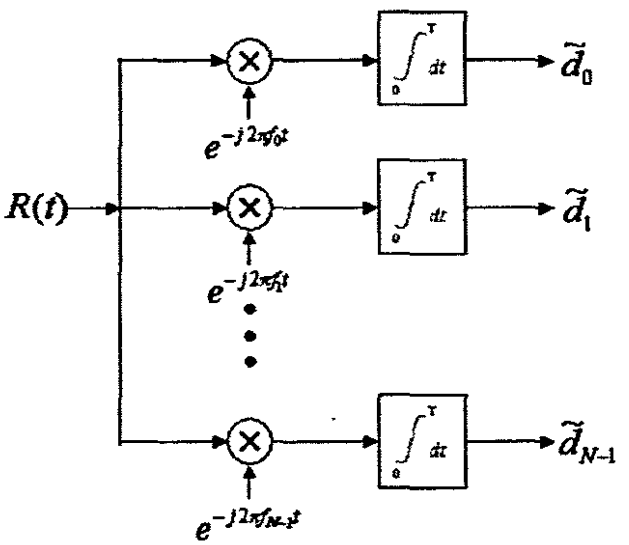

Figure 2.7: Conceptual OFDM Receiver Structure where *R(t)* is the received vector and $\tilde{d}$ is the estimated complex symbol.

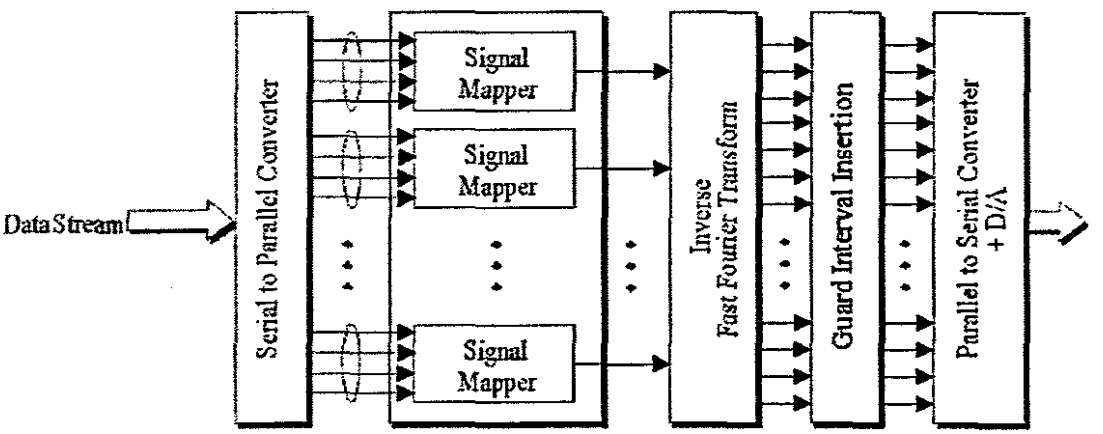

Figure 2.8: Block Diagram of a conventional OFDM Transmitter

of a specific symbol.

The Inverse Fast Fourier Transform (IFFT) modulates the complex numbers in the baseband (Matic 1998). The samples generated by the IFFT represent the OFDM symbol that is a time domain representation of all the multiplexed symbols. A guard interval is inserted in the form of a cyclic prefix. The cyclic prefix appends a copy of the last few samples to the start of the OFDM Symbol. The cyclic prefix is utilised for the minimisation of ISI resulting from multipath delays. Once the cyclic prefix is added, the discrete output waveform is converted to a continuous time domain waveform using a Digital to Analog converter. The output signal is then up-converted for transmission either through a wireless or wired medium.

An example of the output spectrum is given in Figure *2.9*.

2.5.1 Description of stages in an OFDM Transmitter

An analysis of critical stages within the OFDM transmitter is required for a full understanding of the system.

2.5.1.1 Channel Coding

To increase the robustness of OFDM data transmission, channel coding is added to increase the reliability of the transmitted information (Cimini 1985). By appending additional bits to the transmitted data stream, it is possible to detect and even correct certain errors (Education 1999). Among these channel techniques is the use of Trellis coded modulation (TCM) combined with frequency and time interleaving. This method is considered effective for use in a selective fading channel (Cimini 1985).

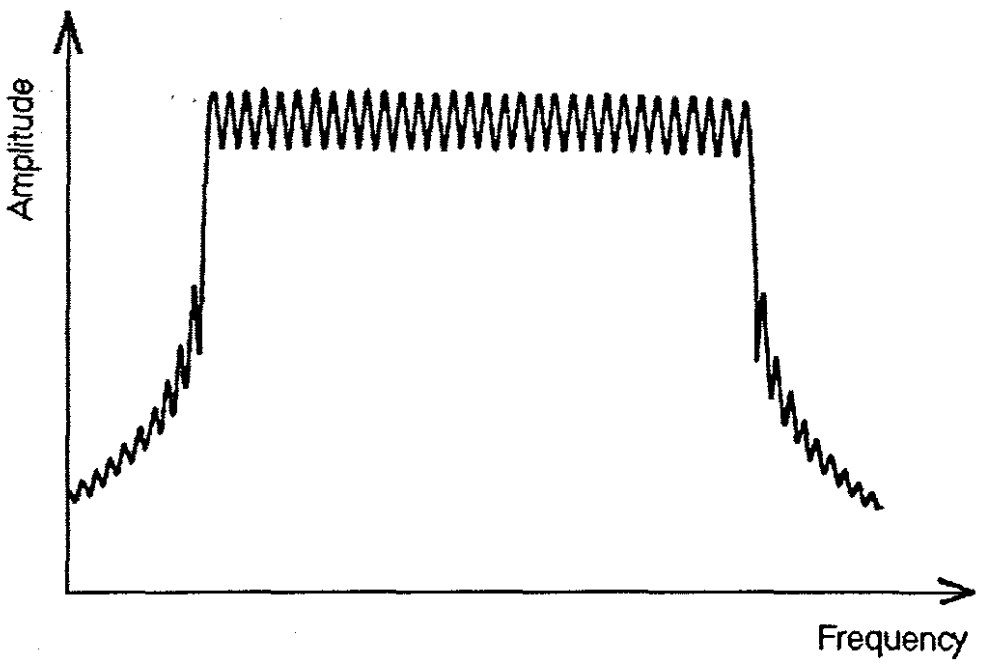

Figure 2.9: Example of a typical resultant OFDM spectrum

When Forward Error Correction (FEC) is used in OFDM, then it is termed as Coded-OFDM or Coded Orthogonal Frequency Division Multiplexing. This is currently being utilised in the Digital Video Broadcasting standard.

2.5.1.2 Signal Mapping / Symbol Encoding

Signal mapping refers to the digital modulation process which produces a set of complex symbols for OFDM transmission. Methods utilised include QAM, QPSK, BPSK, etc. These modulation techniques perform the symbol mapping in the frequency domain. The constellation size is determined by the amount of grouped bits that feed each individual signal mapper.

In certain OFDM architectures, signal mapping can be changed adaptively to suit specific channel conditions. Additionally, with certain OFDM architectures, the sub-carrier signal mapping can be changed according to each sub-channel's condition. For relatively distortion less sub-channels, higher symbol constellations can be used whereas for relatively bad sub-channels, lower symbol constellations will be used.

Differential QAM, QPSK and BPSK are also used as signal mapping techniques to further compensate for frequency or timing errors that occur in typical OFDM systems.

2.5.1.3 IFFT (IDFT) Modulator

The function performed by the IFFT is the process of converting N number modulated sub-carriers into a sampled time domain representation for transmission. From Digital Signal Processing theory, the IFFT or IDFT performs this operation by correlating frequency-domain information with its orthogonal basis functions, which are sinusoids at certain frequencies (Litwin & Puegel 2001).

The basis functions of the IFFT (complex orthogonal sinusoids) from the sub-carriers of the OFDM Transmitter. The input symbols, which are complex, determine both the amplitude and

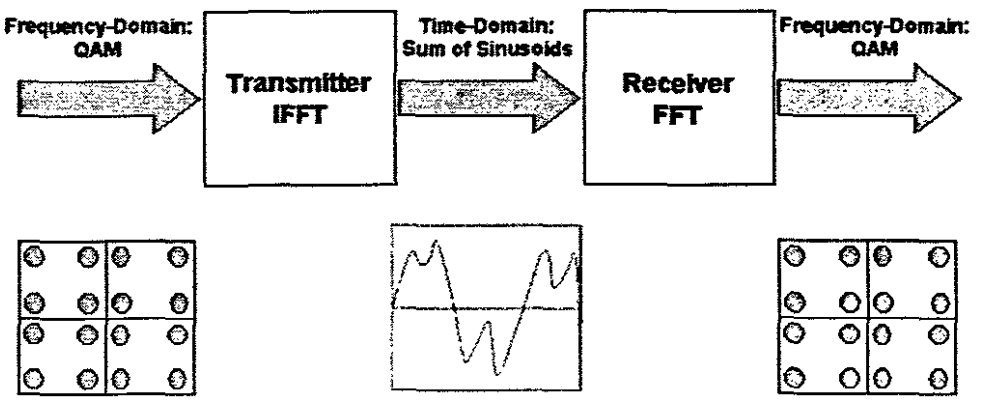

Figure 2.10: The use of the IFFT and FFT for Multiplexing (Litwin & Pugel 2001)

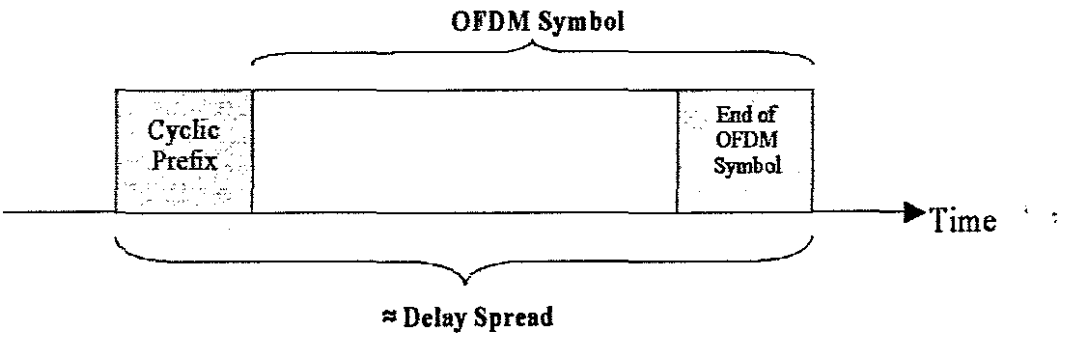

Figure 2.11: Cyclic Prefix

phase of the sinusoid for each sub-carrier. The IFFT output is thus a summation of all N orthogonal sinusoids forming the time domain equivalent signal (Litwin & Puegel 2001).

Evidently the IFFT thus provides an effective method to modulate data onto N orthogonal sub-carriers (Litwin & Puegel 2001).

2.5.1.4 Cyclic Extension / Guard Band Insertion

Orthogonality of sub-carriers can be maintained and individual sub-carriers can be separated by the FFT at the receiver, only if there is no:

– Inter-symbol Interference (ISI) and

– Inter-carrier Interference (ICI)

due to channel distortion.

In practice however, achieving these conditions is not possible. Spectra of individual sub-carriers can spread into adjacent sub-carrier spectra causing ICI and ISI. A simple solution to minimise the effects of ISI is to increase the symbol time. This is accomplished through the aid of a guard band, or cyclic prefix as it is commonly referred to.

A cyclic prefix (as shown in Figure 2.11) extends the OFDM Symbol time to ensure that the total symbol duration is longer than the channel impulse response (which is termed the delay spread). The use of a cyclic prefix as a guard interval also allows the receiver to maintain carrier synchronisation. Using the cyclic prefix the receiver is able to correlate the beginning and the end of the OFDM symbol and thus able to perform synchronisation.

Since the use of a guard interval, reduces data throughput, the guard interval will therefore never exceed more than a quarter of an OFDM symbol's time ($T_g = T/4$), as the efficiency of the transmission will be decreased.

2.6 Description of a conventional OFDM Receiver

In any Digital Communication System, a crucial component of the system is the receiver. The receiver is responsible for the estimation / detection of the transmitted information. it is therefore essential, for providing accurate and reliable information, that the Receiver is capable of estimating, correcting and reconstructing the transmitted data stream.

The complexity of OFDM Receivers can vary from a complex configuration to a relatively straight-forward set-up with standard stages such as the FFT, symbol decoding, etc. The complexity of an OFDM receiver depends on the types of distortions present on the channel to be used. The OFDM receiver should be able to adapt, estimate and compensate for any known error sources that the channel might present. Current innovation and research in OFDM is therefore mainly in the design of OFDM receivers (Ingram 2000).

With no standardisation on receiver configurations and designs, the discussion will therefore focus on a conventional OFDM receiver. The conventional OFDM receiver is depicted in Figure 2.12.

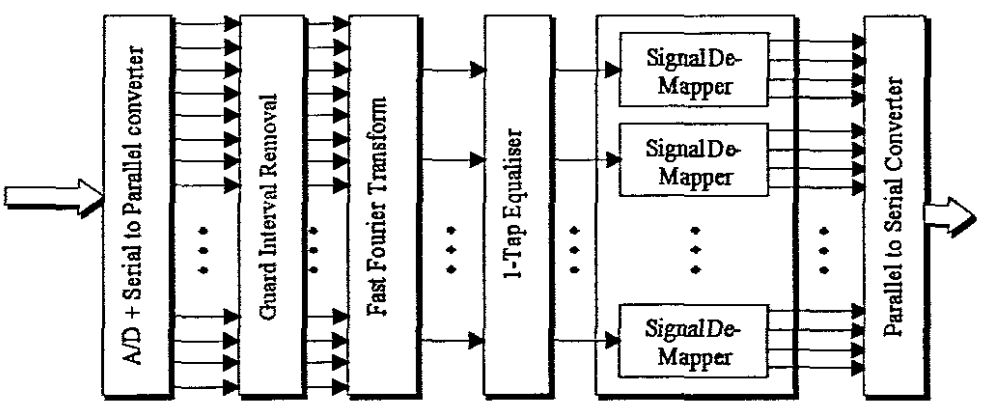

Figure 2.12: Block Diagram of a Conventional OFDM Receiver

The principle operation of a conventional OFDM receiver is a relatively simple concept. The received data (which is in the continuous time domain form) is sampled and converted back to the discrete samples through the use of a Digital to Analog Converter (D/A). A serial data stream is then formed requiring Serial to Parallel conversion so that individual frames can be formed from the buffered samples.

Assuming perfect synchronisation between the transmitter and the receiver, the correctly aligned samples would enable perfect reconstruction of the OFDM frame. In practical systems however, synchronisation has to be performed to estimate the alignment of samples of the OFDM Frame.

Before the Frame is processed by the FFT module, the appended guard interval, or cyclic prefix, is removed. The FFT then extracts the transmitted Frequency Domain information from the OFDM frame. Utilising a relatively simple 1-tap equaliser, channel distortion is compensated for at the equalisation stage. 1-tap equalisation is the process of estimating the channel transfer function H, then compensating for distortion by multiplying discrete sub-carriers by an inverse H, (H_N^{-1} - fourier co-efficient). This is depicted in Figure 2.13.

One of the final stages in this process is the Symbol De-mapper, which estimates the transmitted symbol from a set of known symbols and outputs the respective bit pattern e.g. 16QAM - 4 Bit pattern, QPSK - 2 Bit pattern, etc. The estimated data-stream from the symbol de-mapper is then checked for errors through the use of a channel decoder.

2.6.1 Importance of synchronisation

One of the critical factors for ensuring reliable data transmission, is the maintaining synchronisation between the transmitter and receiver's samplers. This is required to ensure that there are no differences in the transmitter and receiver sampling times. A method utilised for maintaining synchronisation, utilises the pilot symbols at an initial training sequence to align the receiver's

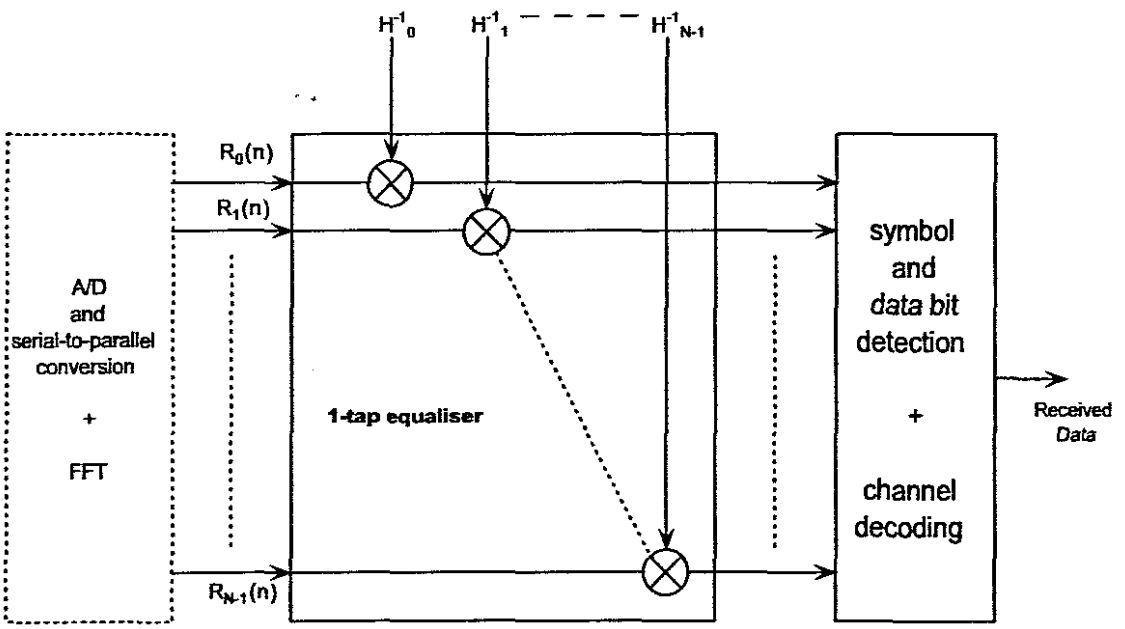

Figure 2.13: Principle operation of a 1-tap equaliser for OFDM - Dostert (2001)

sampling clock. As previously discussed, the cyclic prefix can be used to determine the start of an OFDM frame.

2.6.2 Channel Estimation

The channel estimator performs an important role in trying to determine the effects of channel distortion on individual sub-carriers. Using the estimated transfer function, the equaliser can process the received symbols to minimise channel distortions. With reference to Figure 2.13, equalisation is performed by multiplying individual, discrete sub-carriers $R_0 - R_{N-1}$ with the corresponding fourier coefficient $H_0^{-1} - H_{N-1}^{-1}$ (inverse channel transfer function). As previously discussed, the channel transfer function ($H_0 - H_{N-1}$) is determined during the channel training sequence at the start of transmission.

The necessity of channel estimation and equalisation depends also on the sub-carrier modulation. If a differential modulation scheme is used for sub-carrier modulation, then channel estimation is not required since the encoded information is based on the difference between two consecutive symbols (Edfors et al. 1996). For coherent modulation schemes however, the receiver requires knowledge of the phase and amplitude of the transmitted information in order to decode the symbols.

2.6.3 Description of stages in a typical OFDM Receiver

An analysis of the fundamental stages within the OFDM receiver (depicted in Figure 2.12) is required for a full understanding of the system.

2.6.3.1 A/D and Serial-to-Parallel Converter

The received information is sampled through the use of an analog-to-digital converter. The samples form a binary data stream, which is buffered and later outputted to form the input binary

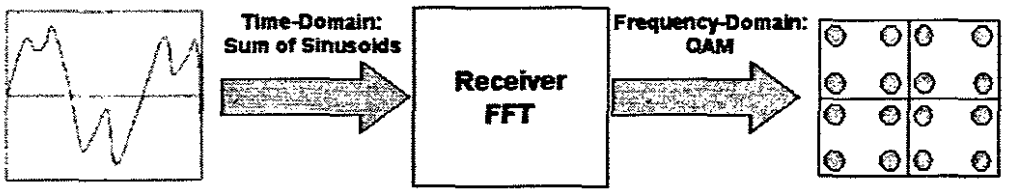

Figure 2.14: OFDM FFT Conversion Process

block for the FFT. Synchronisation is performed before this stage in order to perform the clock and carrier synchronisation tasks.

2.6.3.2 FFT Demodulator (Reconstruction of symbols)

The FFT is a well known technique for extracting frequency domain information from a time domain signal. In the OFDM Receiver, however, the FFT is used to reconstruct the transmitted frequency spectrum contained within the received OFDM signal (Figure 2.14). From the estimated N sub-carriers, the respective complex symbols are extracted.

2.6.3.3 Equalisation

The Equalisation stage uses the estimated channel transfer function, obtained through the channel estimation, to eliminate or minimise the influence of the channel on individual sub-carriers. This stage must be performed before the symbol and bit detection stages to minimise detection errors (Dostert 2001).

Equalisation in OFDM is relatively simple in comparison with single-carrier broadband equalisation techniques (Dostert 2001). This is due to the narrow-band nature of the N sub-carriers where attenuation and group delay are relatively constant for individual sub-carriers (Dostert 2001). Each sub-carrier's (sub-channel's) estimated transfer function H_i can be described by the following equation (Dostert 2001):

$$H_i = \alpha_i e^{j\varphi i} \tag{2.9}$$

where α_i represents the amount attenuation factor and φi represents the phase distortion.

Once again the operation of the equaliser can be displayed graphically (Figure 2.13) where it is shown that the inverse channel estimate H_i^{-1} is used to perform 1-tap equalisation.

2.6.3.4 De-mapping / Symbol Decoding

The symbol decoding stage decodes the complex symbols that have been estimated and equalised. This stage estimates what the transmitted symbol is, given certain boundary and constellation conditions. This process is termed "slicing", in which symbols are estimated based on their position in the symbol constellation. All symbols can be correctly decoded if the received symbol falls within the appropriate symbol's boundaries. With higher order constellation techniques, the boundaries become smaller, which leads to a greater probability of errors occurring.

In the case where differential symbol encoding is used, it is simply a matter of using the previous symbol as the reference for extracting the symbol information. The symbol decoder will thus output the corresponding bit patterns of the decoded symbols, forming the estimated data stream.

2.6.3.5 Channel Decoding

The final stage in the receiver is the channel decoder. Depending on the error correction techniques used, the channel decoder can detect and even correct errors in the recovered bit stream.

This is accomplished either through the use of Forward Error Correction (used in Coded-OFDM) or TCM (Trellis-coded modulation).

2.7 Conclusion

This chapter has described a conventional OFDM Transmitter and Receiver. This forms the theoretical foundation from which the OFDM-PLC simulation was constructed. Consequently, the next chapters will focus on the development of a full OFDM-power line modem simulation, using part of the theory described in this chapter. Naturally, the implementation and theoretical aspects of OFDM will differ slightly, but the fundamental concepts will remain the same.

In beginning the discussion around the simulation development, the next chapter will discuss the measurement and construction of an experimental domestic power network. The research undertaken in this chapter will form the basis for a domestic power network model for use in the OFDM power line modem simulation.

Chapter 3

Domestic power network modeling

A number of approaches can be employed for modeling a domestic power line network. Commonly, these techniques aim to characterise the physical influences of the power cable itself, quantified in terms of a *transfer function*.

The transfer function describes the electrical input/output relationship of the domestic power network, allowing the selection of a communication strategy to mitigate the influence of this medium on the transmitted signal. Methods of determining the transfer function for South African domestic power lines are investigated.

The aim of this portion of the project is to have a general domestic power network model which includes the prominent sources of degradation on this particular communication medium.

Quoting E. Biglieri (2003), "Optimisation of a transmission scheme can only be done after an accurate channel model is made available.", this statement highlights a primary aim of most of the current power line communication research activities today. This problem, of course, is related to the non-availability of an adequate, standardised channel model.

The problem with modeling this particular channel is that it presents a number of characteristics (Figure 3.1), which impede accurate modeling, such as (Biglieri 2003):

– Frequency-varying and time-varying attenuation,

- Substantial non-white background noise,
- Various forms of impulsive noise,
- Topology and location dependence.

In related research (Dostert 2001), (Biglieri 2003), (Anastasiadou & Antonakopoulos 2002) it has been found that load impedance variation on domestic power network can affect the characteristics of the overall transfer function. Thus making the task of modeling even more challenging.

There are, however, unique approaches proposed (Anastasiadou & Antonakopoulos 2002) to overcome these challenges and which have inspired the methodology presented in this paper.

3.1 Chapter Description

The transfer function approximation of an experimental network will be the focus of this chapter. The discussion will include:

- A brief overview of the existing power line channel modeling methods in literature.
- Review of the proposal methodology behind the approximation method, including a mathematical analysis.
- The practical setup and implementation of the approximation method.
- A discussion on post-processing of measured S-parameters to determine the transfer function, utilising MATLAB (Matrix Laboratory).

Finally, an analysis of the results from the approximation method will be given.

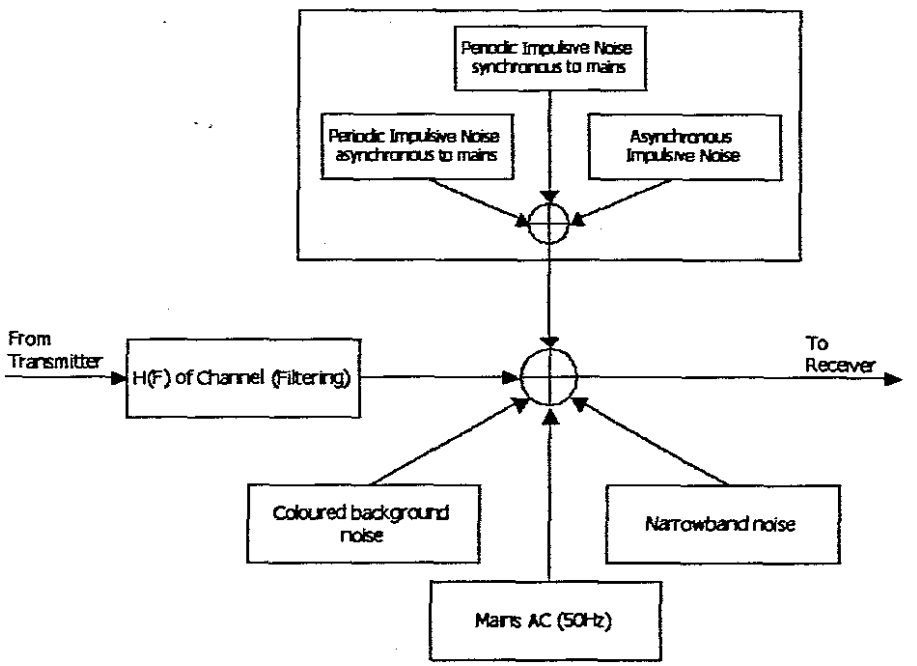

Figure 3.1: Summative characteristics which impede signal transmission

3.2 Literature review on relevant channel models

A literature survey has revealed a few methods for modeling an indoor power line environment. Most of the current models are focused around outdoor power line networks. Bigeliri (2003), discusses methods advocated by certain researchers in the indoor power line environment. A few prevalent methods will be discussed briefly.

The indoor power line network environment can be, and often is, regarded as a multi-path environment with frequency selective fading (Biglieri 2003). A widely known model that uses the principle of multipath fading is the Philips, Zimmerman and Dostert model, or "echo model". The model is given by Equation 3.1.

$$H(f) = \sum_{i=1}^{N} g_i e^{-(a_0 + a_1 f^k) d_i} e^{-j2\pi f \tau_i} \tag{3.1}$$

where N is the number of relevant propagation paths.

a_0 and a_1 are link attenuation parameters

k is an exponent

g_i is the weighting factor for path i,

d_i is the length of path i

τ_i is the electrical delay of path i.

Equation 3.1 is a result of a top-down approach on parametric form (Biglieri 2003). The parameters of the model have to be determined by measurement. The echo model is ideally suited for computer simulations (Biglieri 2003).

Other indoor PLC models utilise transmission line theory to obtain an approximate model of a given indoor PLC network. Banwell and Galli (Banwell & Galli 2001) propose a model which considers the power line channel as a uniform transmission line. Therefore the power line channel can be described as a number of cascaded two-port networks (Banwell & Galli 2001). A similar

channel model is proposed by F. Canete et al for the broadband modeling of indoor power line channels (Cañete, et al. 2002). Their model includes a noise generation component to produce a more realistic model of conditions on the power line network.

Another channel model, which provided the foundation for the work completed in this chapter, is the current research of Anastasiadou and Antonakopoulos (2002). Their proposed model is based on transmission line theory as well, but specifically by a defined experimental power network. The model uses the primary parameters (Pozar 1998) of the power cable. These parameters are utilised to convert specific line sections into 2 port networks that are described by there equivalent ABCD matrices.

$$\begin{bmatrix} A & B \\ C & D \end{bmatrix} = \begin{bmatrix} cosh(\gamma \cdot L) & sinh(\gamma \cdot L) \\ sinh(\gamma \cdot L) & cosh(\gamma \cdot L) \end{bmatrix} \tag{3.2}$$

where γ is the line propagation factor, L is the length and Z_0 is the characteristic impedance of the transmission line.

3.3 Proposed Transfer Function approximation Methodology

The methodology presented here to characterise an experimental network is inspired by D. Anastasiadou and T. Antonakopoulos. As advocated by these researchers, it is advantageous to conduct measurements on an isolated well-defined (in terms of material, topology, dimensions, loading) and controlled domestic power line network. With the physical dimensions known, a channel response of a controlled network topology can be determined (Anastasiadou & Antonakopoulos 2002).

The proposed method for the approximation of the complex transfer function (i.e. magnitude and phase) for an experimental power network includes:

- Measuring the scattering (S-) parameters of consecutive paths in the power network, with and without specific appliances connected.
- Compensation processing to eliminate the effect of coupling circuits on the derived transfer function.
- Post-processing of measured results for the conversion of measured S-parameters to transmission matrix (ABCD) parameters, in order to derive the approximate transfer function for a specific communication scenario.

It is important to note that this proposed modeling process yields a *complex transfer function* as opposed to a *scalar based transfer function*, which would only indicate the attenuation (magnitude of H). The complex transfer function will result in a more realistic simulated performance both in terms of phase and magnitude. This is especially important in OFDM where phase noise can degrade system performance, more than in the single-carrier system case (Litwin & Puegel 2001). The two types of phase noise that could occur in OFDM systems is (Litwin & Puegel 2001):

- Phase noise within subcarriers,
- Phase noise that extends across subcarrier spacings.

It is therefore essential for simulation purposes, that the effect of phase noise be represented in a complex transfer function.

3.3.1 Theory of Scattering matrix parameters

Scattering parameters, or S-parameters as they are commonly termed, is a set of parameters used for relating travelling waves that are scattered or reflected, when an N-port network is inserted into a transmission line (HP S-parameter Application Note).

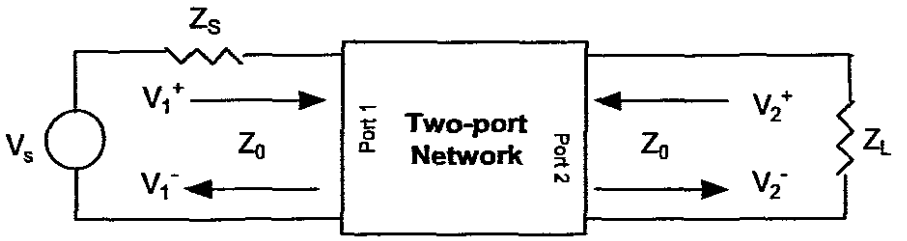

Figure 3.2: Two-port Network

where Z_0 - Characteristic impedance of the line (real-valued)

Z_S - Source impedance

Z_L - Load impedance

V_1^+ and V_2^+ - Represent the incident waves at ports 1 and 2 respectively

V_1^- and V_2^- - Represent the reflected waves at ports 1 and 2 respectively

The network can be described, in terms of its S-parameters as:

$$\begin{bmatrix} V_1^- \\ V_2^- \end{bmatrix} = \begin{bmatrix} S_{11} & S_{12} \\ S_{21} & S_{22} \end{bmatrix} \begin{bmatrix} V_1^+ \\ V_2^+ \end{bmatrix} \tag{3.3}$$

From Equation 3.3 it can readily be shown that the S-parameters of the network can be obtained as follows:

$$S_{11} = \frac{V_1^-}{V_1^+}\Big|_{V_2^+=0} \tag{3.4}$$

In a typical two port scenario (if and only if all ports are matched (Pozar 1998)) the following designations apply: (National-Instruments 2004)

S_{11}	Reflection coefficient of the input
S_{22}	Reflection coefficient of the output
S_{21}	Forward transmission gain
S_{12}	Reverse transmission gain

Table 3.1: Two-Port S-parameter definitions

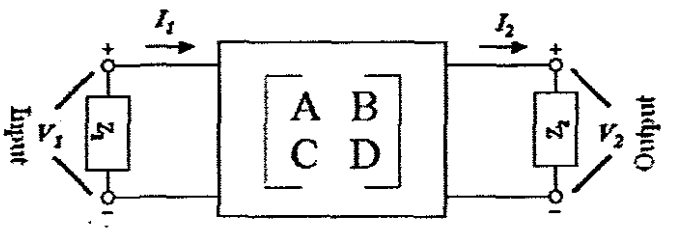

Figure 3.3: Two-port system described by ABCD-parameters

3.3.2 Complex transfer function approximation using S-Parameters

This section will present the methodology for determining a complex transfer function from a given set of S-parameters. Critical to this methodology is the use of ABCD-parameters. A mathematical analysis of this process will now be given.

The general 2-port system shown in Figure 3.3 is described in terms of its ABCD-parameters as:

$$\begin{bmatrix} V_1 \\ I_1 \end{bmatrix} = \begin{bmatrix} cos(\gamma \cdot L) & sinh(\gamma \cdot L) \\ sinh(\gamma \cdot L) & cosh(\gamma \cdot L) \end{bmatrix} \begin{bmatrix} V_2 \\ I_2 \end{bmatrix} \tag{3.5}$$

Using (3.5) and identifying $V_2 = I_2 Z_2$, the transfer function H can be expressed as:

$$H = \frac{V_2}{V_1} = \frac{Z_2}{AZ_2 + B} \tag{3.6}$$

In order to determine both the magnitude and phase of the transfer function, a vector network analyser is used. The measured S-parameters are converted to ABCD-parameters, from which the transfer function can readily be determined, as will be shown below.

From Equation 3.6 it is clear that only the A and B parameters are required to derive the transfer function. Therefore only two conversion equations are required for the conversion from S- to ABCD-parameters (Pozar 1998):

$$A = \frac{(1+S_{11})(1-S_{22})+S_{12}S_{21}}{2S_{21}} \tag{3.7}$$

$$B = Z_L\left[\frac{(1+S_{11})(1+S_{22})-S_{12}S_{21}}{2S_{21}}\right] \tag{3.8}$$

3.3.3 Compensation for Coupling effects

As will be discussed later in Section 3.4, the use of coupling circuits is required to isolate and protect the instrumentation from the AC voltage. This, however, affects the overall Transfer function ($H_{overall}$), since the couplers (H_{C2}, H_{C1}) will introduce their own specific characteristic into the overall measurement. From 2-port Network theory (Pozar 1998), it can be found that the derived transmission matrix T_T can be represented as a series of cascaded Transmission matrices (T), as shown in Figure 3.4.

The ABCD-parameters of the channel alone may be derived by simple matrix manipulation:

$$T_T = T_{C1} \cdot T_{CH} \cdot T_{C2} \tag{3.9}$$

where T_{C1} and T_{C2} represent the coupling circuits transmission matrices. And therefore the Channel's transmission matrix (T_{CH}) can be represented as follows:

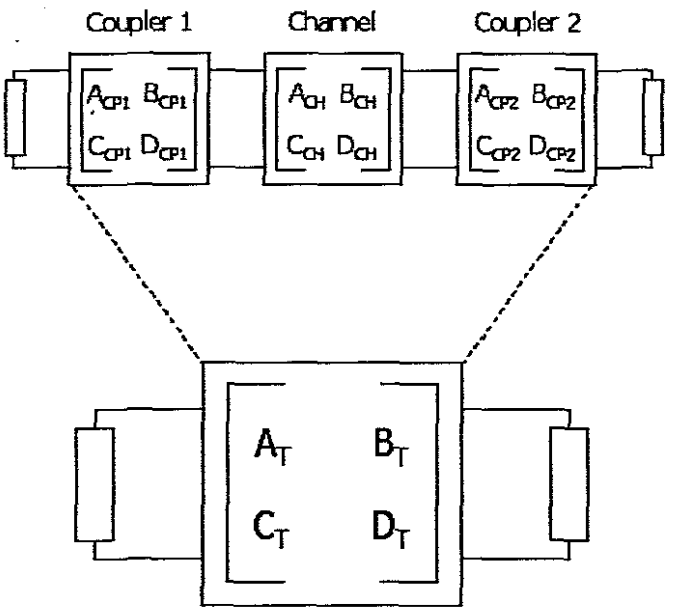

Figure 3.4: System described as a series of ABCD matrices

$$T_{CH} = T_{C1}^{-1} \cdot T_T \cdot T_{C2}^{-1} \tag{3.10}$$

Once T_{CH} is derived, it can then be converted to the approximate transfer function $H_{overall}$ of the power line, without the effects of the coupling circuits, using Equation 3.6.

3.4 Practical Setup and implementation

This section will review how the proposed methodology was implemented practically. As will be discussed further in this section, this has entails constructing an experimental power network as well as the design and construction of coupling circuits for instrumentation protection. Instrumentation employed for this particular procedure consisted of:

- HP Vector Network Analyser (Model 4396B)
- HP S-Parameter Test Kit (Model 85046A)

The VNA (Vector Network Analyser) was calibrated using a 3.5mm Economy Calibration kit using the SOLT (Short, Open, Load, Thru) method (discussed further in Section 3.4.2).

All measurements were conducted in the band 4.49MHz to 25MHz. The decision to simulate in this band is based on the specifications of Homeplug 1.0 (Lee, et al. 2003), which provides a reference specification for the simulations. It is therefore essential to measure the effects of the experimental network in this particular band.

As will be discussed later in Chapter 4, similarly to the Homeplug 1.0 standard, the simulation will also utilise 84 to 100 carriers to analyse the performance of an OFDM-based PLC modem.

3.4.1 Coupling circuit design and construction

To protect the instrumentation from the hazardous AC supply voltage, coupling circuits were constructed and tested in the band of interest. As stated previously, the specification of the project

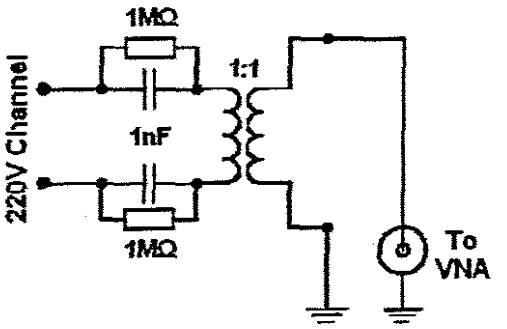

Figure 3.5: Circuit Diagram of the Coupler circuit utilised in measurments

required measurements to be conducted within the range of 4.49MHz to 25MHz.

The practical coupling circuits therefore needed to be tested for minimal degradation in the band of interest. The coupler circuit consists of a ferrite-core transformer, which provides galvanic isolation from the mains supply as shown in Figure 3.5:

The two frequency responses for the respective couplers are shown in Figure 3.6, depicting an acceptable, relatively flat response.

It should be noted that, because the couplers will be compensated for through mathematical manipulation, they need not be optimal.

3.4.2 VNA (Vector Network Analyser) Calibration

Systematic and random errors are inherent in VNA measurements. It is therefore essential, in order to minimise these errors, to perform calibration on the VNA.

VNA Calibration also attempts to compensate for:

– Imperfect impedances at VNA test ports

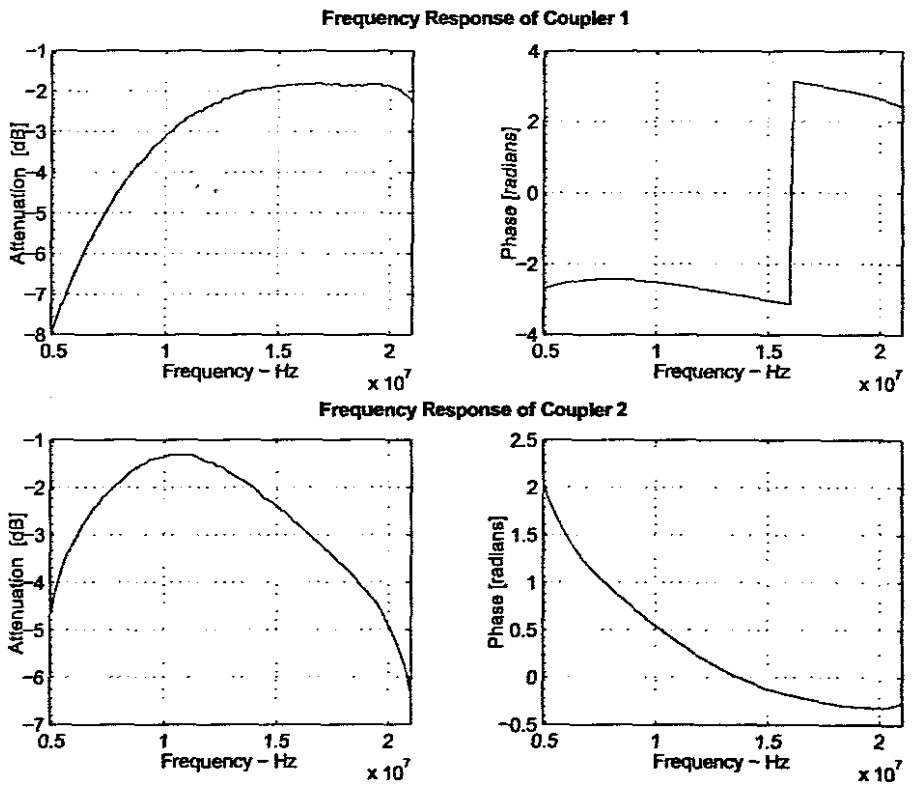

Figure 3.6: Magnitude and Phase response of Coupler circuits

- Loss, phase shift and reflections caused by connectors and cables connecting the VNA and the DUT (device under test).
- Internal leakage between test ports of the VNA.

When performing a VNA calibration, the following assumptions are made:

- The VNA is perfect (assumed to be calibrated and error free).
- All systematic errors are lumped into one error adapter network.

Calibration was performed using the SOLT (Short, Open, Load and Thru) method. The SOLT standards used were from the HP 3.5mm Economy Calibration kit. For the purposes of the project, a complete two-port calibration was performed. This entailed connecting each of the standards (Short, Open, Load and Thru) to the respective ports to allow the VNA to compensate for specific types of errors.

The calibration procedure utilised for the measurement of the experimental networks is depicted in the figure below. it therefore can be seen that the VNA is not calibrated to include the effects of the coupler circuits.

3.4.3 Construction of an experimental power network

An experimental network was constructed for the purposes of transfer function approximation. It is based on the same topology found in (Anastasiadou & Antonakopoulos 2002) and depicted in Figure 3.8. The motivation for utilising an experimental network was to ensure that measurements were conducted on a well-defined network, eliminating or minimising external factors that could affect the results.

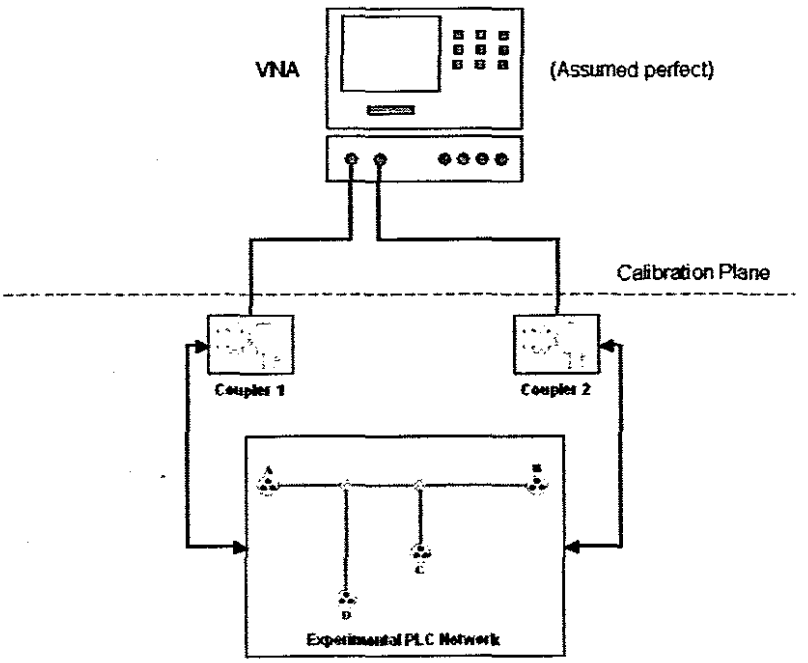

Figure 3.7: Calibration of VNA

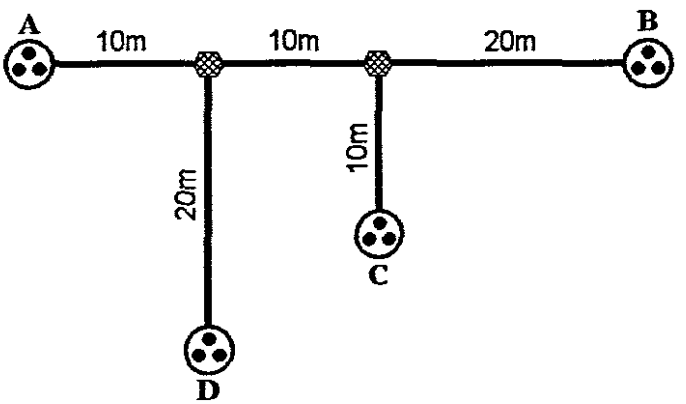

Figure 3.8: Experimental Network Setup

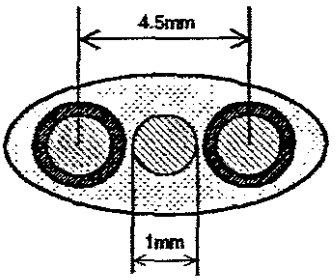

Figure 3.9: Cross-section of Flex-three-core wiring

The experimental network (as in the case (Anastasiadou & Antonakopoulos 2002)) was constructed using common South African, three-core flex, household wiring (cross-section depicted in Figure 3.9).

3.4.4 Load impedances

To produce a relatively good estimate of the domestic power network environment, appliance loads were added when conducting S-parameter measurements. The resultant disturbance of both the power network and load impedance (appliance) would therefore be measured.

For this particular set of measurements, the following appliances were used (Figure 3.10):

- Handheld Drill
- Handheld Dryer
- Handheld Mixer
- Light Dimmer
- Television
- Personal Computer
- Vacuum Cleaner

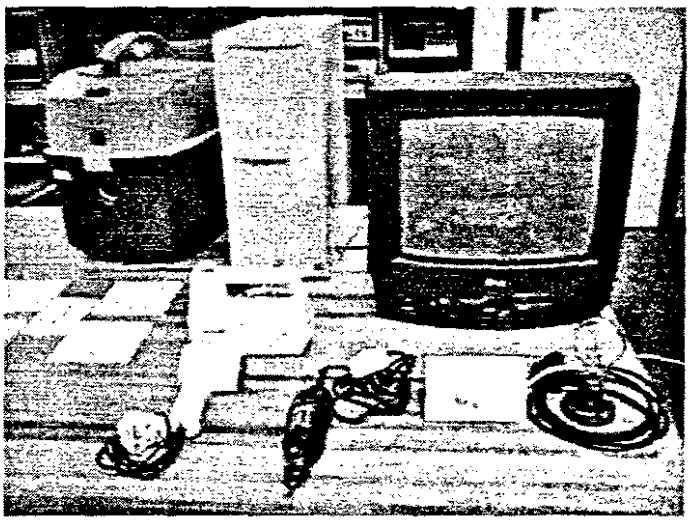

Figure 3.10: Appliances utilised in measurements

As will be discussed later, the total effect of the varying impedance of the appliances are included in the overall frequency response measurement.

3.4.5 Measurement procedure for transfer function approximation

The measurement procedure can be summarised as follows:

- Retrieving the calibrated configuration of the VNA.
- Connecting the S-Parameter test kit to the measured path (e.g. Path AB) via couplers.
- The addition of the appliance at one of the open entry points of the experimental network, e.g. C or D for Path AB.
- Powering the experimental network to power the appliance for measurement. Measuring individual S-Parameter ($S_{11}, S_{12}, S_{21}, S_{22}$).
- Storage of the measured S-parameters for post-processing in MATLAB.

The above procedure was conducted for every possible path on the unloaded experimental network, as well as for the addition of every appliance at all entry points. This resulted in a total of

84 measurements being required. Figure 3.11 shows the checklist used during the measurements.

Additionally, S-parameter characterisation of the individual coupler circuits were also needed. These measurements are required for coupling effect compensation.

3.5 Post-processing

The post-processing applies the methodology described in Section 3.3. The post-processing is performed utilising a computer-aided mathematical analysis program, namely MATLAB (Matrix Laboratory).

Firstly, the stored measurements (all 84) are categorically stored so that each path has a defined set of measured scenarios. Measurements are saved to spreadsheet files to allow easy importation into the MATLAB environment. The spreadsheet file will contain both phase and magnitude information of the individual, measured S-parameters.

3.5.1 Post-processing Procedure

Once the spreadsheet file has been successfully imported into MATLAB, a MATLAB script will:

- Convert the S-parameters of the overall channel (including couplers) to the required A and B parameters (Equations 3.7 and 3.8).
- Convert the S-parameters of the individual couplers to their respective A and B parameters.
- Approximate the overall transfer utilising Equation 3.6.
- Using the stored ABCD-parameters of the coupler, the desired transfer function of the channel alone is determined using Equation 3.6 and 3.2.

3.5.2 MATLAB Script Design

In this specific application, the conversions from S- to Transmission Matrix parameters and Transmission Matrix to Transfer function, are the two essential operations to be calculated using MATLAB.

Therefore two scripts were designed and implemented based on flowcharts shown in Figures 13 and 14. The script *s2t.m* converts a given set of S-parameters to the equivalent (ABCD) parameters.

The script *tmath.m* obtains the overall response (by removing the effects of the coupling circuits) and converting the result (in ABCD parameter format) to an equivalent transfer function. The respective script codes are listed in Appendix C.

	Path CD	Path BD	Path BC	Path AD	Path AC	Path AB		
S11							Drill	Noise sources connected without Power
S12								
S21								
S22								
S11							Dryer	
S12								
S21								
S22								
S11							Mixer	
S12								
S21								
S22								
S11							Dimmer	
S12								
S21								
S22								
S11							TV	
S12								
S21								
S22								
S11							PC	
S12								
S21								
S22								
S11							Vacuum	
S12								
S21								
S22								
S11							Drill	Noise sources connected with Power
S12								
S21								
S22								
S11							Dryer	
S12								
S21								
S22								
S11							Mixer	
S12								
S21								
S22								
S11							Dimmer	
S12								
S21								
S22								
S11							TV	
S12								
S21								
S22								
S11							PC	
S12								
S21								
S22								
S11							Vacuum	
S12								
S21								
S22								

Figure 3.11: Checklist for measurements

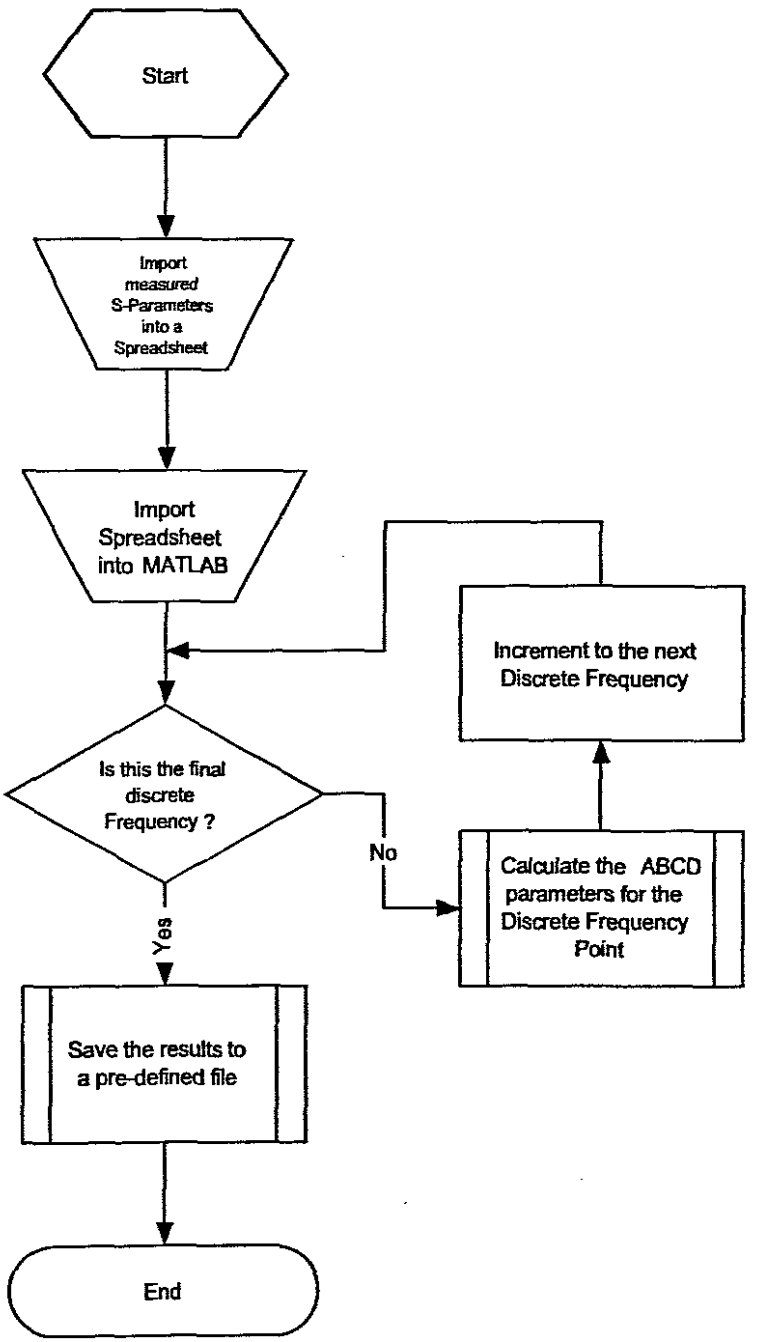

Figure 3.12: Flowchart design for *s2t.m* script (See Appendix C for listing)

3.6 Analysis of Results

The measured transfer functions for Path AC are shown in Figure 3.14 and 3.15. The appliances are connected at point B and D respectively. A graphical analysis reveals that there were no significant differences when appliances were powered or not powered. The transmission nulls are clearly defined as a result of multipath reflections which cause partial signal cancellation. Similarities with the results found in (Dostert 2001), (Cañete et al. 2002), (Anastasiadou & Antonakopoulos 2002), et al, are present.

Further analysis of these and other measurements have also revealed that there is a general increase in attenuation with frequency which confirms with other studies the low-pass filtering effect of a power network. A decrease of multipath reflections is observed and can be attributed to the fact that the connection of appliance, absorbs a fraction of the power incident.

It can therefore be concluded that the results found are similar to those obtained by current researchers in in-door power line measurement (Dostert 2001), (Cañete et al. 2002), (Anastasiadou & Antonakopoulos 2002).

3.7 Conclusion

The methodology presented in this chapter, has resulted in the availability of a domestic power network model. This model will form part of the core simulation model to determine the overall characteristics.

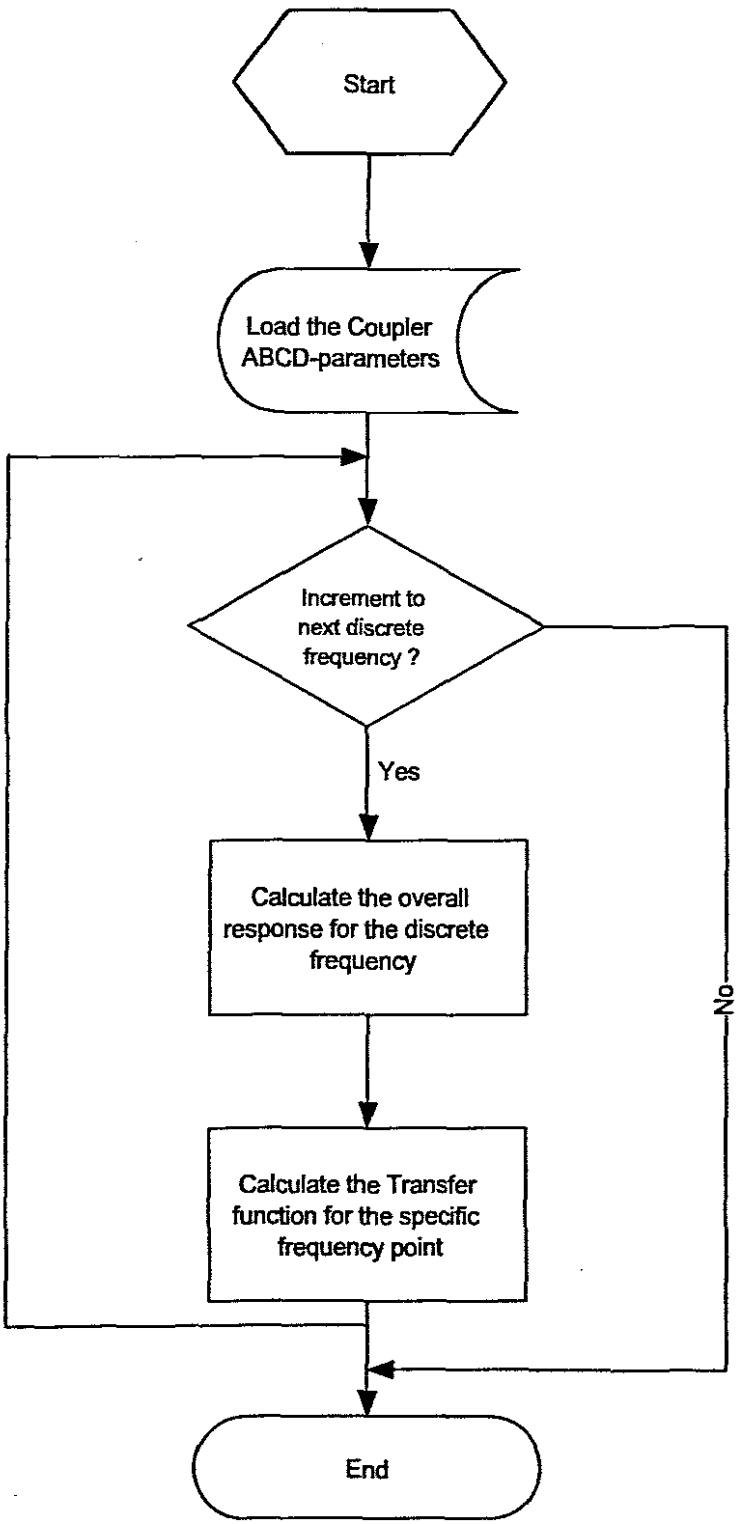

Figure 3.13: Flowchart for *tmath.m* for script (See Appendix B for listing)

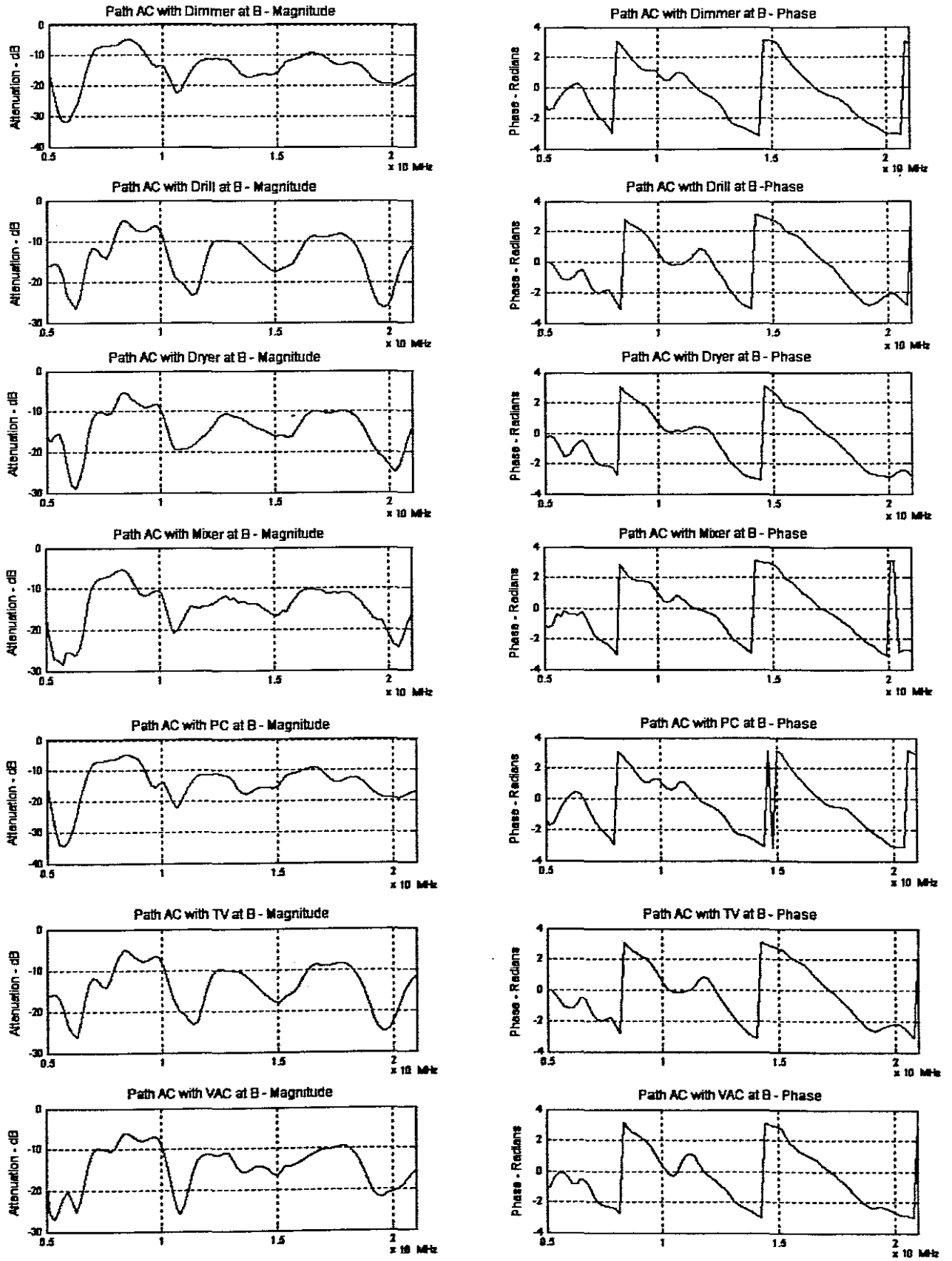

Figure 3.14: Measurement results for Path AC

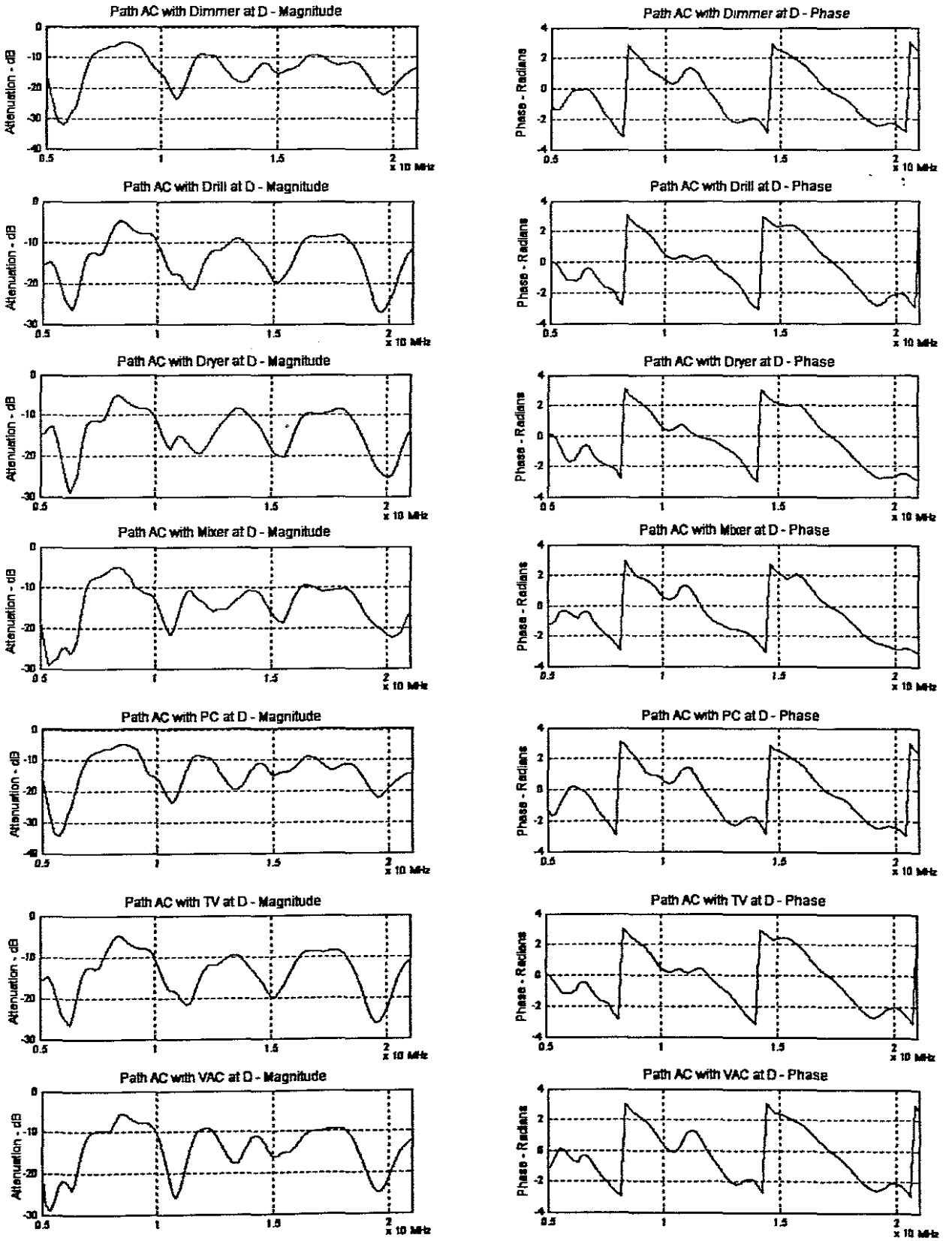

Figure 3.15: Measurement results for Path AC (continued)

Chapter 4

OFDM Communication System Simulation in MATLAB

Simulation can be described as the prediction of probable system behavior, and thus in the case of telecommunications, the estimated performance. A simulation provides the engineer with a likely estimate of how the system would function in a given scenario. Measuring system performance is achieved using specific methods such as BER (bit error rate), as in the case of Digital communications.

For the purposes of this project, the use of simulation is imperative in achieving the overall project objective. The performance estimation, through simulation, aids the author in the analysis of the various encoding schemes. The model presented in this chapter is a customisation of an OFDM Simulation model from (Harada & Prasad 2002). As will be discussed in this chapter, the model has been adapted to suit project requirements.

The simulation environment used in this case is MATLAB, which is an industry, and academic standard for the application of numerical processing, especially using matrix-based methodologies to solve/simulate large problems.

4.1 Chapter Description

This chapter will cover the construction of an OFDM-based communication system in MATLAB, including the integration of the proposed channel model (discussed in Chapter 3). The

system is based on that of Prasad and Harada (Harada & Prasad 2002).

The layout of the chapter will be the following:

- Overview of the simulated OFDM architecture
- OFDM Transmitter simulation
- OFDM Receiver simulation
- PLC Channel simulation
- Integration of simulation blocks
- Verification of model using AWGN Noise

This chapter will contain extracts of MATLAB script code to provide the reader with an understanding of how concepts were implemented in the simulation environment. All MATLAB scripts produced for the project are listed in the Appendices.

4.2 OFDM Simulation Concepts

4.2.1 Overall Description

The envisaged simulation model is the combination of both an OFDM communication system and a domestic power line channel. The overall model is graphically illustrated in Figure 4.1, where the three fundamental simulation stages are shown, namely the OFDM Transmitter, Domestic Power and OFDM Receiver.

The principle requirement for this simulation is the ability to vary parameters i.e. encoding / modulation techniques for various sub-carriers, with selected communication scenarios. This provided the author with an analysis tool for determining and comparing the performance of different simulated approaches in achieving efficient high speed power line communication.

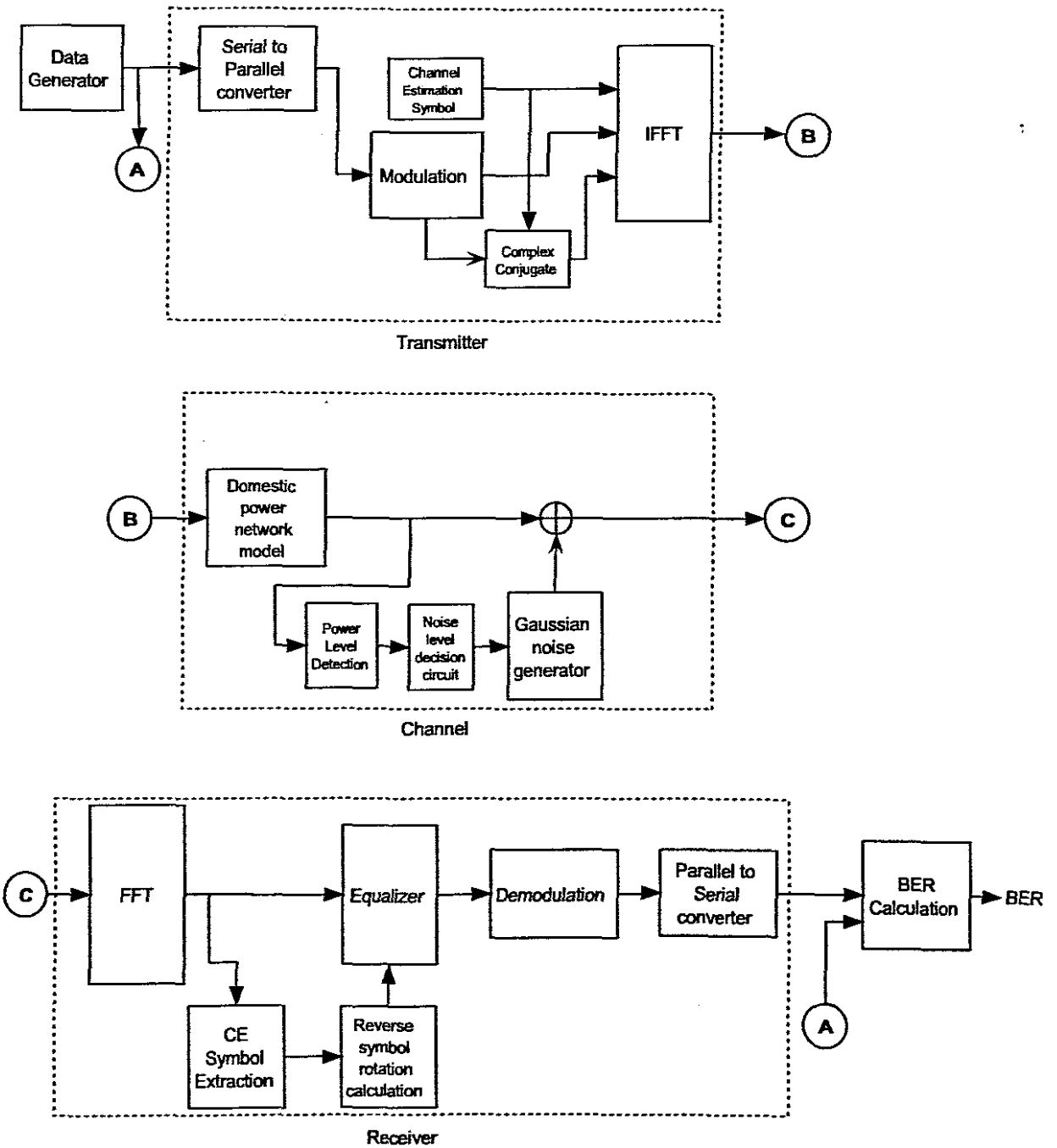

Figure 4.1: Overall Simulation Diagram

As mentioned in Chapter 1, due to time and specification constraints, omitted components of the simulation were:

- Channel coding techniques
- Synchronisation techniques

4.3 OFDM Transmitter Simulation

The construction of an OFDM transmitter in MATLAB requires the implementation (in MATLAB) of mathematical functions associated with the OFDM transmission process.

In this section of the simulation, randomly generated data (at *Point A*) is packaged into OFDM packets, which will then be transmitted through a simulated channel scenario (at *Point B*). The fundamental stages within this process are the modulation and IFFT (Inverse Fast Fourier Transform) stages. As mentioned before, the basis for this study is the focus on the performance effect of different modulation methods.

4.3.1 OFDM Transmitter Algorithm

The algorithm for an OFDM Transmitter is quite simple. The algorithm is the process of generating of a time-domain signal that represents the encoded information in the frequency domain. The stages for generating an OFDM signal will now be discussed.

4.3.1.1 Serial to Parallel Converter

The input binary stream, which is assumed to be in a serial form, has to be converted to a parallel form. This requirement serves the purpose of buffering the input serial stream as well as allows the S/P (Serial to Parallel) stage to output a specific amount of parallel bits. The amount of parallel bits required depends on the type of sub-carrier encoding to be used e.g. QPSK (2 bit

input), QAM (4 bit input), BPSK (1 bit input), etc.

4.3.1.2 Modulation / Encoding

Using the grouped input parallel bits from the S/P (Serial to Parallel) stage an equivalent Complex symbol is outputted from the Encoder. It should be noted, however, that the encoding can also be any other multi-level signaling encoding technique e.g. BPSK, QPSK, DQPSK, etc.

4.3.1.3 Discrete Frequency Mapping

This is an important stage in the OFDM signal generation process. In order to generate a real-valued time signal, OFDM carriers must be defined in complex conjugate pairs which would be symmetric about the Nyquist Frequency (Cosby 2001). The Nyquist frequency as well as the DC component would have no complex conjugate pair and therefore no Complex symbol will be assigned to these frequency bins. Zeros are also added to ensure that the length of the input to the IFFT is a power of 2 bits to ensure efficiency in the computation of the IFFT.

Figure 4.2 and 4.3 illustrate an example of how four Complex symbols are mapped for a 64 bin OFDM Frame. The first 32 bins contain the transmitted complex symbols, and the last 32 bins are the complex conjugate of the complex symbols. The result after an IFFT, will be a real-valued signal.

4.3.1.4 Channel Estimation - Pilot symbol generation

Channel estimation provides a method of estimating the amount of fluctuation, of the amplitude and phase due to channel distortion. A pilot-symbol based system is usually employed, for at specific time intervals, a pilot-symbol is transmitted (which is known to both the transmitter and receiver). The receiver can then estimate the amount of distortion incurred (both phase and

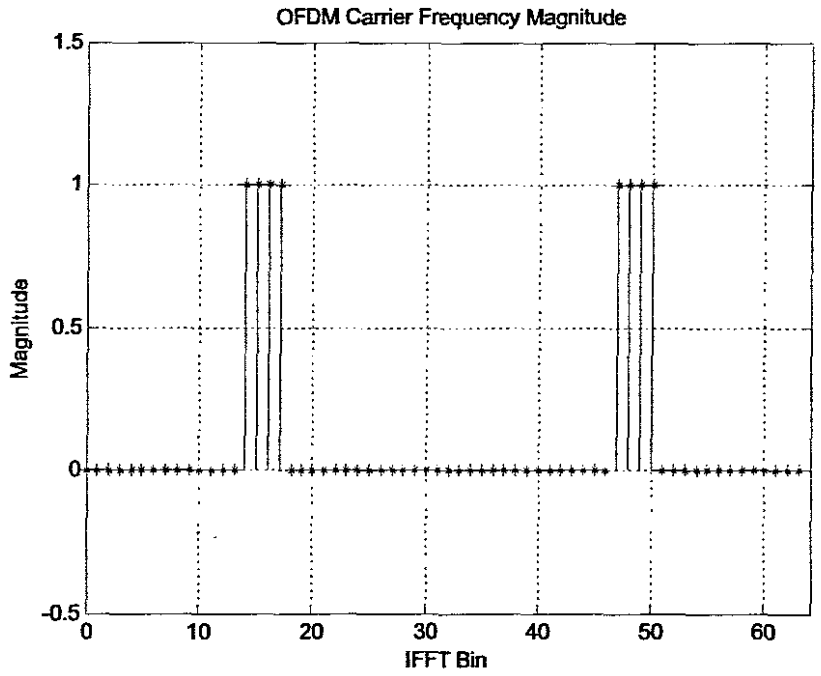

Figure 4.2: Discrete Frequency Mapping - Magnitude

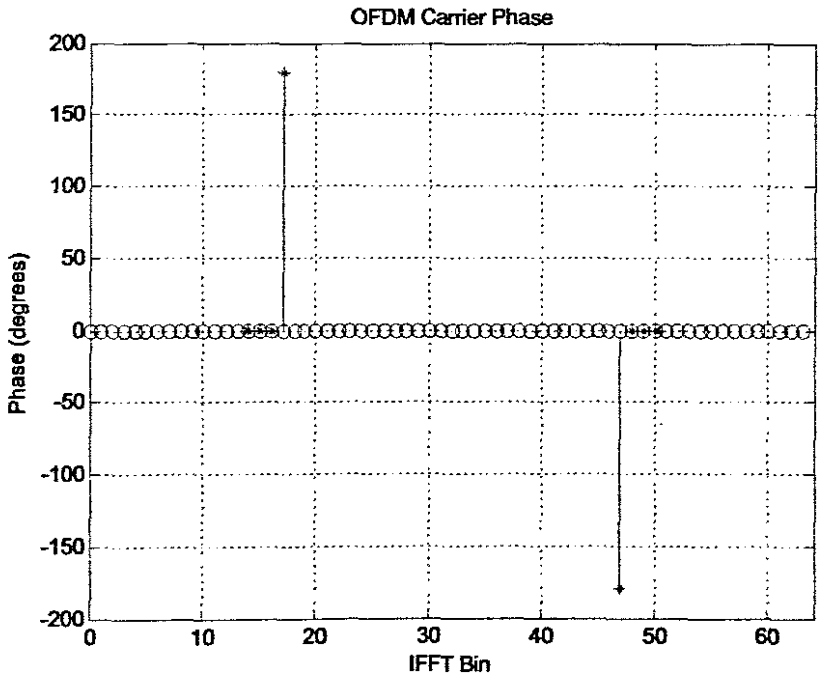

Figure 4.3: Discrete Frequency mapping - Phase

amplitude), thus making the symbol estimation more accurate.

4.3.2 MATLAB OFDM Transmitter Implementation

The MATLAB implementation of the OFDM Transmitter is based on the framework MATLAB scripts provided by Harada / Prasad (Harada & Prasad 2002). The transmission methodology utilised in Harada / Prasad (Harada & Prasad 2002) involves the use of all the discrete frequencies to transmit information, which results in a complex signal at the output of the OFDM transmitter.

It was therefore necessary to alter the scripts, in order to:

- Change the transmission methodology, as discussed in Section 4.3.1
- Adapt for different encoding / modulation methods, e.g. BPSK, QPSK, 8QAM, 16QAM, etc.

The specification used for the OFDM transmitter, is based on the HomePlug Standard (Lee et al. 2003). It specifies using a 256 IFFT, 84 data carriers and a guard interval length of 172. A typical spectrum is shown in Figure 4.4.

The algorithm for the OFDM transmitter is comparatively simple. Its core function is to form the OFDM symbols for transmission from a given, random serial data input. For the purposes of this simulation, pilot-symbols are transmitted at the beginning of transmission. Figure 4.5 displays the flowchart for the OFDM Transmitter algorithm.

4.4 Domestic Power network simulation

The objective of the domestic power network simulation, is the inclusion of the distortion effects (from the various measured scenarios), into the overall OFDM Simulation. Again, this

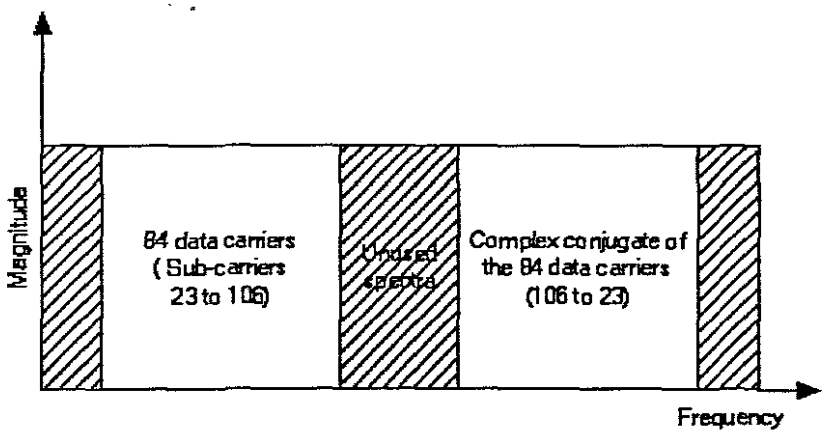

Figure 4.4: Spectrum usage for OFDM Transmission and Reception

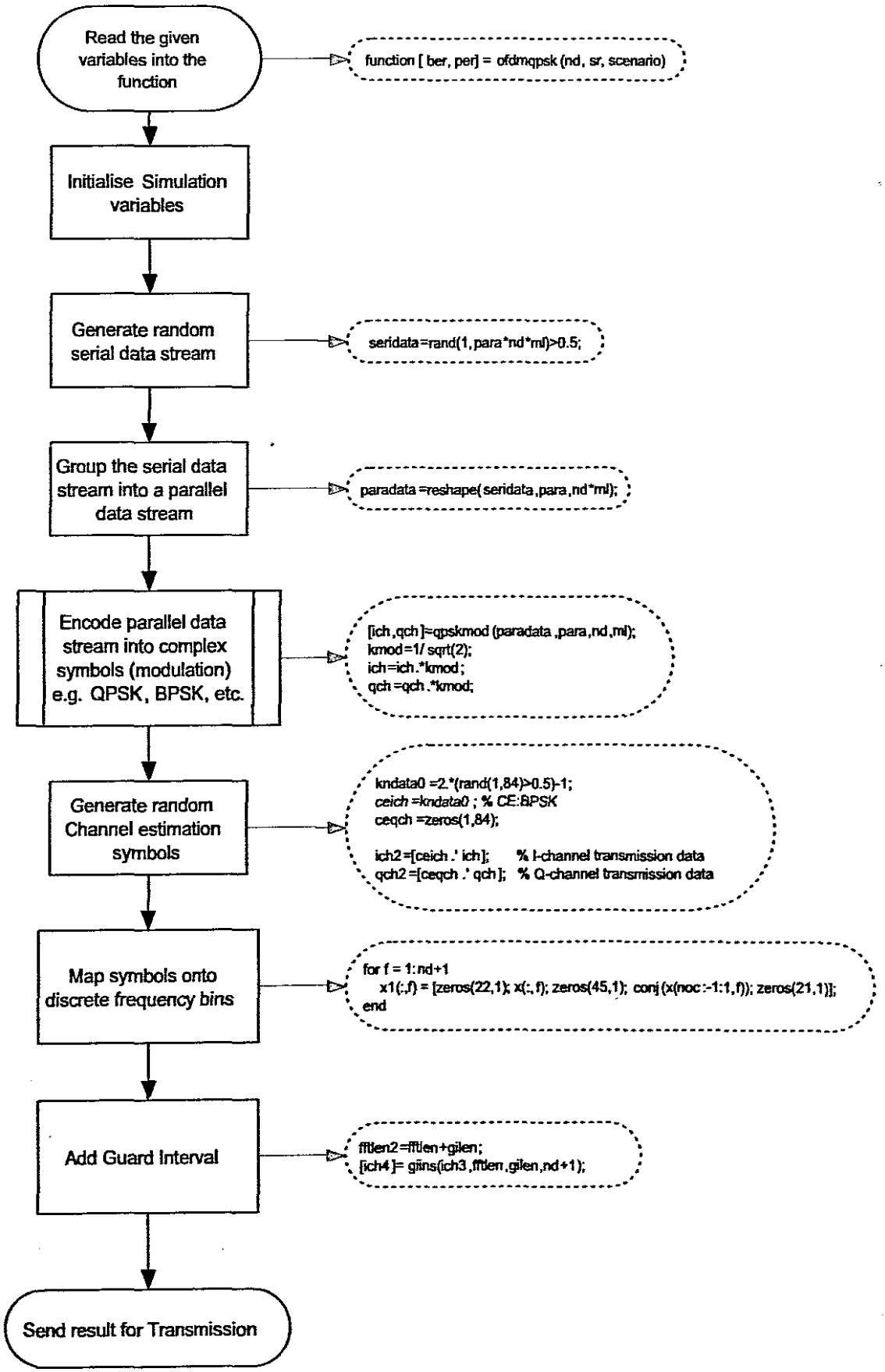

Figure 4.5: Flowchart for MATLAB OFDM Transmitter

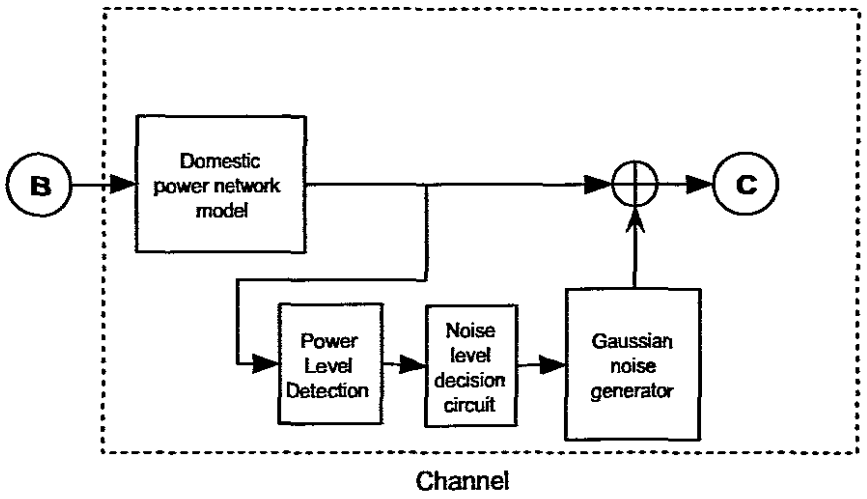

Figure 4.6: Block Diagram of Domestic power line model

*provides the required functionality to enable the performance analysis of various encoding / mod*ulation techniques.

This particular model utilises the results generated in Chapter 3, which are in the form of MAT Files (MATLAB Data files). The files provide the necessary distortion characteristics of a particular scenario. Combined with AWGN (Additive White Gaussian Noise), the model represents the estimated distortion effect of the transmitted signal, through the selected scenario. Figure 4.6 is a graphical representation of the processes followed when the output of the OFDM Transmitter (*Point B*) is sent through the channel model, resulting in the output at *Point C*.

4.4.1 Domestic Power network Algorithm and implementation

As mentioned previously, this particular domestic power network model is based on measurements made on the experimental power network, i.e. a particular path with a specific noise source connected at an open power point.

All 84 measurements of the possible scenarios are stored in individual MAT files. The files are stored in the MATLAB work directory, under the respective Path folder e.g. 'pathac' for Path AC. The filename is designated by the respective path, the point on the experimental network where the noise source is connected and the noise type e.g. pathacdtv.mat for Path AC, with TV noise source connected at D. This ensures that the correct file is loaded when the MATLAB function is called, as the scenario is one of the variables that have to be passed to the model function.

The MAT files contain the measured transfer functions for the respective scenarios, and hence all calculations have to be performed in the frequency domain. Therefore it is essential that the input OFDM time signal has to be converted to the frequency domain as well, so that it can be processed. Once in the frequency domain, the following equation is applied to determine the distorted signal for the simulated scenario:

$$S_{distorted} = \mathfrak{F}^{-1}\{\mathfrak{F}(S_{OFDM}) \cdot H_{scenario}\} \tag{4.1}$$

Where $S_{distorted}$ is the resultant signal, S_{OFDM} is the input OFDM signal and $H_{scenario}$ is the selected scenario for simulation.

The next step in this process is the addition of AWGN. This is required:

- since the measured distortion does not contain any noise information, other than that generated by the appliances.
- for plotting BER plots, the AWGN needs to be varied and included in the simulation.

The process of adding AWGN is based on (Harada & Prasad 2002). As can be seen in Figure 4.6, this process consists of the detection of signal power level, so that the appropriate attenuation level can be calculated. Once the proper attenuation level has been calculated for a given Eb/No, the Gaussian noise is then added to the distorted signal $S_{distorted}$. The following derivation shows how

the attenuation level (required for plotting purposes) is determined, with a given Eb/No (Harada & Prasad 2002):

$$E_b = \frac{spow}{br} \tag{4.2}$$

$$N_o = \frac{npow}{sr} \tag{4.3}$$

$$\therefore E_b/N_o = \frac{spow}{br} \cdot \frac{sr}{spow} \tag{4.4}$$

Since E_b/N_o is in decibels, *npow* can therefore be expressed as:

$$\therefore npow = \frac{spow}{br} \cdot \frac{sr}{E_b/N_o} \tag{4.5}$$

$$\therefore npow = \frac{spow}{br} \cdot \frac{sr}{10^{\frac{Eb/No}{10}}} \tag{4.6}$$

where E_b = Energy per bit

spow = Signal Power

N_0 = Noise power density

br = Bit Rate

sr = Symbol Rate

npow = Noise power

Since the simulated signal is expressed in voltage, the noise signal will be as well, and since Gaussian noise is normally distributed equally in in-phase and quadrature-phase channels, the attenuation factor (*attn*) can be expressed as (Harada & Prasad 2002):

$$attn = \sqrt{\frac{1}{2} \cdot npow} \tag{4.7}$$

The attenuation factor, *npow*, is calculated at the beginning of the process, using the input OFDM signal.

Figure 4.7 shows the flowchart for the entire process.

4.5 OFDM Receiver Simulation

The objective of the OFDM receiver, in short, is the estimation of transmitted symbols from received OFDM symbols. The received OFDM symbols are the distorted versions of the transmitted data.

As the final stages in the OFDM system, the performance of the OFDM system is directly linked to the OFDM receiver's ability to effectively estimate the transmitted data from received OFDM symbols. The measurement of efficiency / performance in this case (as with any digital communication system) is the BER (bit error rate).

4.5.1 OFDM Receiver Algorithm

The algorithm for the OFDM receiver comprises of the three major sub-algorithms, namely the:

- Fast Fourier Transform
- Equalization using Channel Estimation
- Demodulation / Symbol decoding

These processes will be discussed in the following sections. It should again be noted that *synchronization* and *channel coding* have been omitted for this particular implementation. Figure 4.8 represents the simulation block diagram for the OFDM receiver.

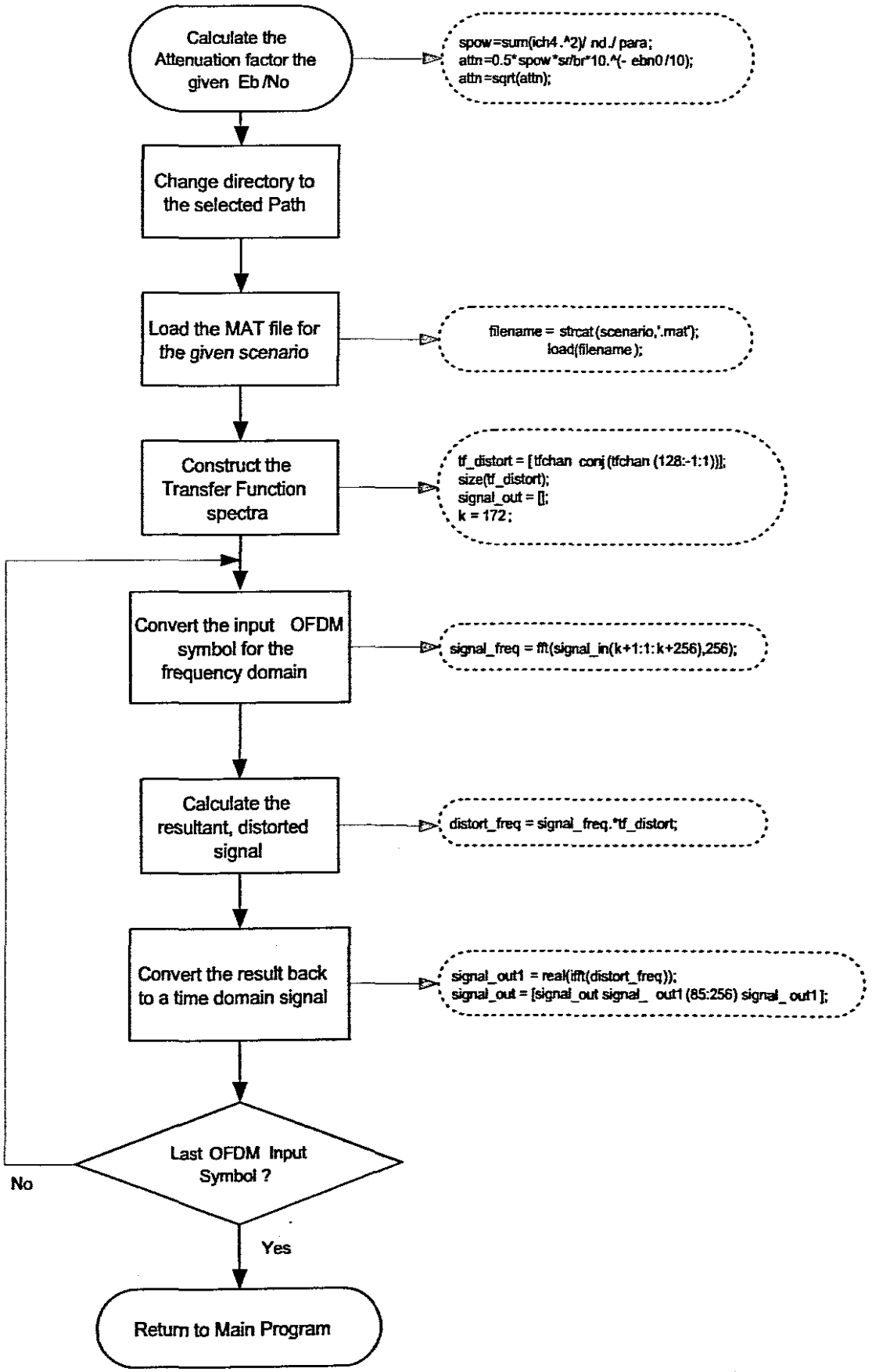

Figure 4.7: Flowchart for determination of E_b/N_o for a selected communciation scenario

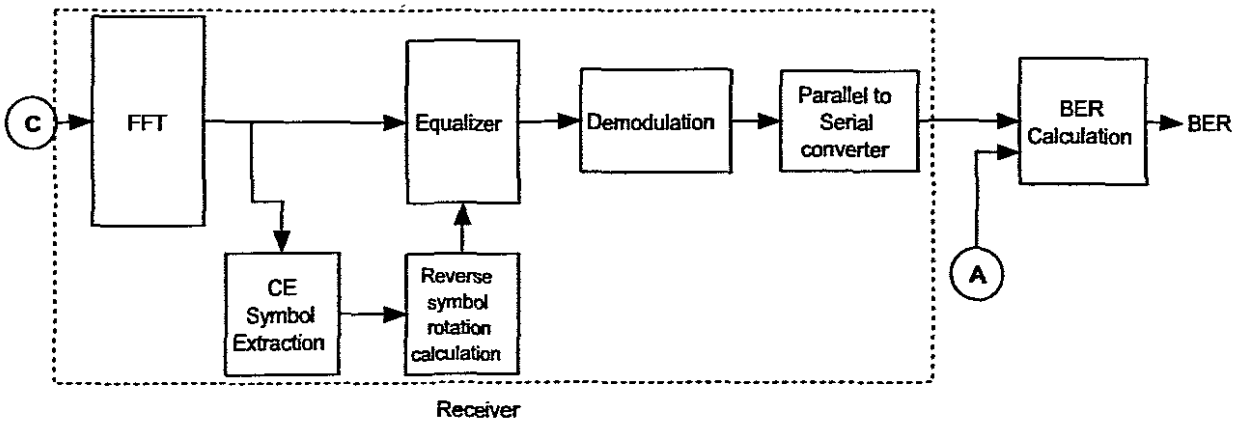

Figure 4.8: Block Diagram of OFDM Receiver

4.5.1.1 Fast Fourier Transform

Before the FFT is applied to a received OFDM symbol, the symbol's guard interval has to be removed before processing can take place. As discussed in Chapter 2, the guard interval's length can range to a maximum of $1/4$ of an OFDM symbol's length.

An FFT is then applied to the input OFDM signal for the conversion from time domain to frequency domain for processing. This aids in the recovery of the frequency frame which contains the mapped complex symbols at the specific OFDM carriers. This operation can also be seen as a de-multiplexing technique, where discrete carriers are separated in the frequency domain through the FFT operation.

Due to channel distortion, individual discrete carrier information will be distorted, or, as it is also termed, rotated (in terms of a constellation map). To minimize the distortion, equalization is applied through the use of channel estimation symbols to estimate the degree of symbol rotation.

4.5.1.2 Equalisation

Equalisation is the process of compensating for channel distortion. In this implementation, a pilot symbol-aided scheme is utilized, to estimate and compensate for channel distortion. This is achieved by sending a known OFDM symbol (which is known to both the transmitter and receiver) at regular intervals between OFDM symbol transmissions (as depicted in Figure 4.9 (Harada & Prasad 2002)).

At the receiver, the distorted pilot-symbols are used to calculate an estimate of the channel transfer function. Equalisation is then applied to received OFDM symbols, in order to recover transmitted data corrupted by channel distortion (Harada & Prasad 2002) (Dostert 2001)

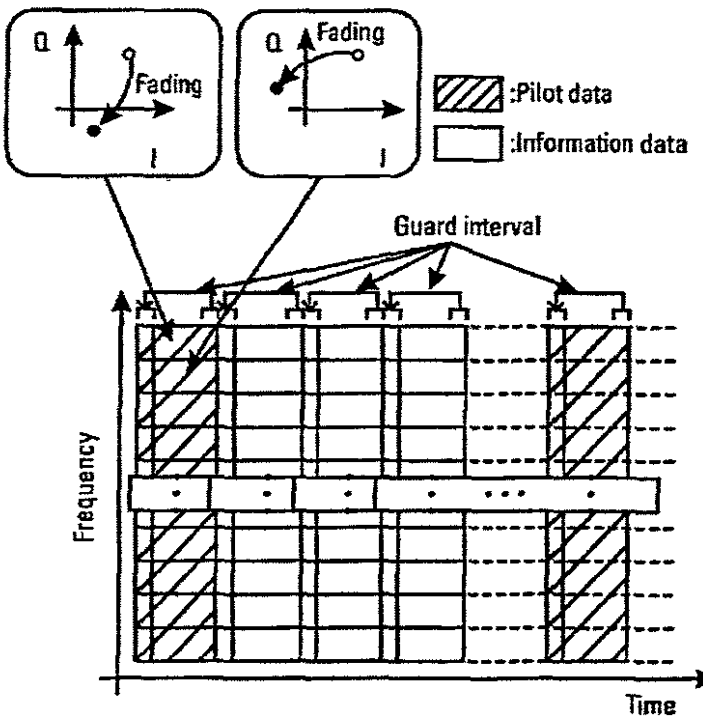

Figure 4.9: Pilot data is used to estimate the amount of fading during transmission, and compensate the information data appropriately (Harada & Prasad 2002)

4.5.1.3 Demodulation / Decoding

Depending on the type of encoding / modulation method utilized during the simulation, the demodulation / decoding process will estimate, from a given set of complex symbols, the equivalent data output.

The symbol estimation is performed by using a "slicer", which uses decision boundaries to estimate the likeliest symbol that could have been transmitted. Graphically this can be viewed in terms of a constellation diagram.

4.5.1.4 Parallel to serial Converter

The Parallel to Serial Converter's function is to buffer decoded data streams, then convert the resultant parallel data stream into a serial data stream. The estimated data stream will thus be formed. This data stream will then be compared to the transmitted data stream, for BER calculations.

4.5.2 MATLAB OFDM Receiver Implementation

As mentioned before, the framework MATLAB scripts used for the Receiver implementation are from (Harada & Prasad 2002). As with the OFDM Transmitter implementation, the scripts have been adapted for the change in:

- *the discrete frequency mapping technique*
- various encoding / modulation techniques e.g. QAM, QPSK, DQPSK, etc.

The specifications of the receiver comply to the Homeplug standards (Lee et al. 2003) where a 256 FFT is utilized for the time-to-frequency conversion.

The first step in the OFDM receiver is the removal of the guard interval before processing. Once the guard interval is removed, an FFT is applied to the received OFDM signal to obtain a spectral representation, wherein the received complex symbols (real and imaginary) can be found.

Compensation for the channel distortion follows, requiring the calculation of the amount of symbol rotation (distortion in terms of phase and amplitude), per discrete sub-carrier. As explained in (Harada & Prasad 2002), the pilot data symbols are used to calculate the amount of symbol rotation. The relationship between transmitted pilot data (real component - *ice0*, imaginary component - *qce0*) and the received pilot data (real component - *ice1*, imaginary component - *qce1*) is given by (Harada & Prasad 2002):

$$\begin{pmatrix} ice1 \\ qce1 \end{pmatrix} = A \cdot \begin{pmatrix} ice0 \\ qce0 \end{pmatrix} \tag{4.8}$$

where A is the transition matrix of the fading environment and represented as follows (Harada & Prasad 2002):

$$A = \begin{pmatrix} iv & -qv \\ qv & iv \end{pmatrix} \tag{4.9}$$

where *iv* and *qv* represent the rotation vectors (real and imaginary respectively).

Thus, to provide compensation, all received OFDM symbols must be multiplied by A^{-1}, which is defined as (Harada & Prasad 2002):

$$A^{-1} = \frac{1}{\sqrt{iv^2 + qv^2}} \cdot \begin{pmatrix} iv & qv \\ -qv & iv \end{pmatrix} \tag{4.10}$$

Using the above equations, the values of *iv* and *qv* are given by:

$$iv = \frac{1}{\sqrt{ice1 + qce1}} \cdot (ice0 \cdot ice1 + qce0 \cdot qce1) \tag{4.11}$$

$$iv = \frac{1}{\sqrt{ice1 + qce1}} \cdot (qce0 \cdot ice1 - ice0 \cdot qce1) \tag{4.12}$$

Using *iv* and *qv*, inverse rotation matrices are produced, which is multiplied with all received complex symbols to provide compensation for channel distortion.

Once individual symbols are estimated from individual discrete carriers, the data stream is recreated. Using the recreated data stream (estimated data stream), the BER is calculated to determine the performance of the transmission.

BER is defined as:

$$BER = \frac{noe}{nod} \tag{4.13}$$

where *noe* represents the number of bit errors and *nod* represents the total number of transmitted bits.

The flowchart in Figure 4.10, depicts the processes followed in the MATLAB OFDM Receiver.

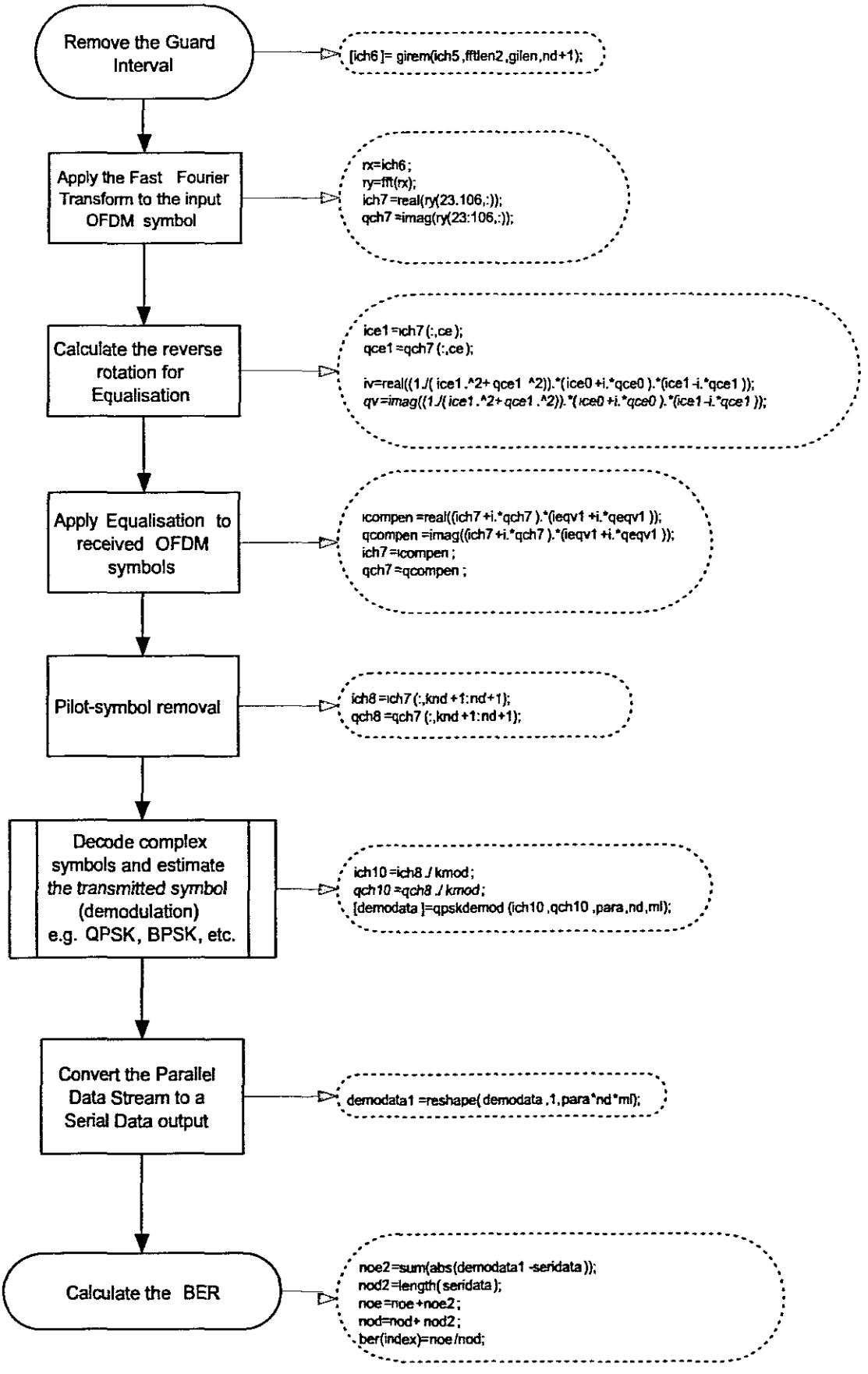

Figure 4.10: Flowchart for MATLAB OFDM Receiver

4.6 Algorithm verification

An essential component to this thesis, in ensuring the highest possible accuracy from simulation runs, is to verify that the base algorithms (all six simulation programs i.e. QPSK, BPSK, etc.) are functioning within specific theoretical limits. The following discussion is related to this component, where algorithm verification was undertaken.

4.6.1 Process of Algorithm verification

The process of algorithm verification involved customising the six MATLAB scripts of the different encoding schemes used e.g. QAM, QPSK, etc. where only AWGN noise is utilised and with no equalisation / symbol training. The resultant BER plots would then form part of the analysis component to verify that the outputs are with the expected theoretical limits.

The theoretical BER plots of the individual encoding schemes, used in the six OFDM implementations, will be used to compare and validate the individual algorithm's BER response. As mentioned in (Harada & Prasad 2002), in OFDM transmission, if orthogonality is preserved, then the expected BER performance should be identical to the theoretical BER response of the modulation scheme used in each subchannel. This means that if QPSK is used for the subchannel modulation through an AWGN channel, then the expected BER response should be relatively the same as the theoretical AWGN QPSK BER response.

But, it is also important to note, as in (Harada & Prasad 2002), that *the use of a guard interval*, introduces *a shift from the theoretical BER value*. This is related to (Harada & Prasad 2002) the guard interval power for received signal, and can be equated as the following (Harada & Prasad 2002):

$$bershift = -10log_{10}\left(\frac{gilen}{fftlen2}\right) \tag{4.14}$$

where *gilen* refers to the guard interval length and *fftlen2* refers to the sum of the guard interval length and FFT length.

Using the specifications of the simulations, a maximum shift of *3.9dB* can be expected according to (Harada & Prasad 2002).

4.6.2 Results of Algorithm verification

After successfully customising the six algorithms (removing the power line model component and symbol training), a batch simulation was performed using the following criteria:

- Symbol Rate - 250 000 symbols/sec
- Number of bits transmitted - 4000

The results of the simulations are depicted in Figures 4.11 to 4.16. From these figures, the expected shift is evident. Differences between theoretical and simulated BER values, for individual encoding methods, are tabulated in Tables 4.1 to 4.6.

The simulated average shift for individual encoding methods are summarised as follows:

- BPSK : 2.2dB
- QPSK : 2.5dB
- DBPSK : 2.2dB
- DQPSK : 2dB

- 8QAM : 2.4dB

- 16QAM : 2.5dB

with an overall average shift of 2.4dB.

Looking at this result, it can therefore be concluded that all the individual simulations algorithms result in approximately the same amount of dB shift and that secondly, the simulations are functioning within the theoretical limits.

4.7 Conclusion

Chapter 4 has discussed the development of the necessary simulation tools which is required for the benchmarking modulation performance. Insight has been given into the algorithms and methodologies used to develop and produce the MATLAB scripts needed for producing the simulation results.

It should be noted that since the framework utilized from (Harada & Prasad 2002) has been verified to be working within the necessary parameters of an OFDM simulation, the model presented in this chapter thus is validated, since the same framework is utilized throughout the simulation.

This chapter thus completes the final stage of the design process. An entire OFDM-PLC system has been developed in MATLAB, which completes one of the author's objectives.

The subsequent chapter will concentrate on the analysis of the results produced by this simulation model and the recommended strategies for improving system performance.

BER	EbN0 (Theory)	EbN0 (Simulation)	Shift
1e-02	4.295dB	6.519dB	2.224dB
1e-03	6.768dB	8.981dB	2.213db
1e-04	8.359dB	10.55dB	2.191dB
1e-05	9.559dB	11.75dB	2.191dB

Table 4.1: Verification Results - BPSK

BER	EbN0 (Theory)	EbN0 (Simulation)	Shift
1e-02	4.242dB	7.067dB	2.825dB
1e-03	6.761dB	9.32dB	2.559db
1e-04	8.366dB	10.83dB	2.464dB
1e-05	9.55dB	11.85dB	2.3dB

Table 4.2: Verification Results - QPSK

BER	EbN0 (Theory)	EbN0 (Simulation)	Shift
1e-02	5.894dB	8.126dB	2.232dB
1e-03	7.919dB	10.13dB	2.211db
1e-04	9.27dB	11.47dB	2.2dB

Table 4.3: Verification Results - DBPSK

BER	EbN0 (Theory)	EbN0 (Simulation)	Shift
1e-02	6.71dB	9.494dB	2.784dB
1e-03	9.179dB	11.73dB	2.551db
1e-04	10.76dB	13.21dB	2.45dB
1e-05	11.91dB	14.35dB	2.44dB

Table 4.4: Verification Results - DQPSK

BER	EbN0 (Theory)	EbN0 (Simulation)	Shift
1e-02	7.02dB	9.508dB	2.488dB
1e-03	9.593dB	11.96dB	2.367db
1e-04	11.27dB	13.84dB	2.57dB
1e-05	12.48dB	14.8dB	2.32dB

Table 4.5: Verification Results - 8QAM

BER	EbN0 (Theory)	EbN0 (Simulation)	Shift
1e-02	7.823dB	10.5dB	2.677dB
1e-03	10.48dB	13.02dB	2.54db
1e-04	12.18dB	14.44dB	2.26dB

Table 4.6: Verification Results - 16QAM

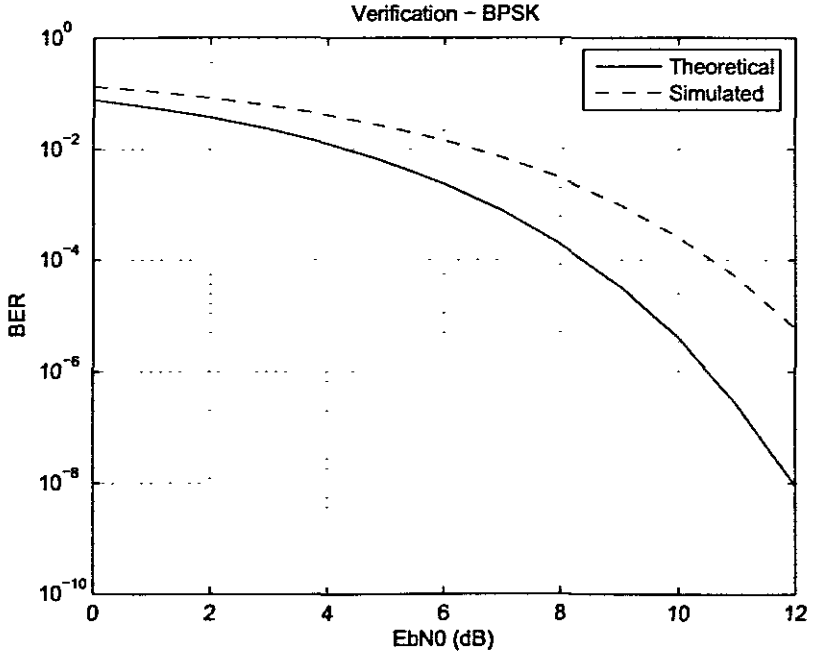

Figure 4.11: Results of Verification for OFDM-BPSK Simulation

BER	EbN0 (Theory)	EbN0 (Simulation)	Shift
1e-02	7.02dB	9.508dB	2.488dB
1e-03	9.593dB	11.96dB	2.367db
1e-04	11.27dB	13.84dB	2.57dB
1e-05	12.48dB	14.8dB	2.32dB

Table 4.5: Verification Results - 8QAM

BER	EbN0 (Theory)	EbN0 (Simulation)	Shift
1e-02	7.823dB	10.5dB	2.677dB
1e-03	10.48dB	13.02dB	2.54db
1e-04	12.18dB	14.44dB	2.26dB

Table 4.6: Verification Results - 16QAM

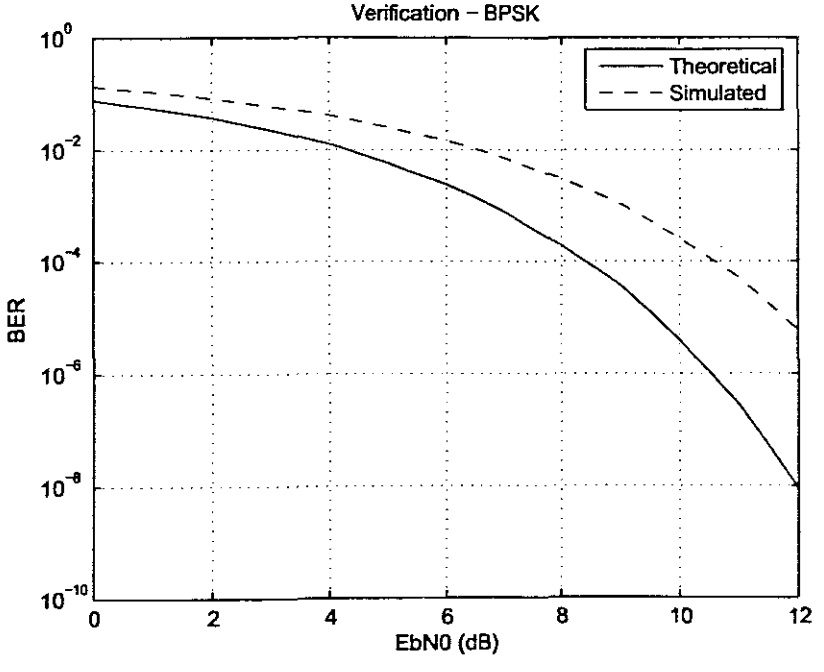

Figure 4.11: Results of Verification for OFDM-BPSK Simulation

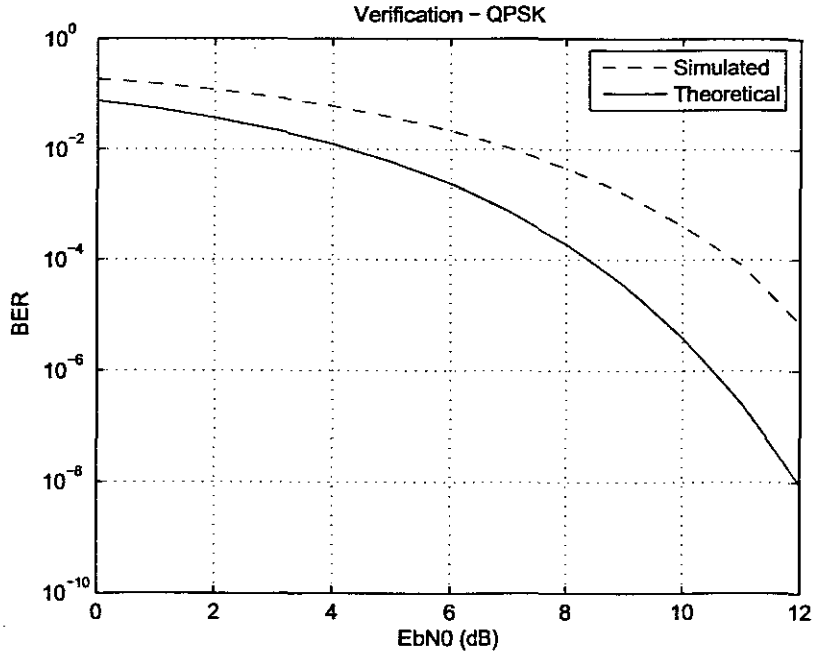

Figure 4.12: Results of Verification for OFDM-QPSK Simulation

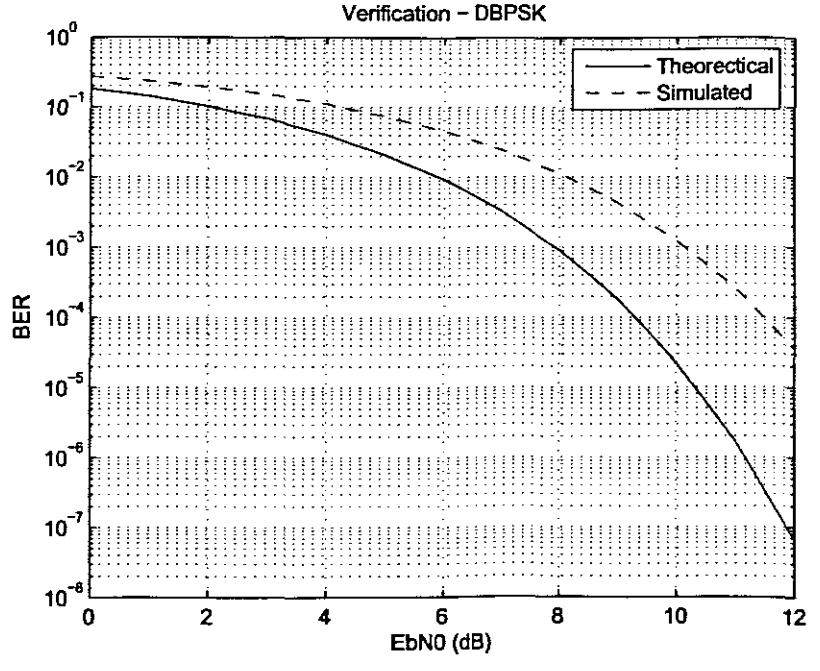

Figure 4.13: Results of Verification for OFDM-DBPSK Simulation

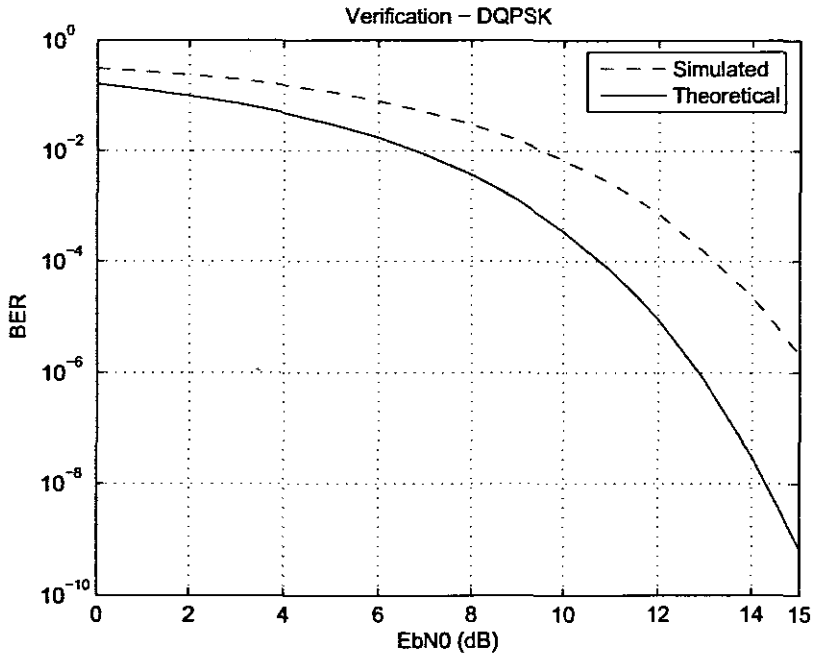

Figure 4.14: Results of Verification for OFDM-DQPSK Simulation

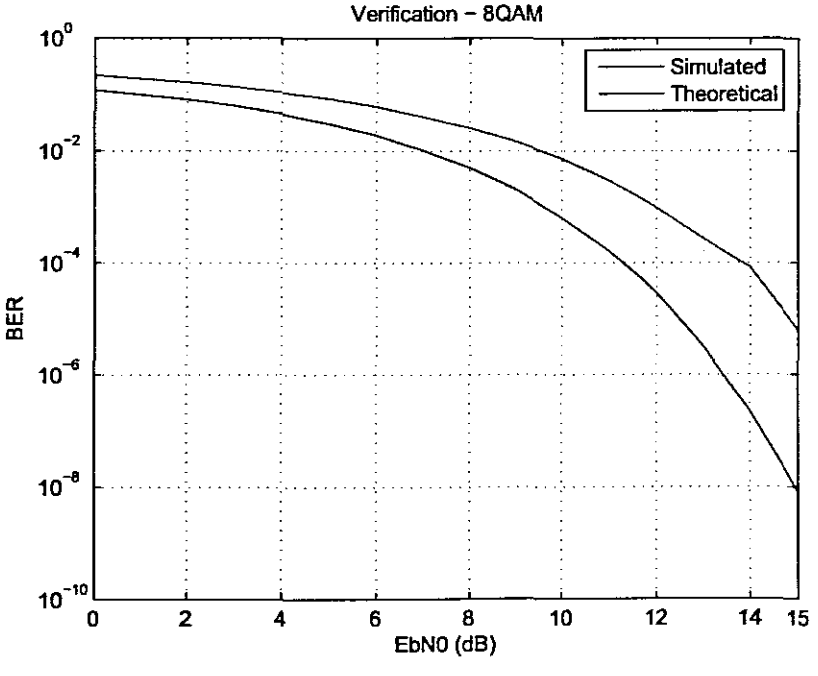

Figure 4.15: Results of Verification for OFDM-8QAM Simulation

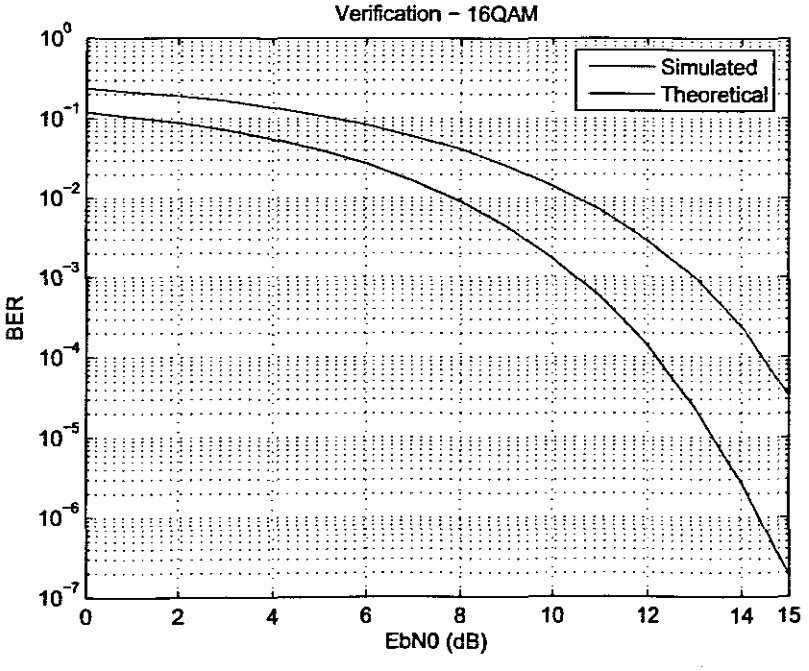

Figure 4.16: Results of Verification for OFDM-16QAM Simulation

Chapter 5

Results of simulated communication scenarios

5.1 Chapter Description

In this chapter, the author will be presenting the results from a series of simulated scenarios. The simulation tools developed were utilised in order to generate the necessary BER plots, required for performance analysis.

The structure of the chapter is as follows:

- An evaluation of the simulated results of individual encoding groups, e.g. PSK-based encoding, QAM-based encoding, etc.
- Comparative analysis of the various encoding techniques.

5.2 Simulation Criteria

For the purposes of analysis, five typical scenarios were used for comparative simulations. The selected scenarios were:

- Scenario 1: Path AB with a PC at C
- Scenario 2: Path AC with a Vacuum at D
- Scenario 3: Path BC with a Mixer at D
- Scenario 4: Path BD with a TV at A
- Scenario 5: Path CD with a Hair-dryer at A

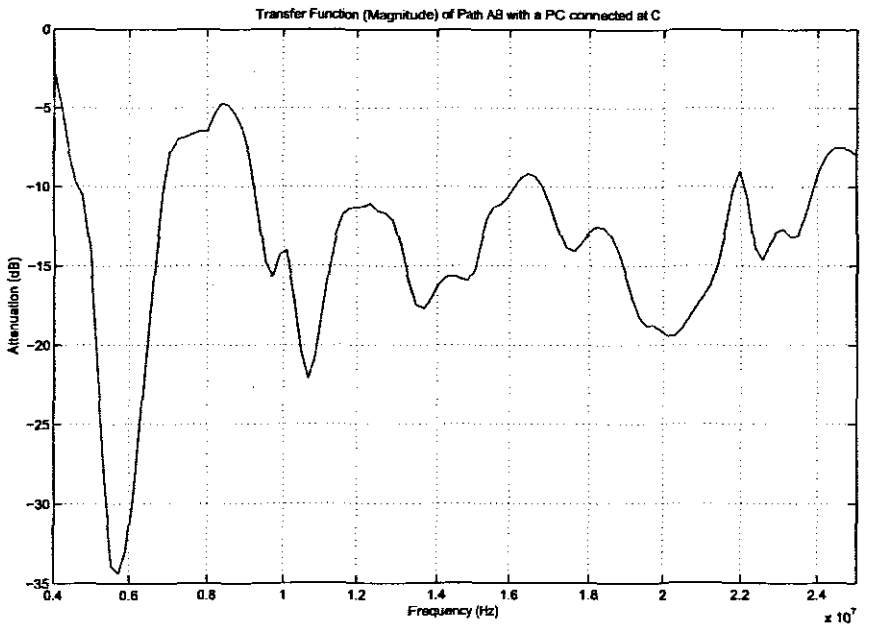

Figure 5.1: Transfer function (Magnitude) - Path AB with PC at C

The series of scenarios provides the author with a balanced range of transfer functions, especially degrees of attenuation as well as phase noise. This can be seen in Figures 5.1 to 5.5, which depict both the magnitude variations of the 5 scenarios.

The simulation criteria is as follows:

– Throughput - 42Mbps

– No. of bits transmitted - 1 000 000 bits

It should also be noted that no error correction or detection schemes were utilised during the simulations. The results are based on uncoded-OFDM transmissions.

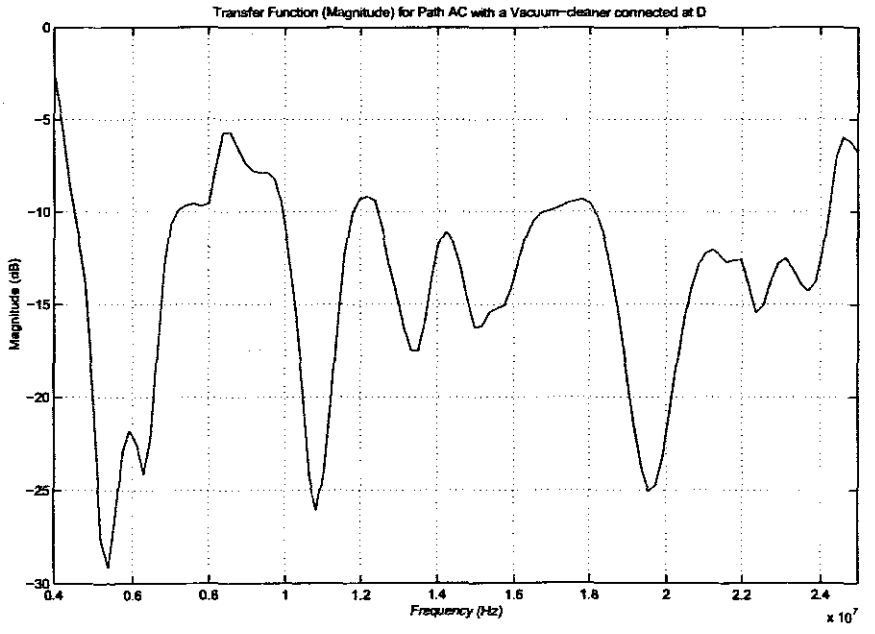

Figure 5.2: Transfer function (Magnitude) - Path AC with Vacuum-cleaner at C

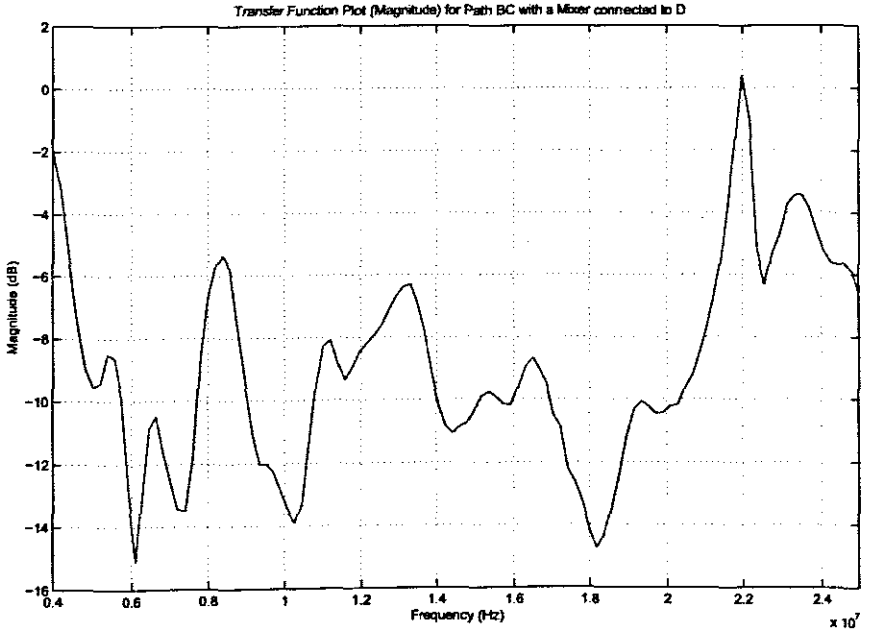

Figure 5.3: Transfer function (Magnitude) - Path BC with Mixer at C

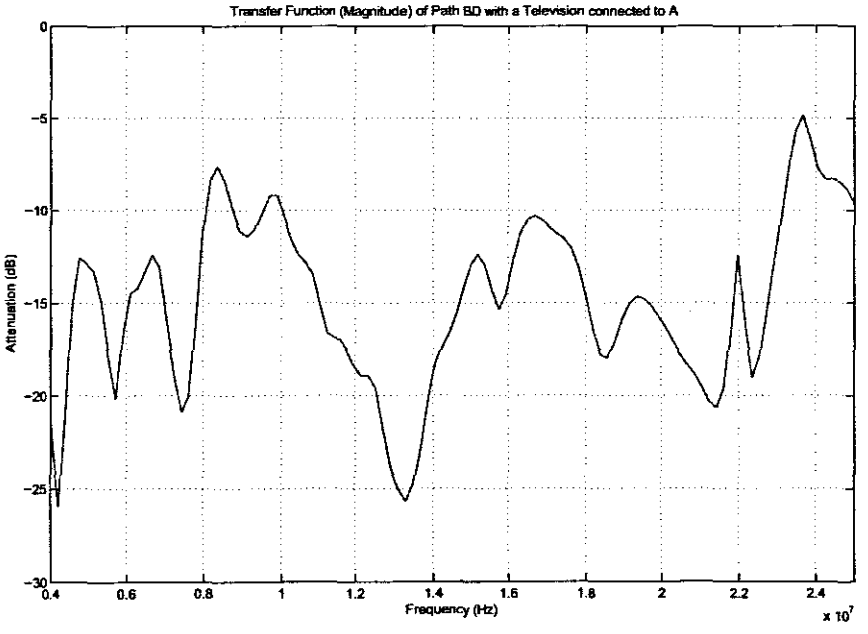

Figure 5.4: Transfer function (Magnitude) - Path BD with Television at A

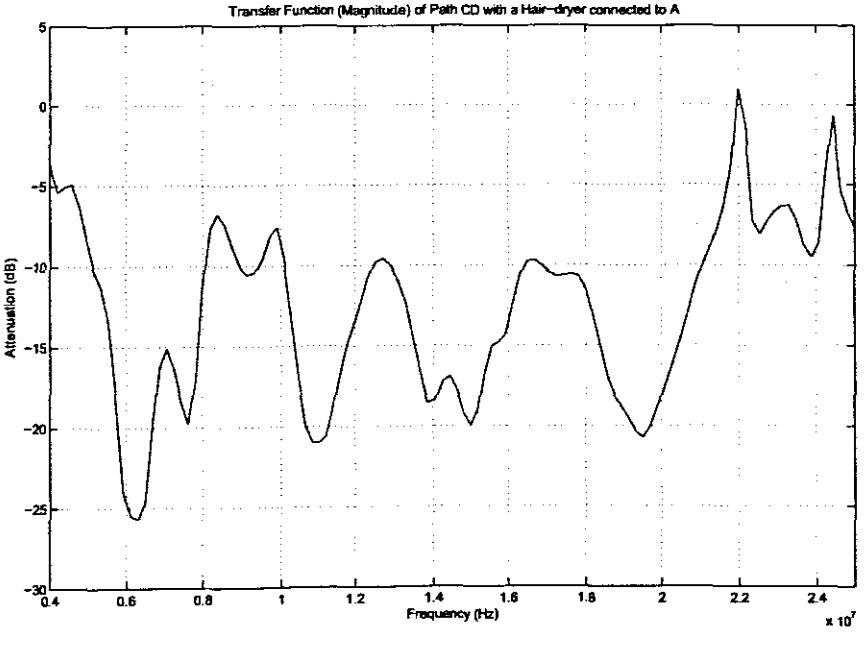

Figure 5.5: Transfer function (Magnitude) - Path CD with Hair-dryer at A

5.3 Simulation Results

5.3.1 PSK

The results presented in Figures 5.6 to 5.10 are for the five scenarios, for PSK-based modulation / encoding.

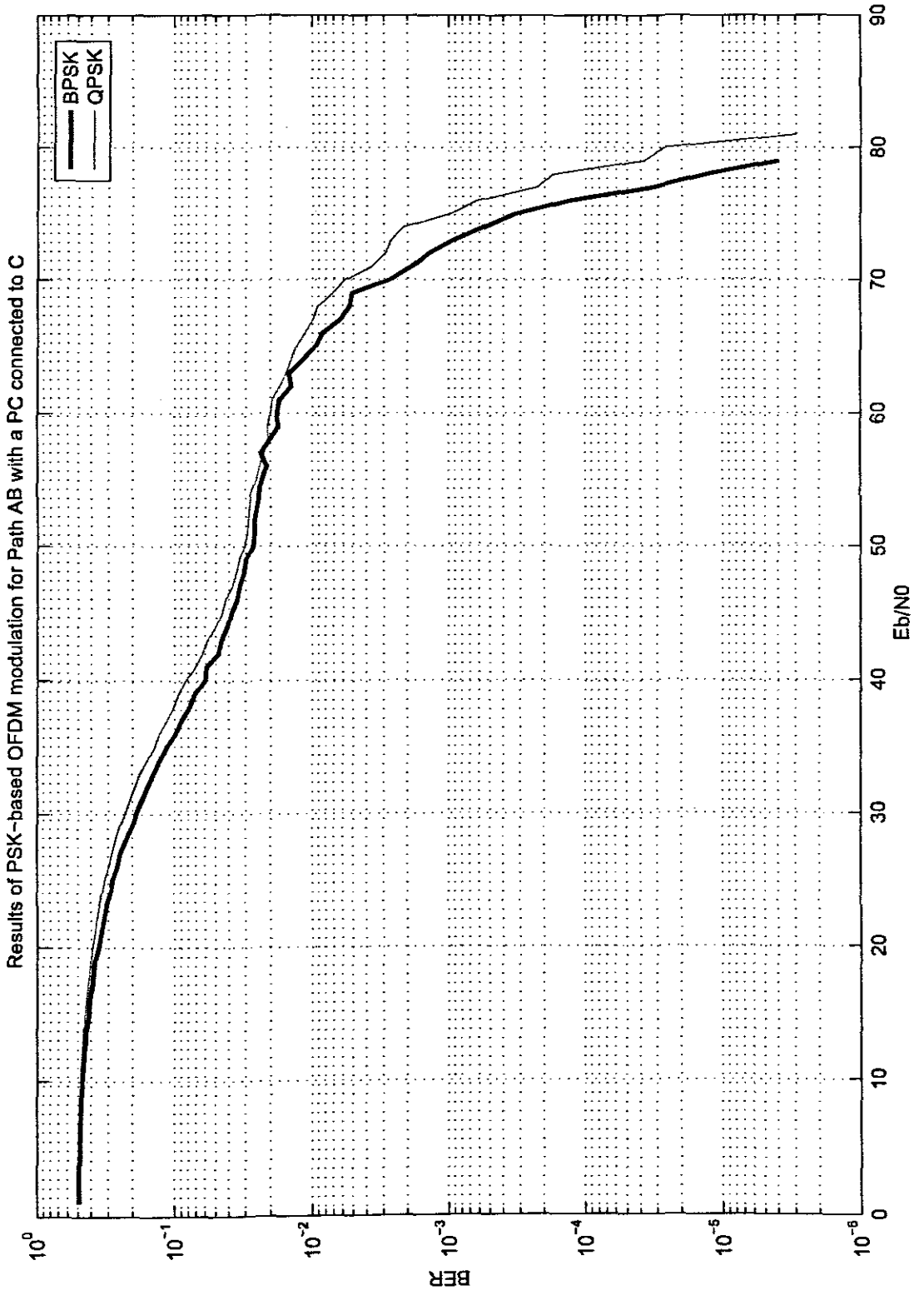

Figure 5.6: Results (PSK) - Scenario 1

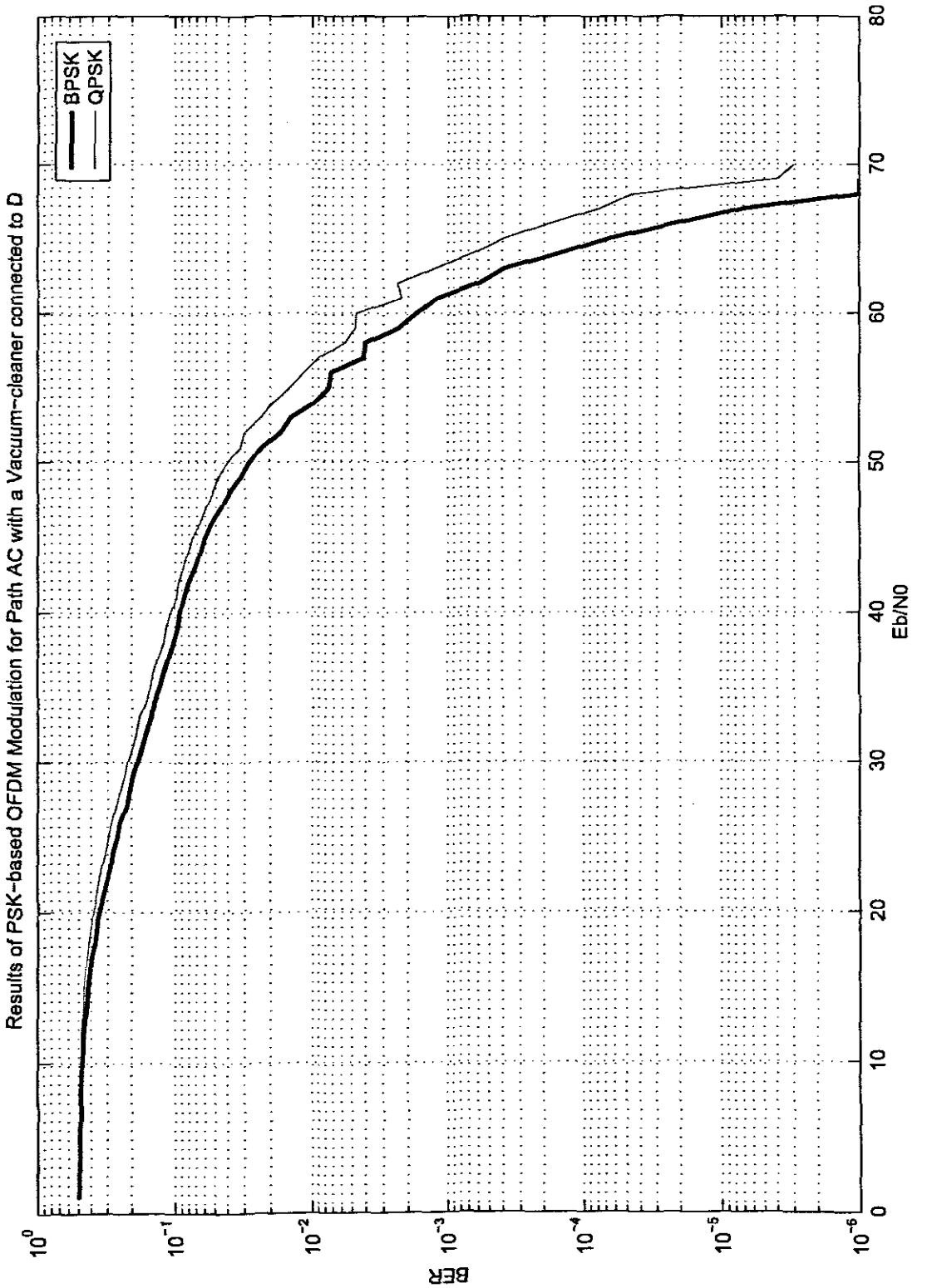

Figure 5.7: Results (PSK) - Scenario 2

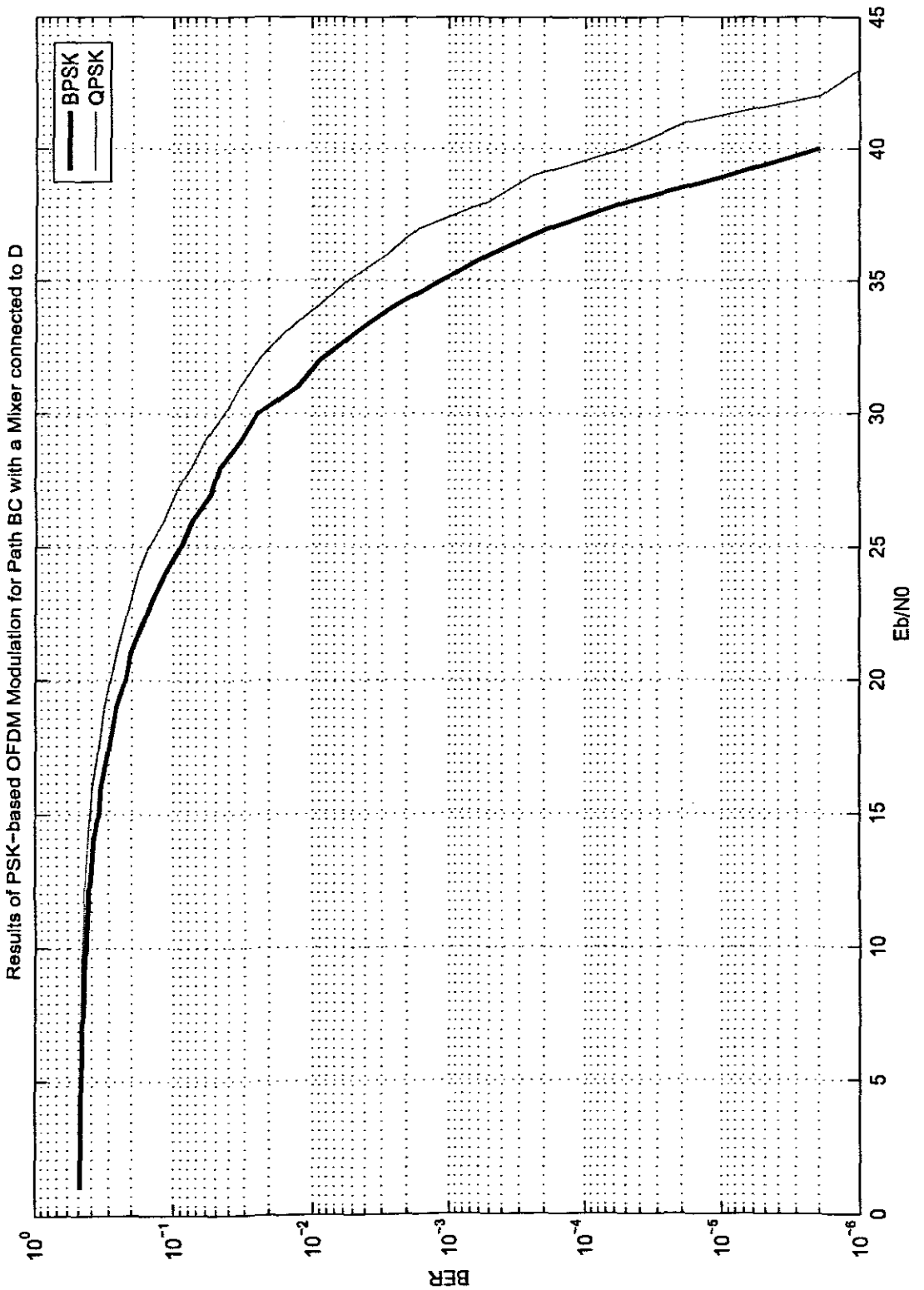

Figure 5.8: Results (PSK) - Scenario 3

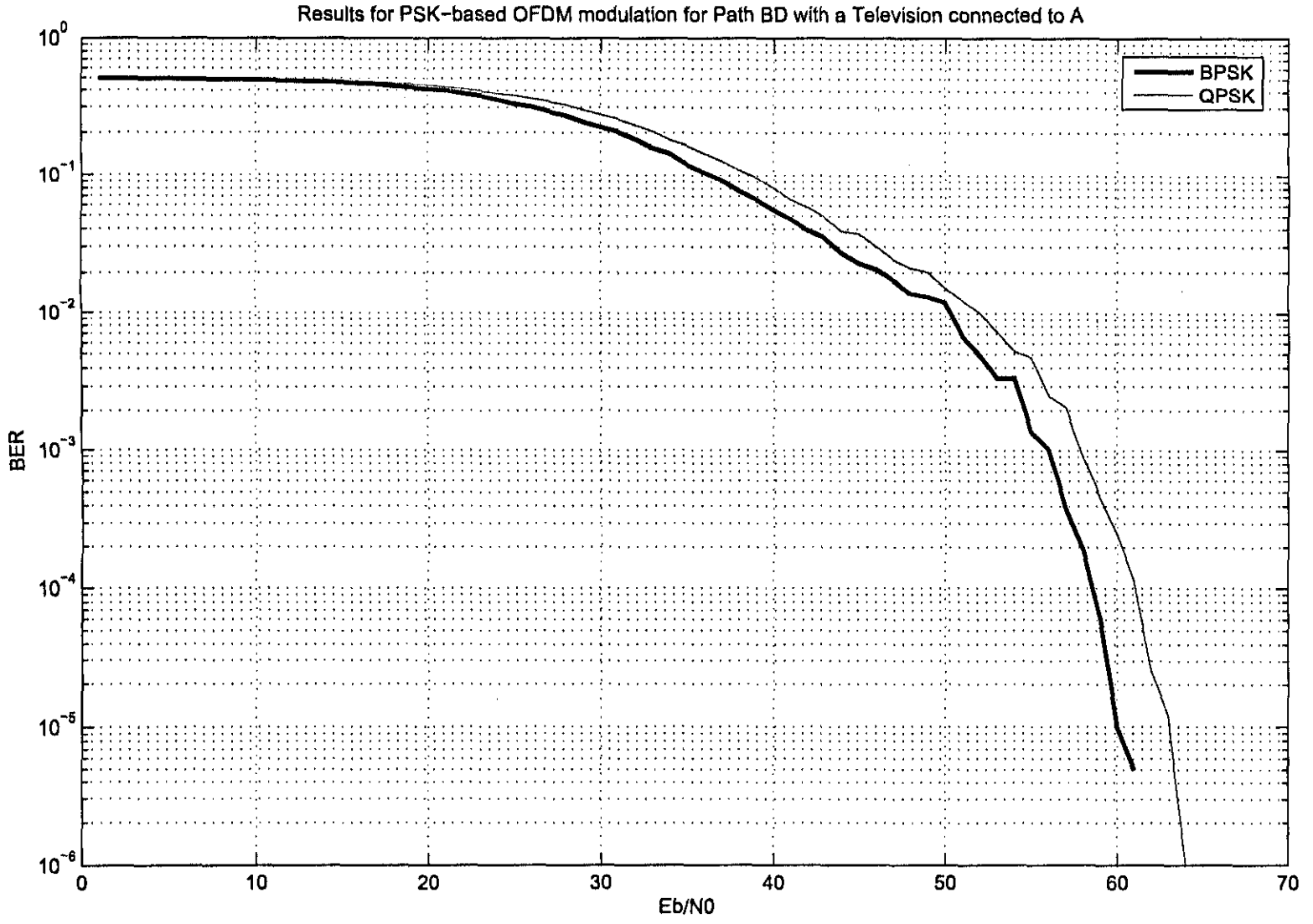

Figure 5.9: Results (PSK) - Scenario 4

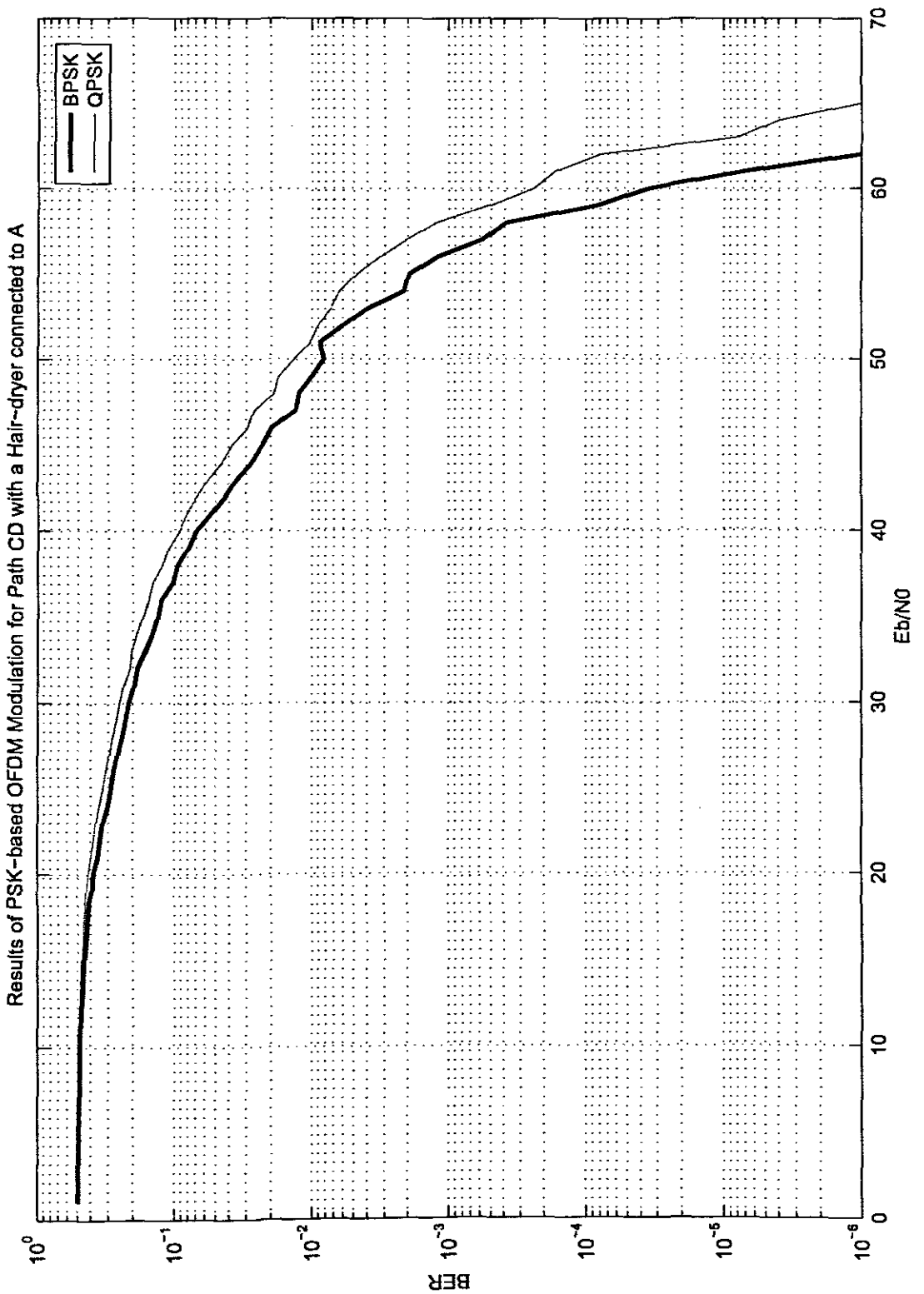

Figure 5.10: Results (PSK) - Scenario 5

5.3.1.1 Scenario 1

In the first scenario, examining the magnitude TF (Transfer Function) plot (Figure 5.1) it is clear that the attenuation level is quite high, especially at 6MHz where the attenuation level lies at $\approx$ 35dB. The resultant average attenuation level (with reference to the lower carriers) is higher.

Examining the resultant BER plot for the scenario (Figure 5.6), OFDM-BPSK and OFDM-QPSK have almost similar performances as expected in theory (Harada & Prasad 2002). The poor performance in terms of BER, can be explained by examining the physical layout of the scenario, where the signal path has two inter-connects. The two inter-connects add to the detriment of signal quality by presenting a High Z (at D) and an unmatched impedance at C (the PC), which results in an unmatched impedances, causing a high amount of reflections (Pozar 1998). Combined with relatively high attenuation, the resultant is a heavily degraded signal and hence a higher average Eb/N0 required to reach a sustainable BER of 10^{-5}.

5.3.1.2 Scenario 2

The second scenario slows a slight improvement in terms of BER (Figure 5.7). OFDM-BPSK has a slightly better performance (1dB) than OFDM-QPSK in this scenario, where the Eb/N0 at 10^{-5} is approximately *69dB*. When examining the transfer function plot (magnitude) of the scenario, there are three major attenuation dips (-25dB).

As expected, this influences the overall BER performance.

5.3.1.3 Scenario 3

From the third scenario's BER plot, an improved performance can be seen. When examining the Transfer function (magnitude) plot, Figure 5.3, it is evident that the average attenuation is low ($\approx$ -12dB). The result is a relatively good BER plot, considering the transmission is uncoded.

Comparatively, OFDM-BPSK has an advantage (2dB difference) against OFDM-QPSK (Figure 5.8).

5.3.1.4 Scenario 4

An analysis of the Transfer Function (magnitude) plot, Figure 5.4, reveals one large attenuation dip at 12MHz (≈ -25dB), with a series of smaller attenuation dips of ≈ -20dB. Compared to the transfer function of scenario 3, the estimated performance would be average.

Figure 5.9 thus confirms the expected (average) performance, in which OFDM-BPSK and OFDM-QPSK have similar BER responses.

5.3.1.5 Scenario 5

In the final scenario, an average performance can be estimated, when examining the transfer function. An average attenuation of ≈ -18dB is present. At a BER of 10^{-5}, OFDM-BPSK has an Eb/N0 of 60dB, which are comparatively good, taking into account that the OFDM transmission is uncoded (no error correction / detection techniques) except for the 1-tap equalisation.

Both OFDM-QPSK and OFDM-BPSK have similar responses.

5.3.2 DPSK

Figures 5.11 to 5.15 represent the results for OFDM-DPSK based simulations, for the five scenarios.

5.3.2.1 Scenario 1

Upon analysis of the first set of BER results for OFDM-DPSK simulation (Figure 5.11), it is evident that the results for OFDM-DBPSK and OFDM-DQPSK, are identical to OFDM-BPSK and OFDM-QPSK respectively. This indicates that even when a non-coherent transmission method (DPSK), which in certain cases should perform slightly better than their coherent counterparts, shows similar results to that of the equivalent coherent transmission method.

It should be noted (as mentioned in the previous PSK-based results) this particular scenario can be considered to be the worst case scenario, as the average attenuation is higher, resulting in substantial signal degradation. Differential PSK methods are most suited to communication scenarios which are plagued by phase rotation.

5.3.2.2 Scenario 2

In this scenario, the BER responses for DBPSK and DQPSK have almost similar responses. Also, the OFDM-DPSK BER responses are identical to their OFDM-PSK equivalents i.e. OFDM-DBPSK = OFDM-BPSK and OFDM-DQPSK = OFDM-QPSK (Figures 5.7 and 5.12).

5.3.2.3 Scenario 3

Comparing Figure 5.8 and Figure 5.13, it is evident that OFDM-BPSK has a slightly better response in this scenario. Although examining the BERs of OFDM-QPSK and OFDM-DQPSK, they have similar responses.

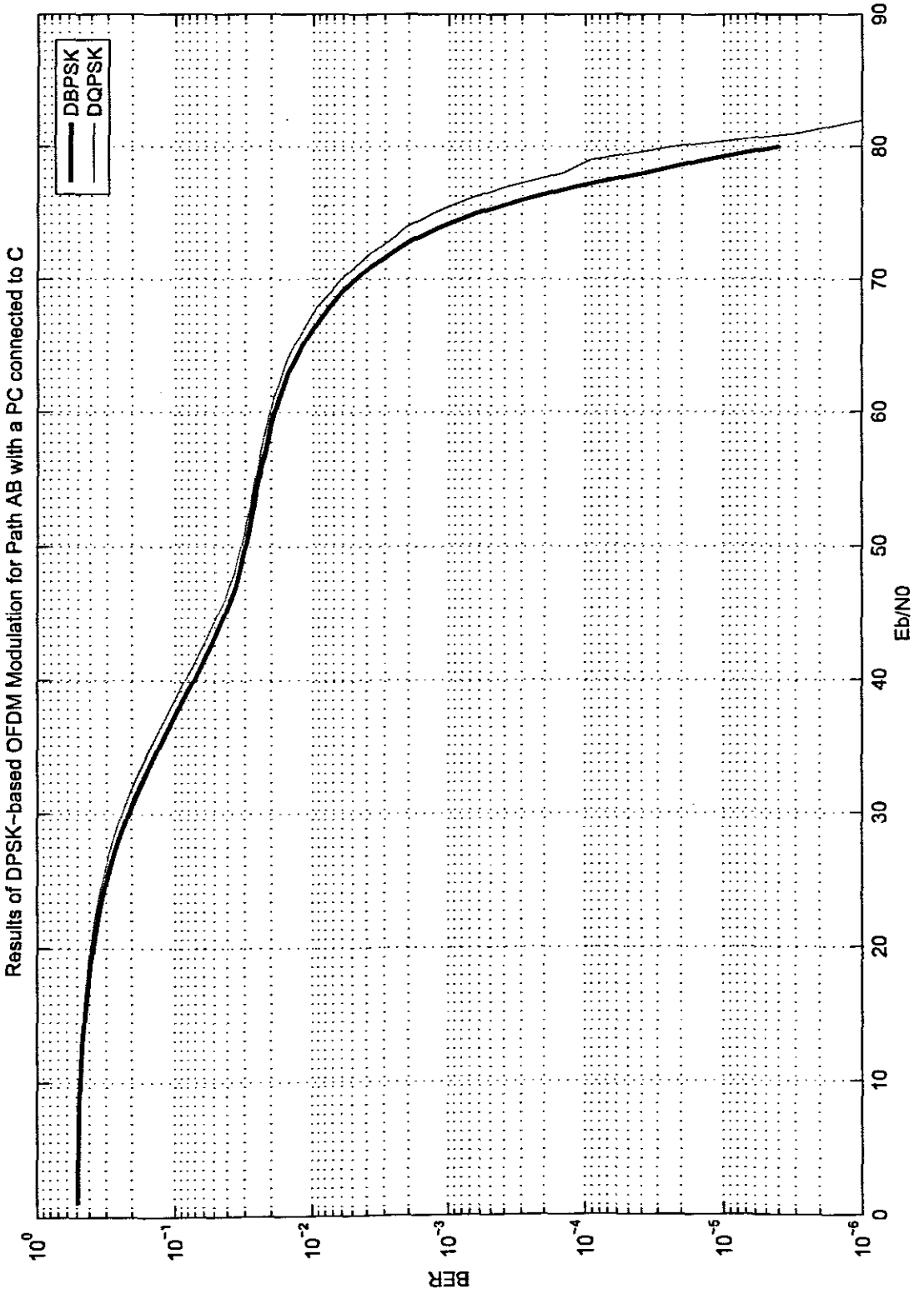

Figure 5.11: Results (DPSK) - Scenario 1

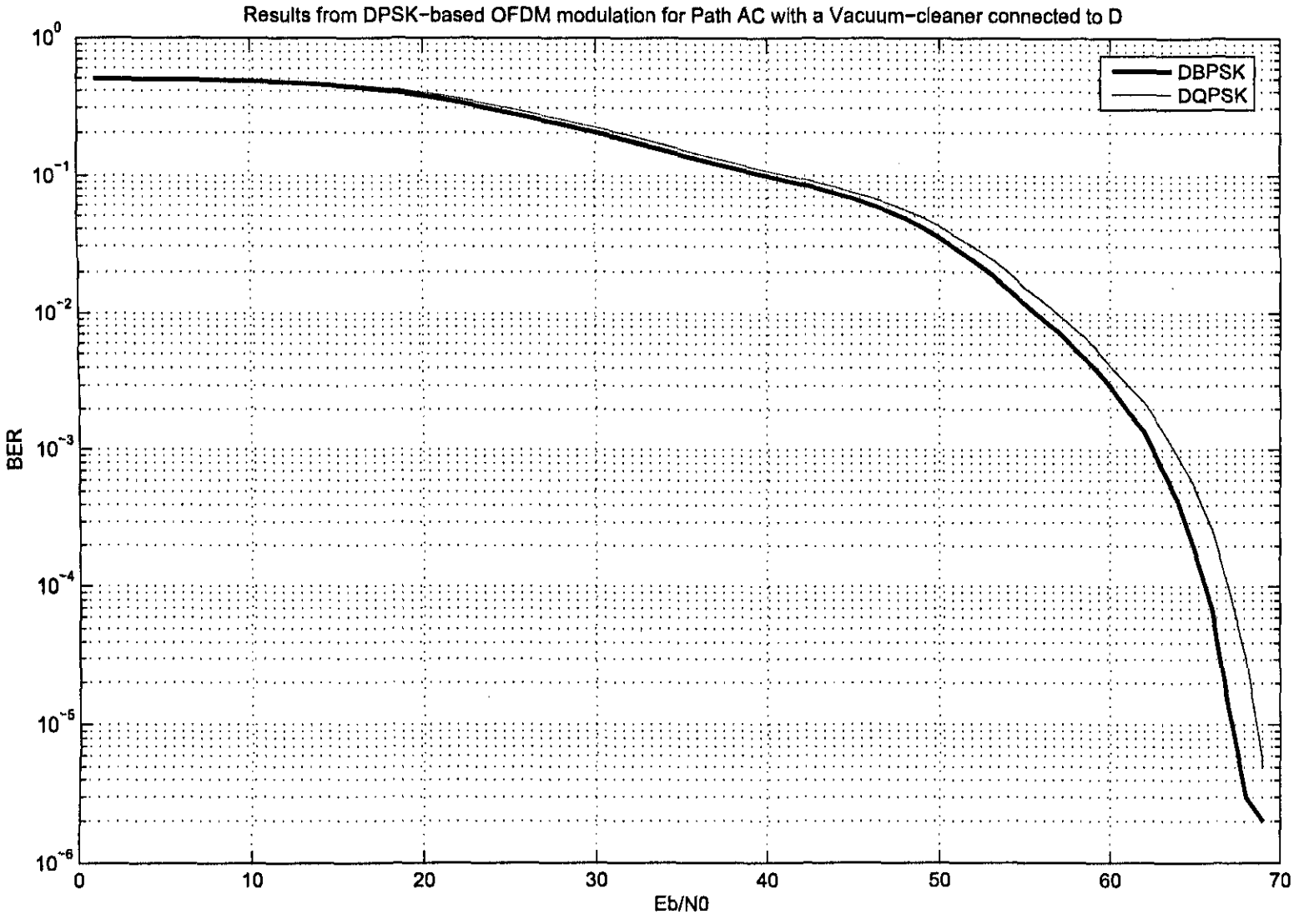

Figure 5.12: Results (DPSK) - Scenario 2

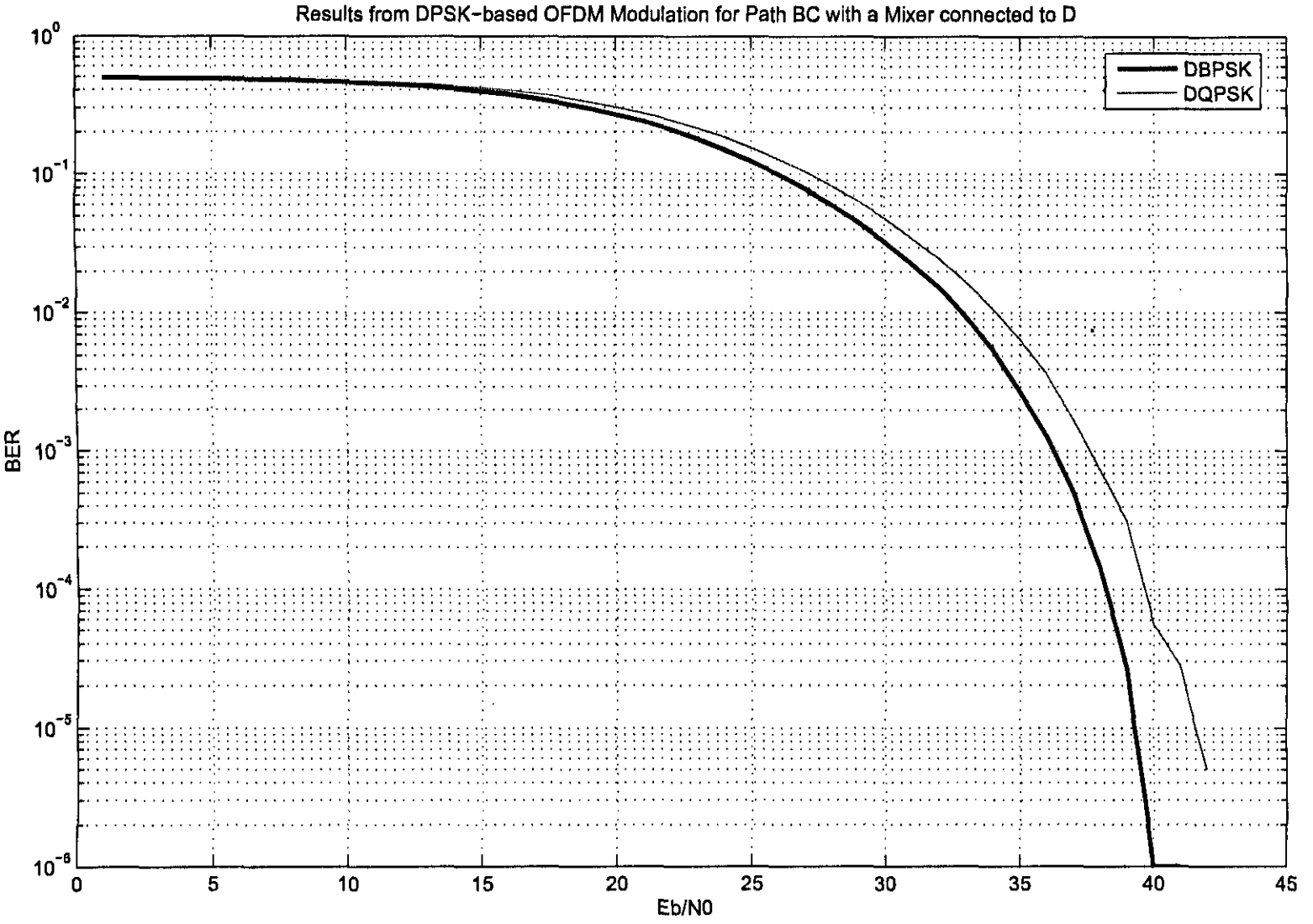

Figure 5.13: Results (DPSK) - Scenario 3

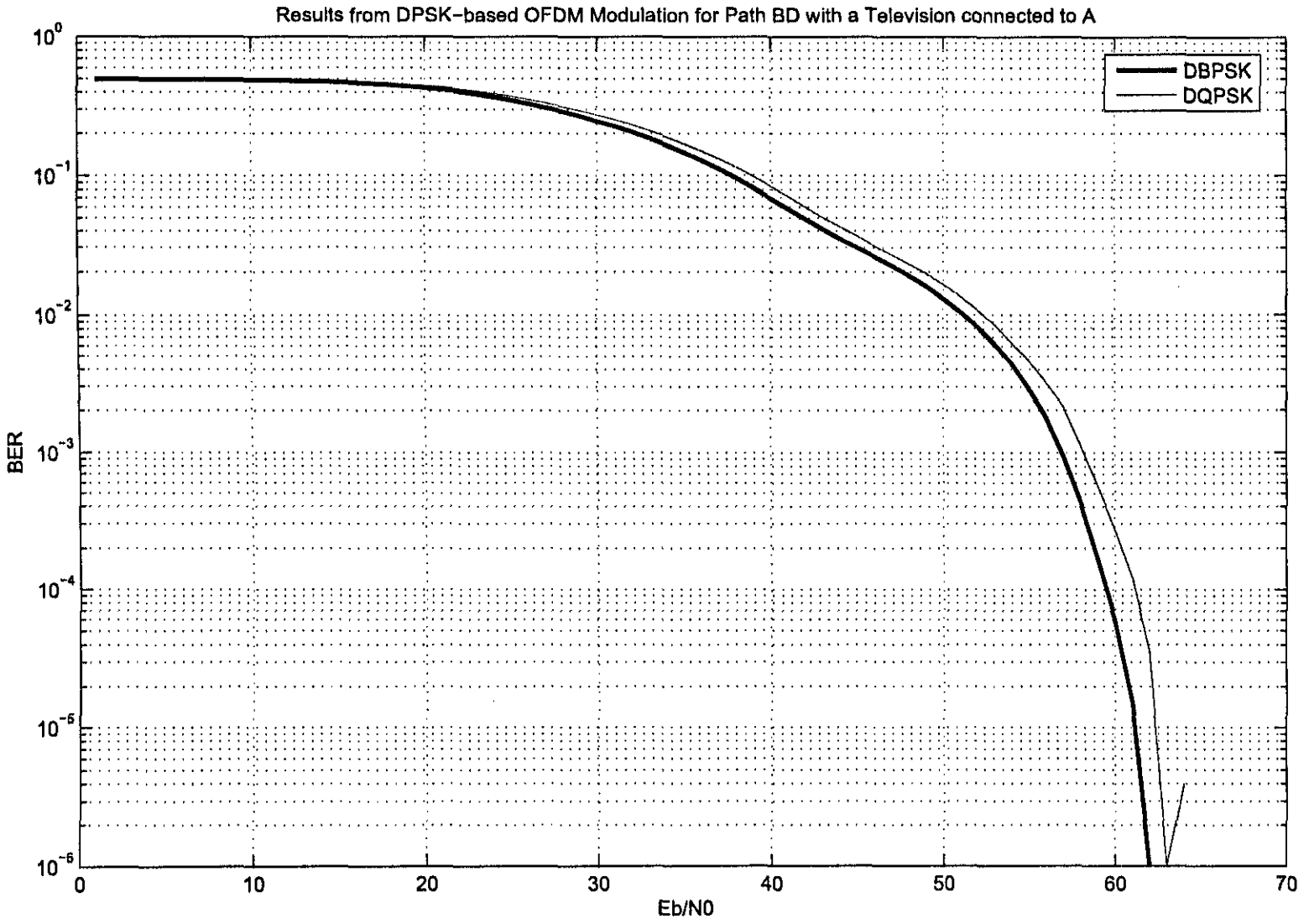

Figure 5.14: Results (DPSK) - Scenario 4

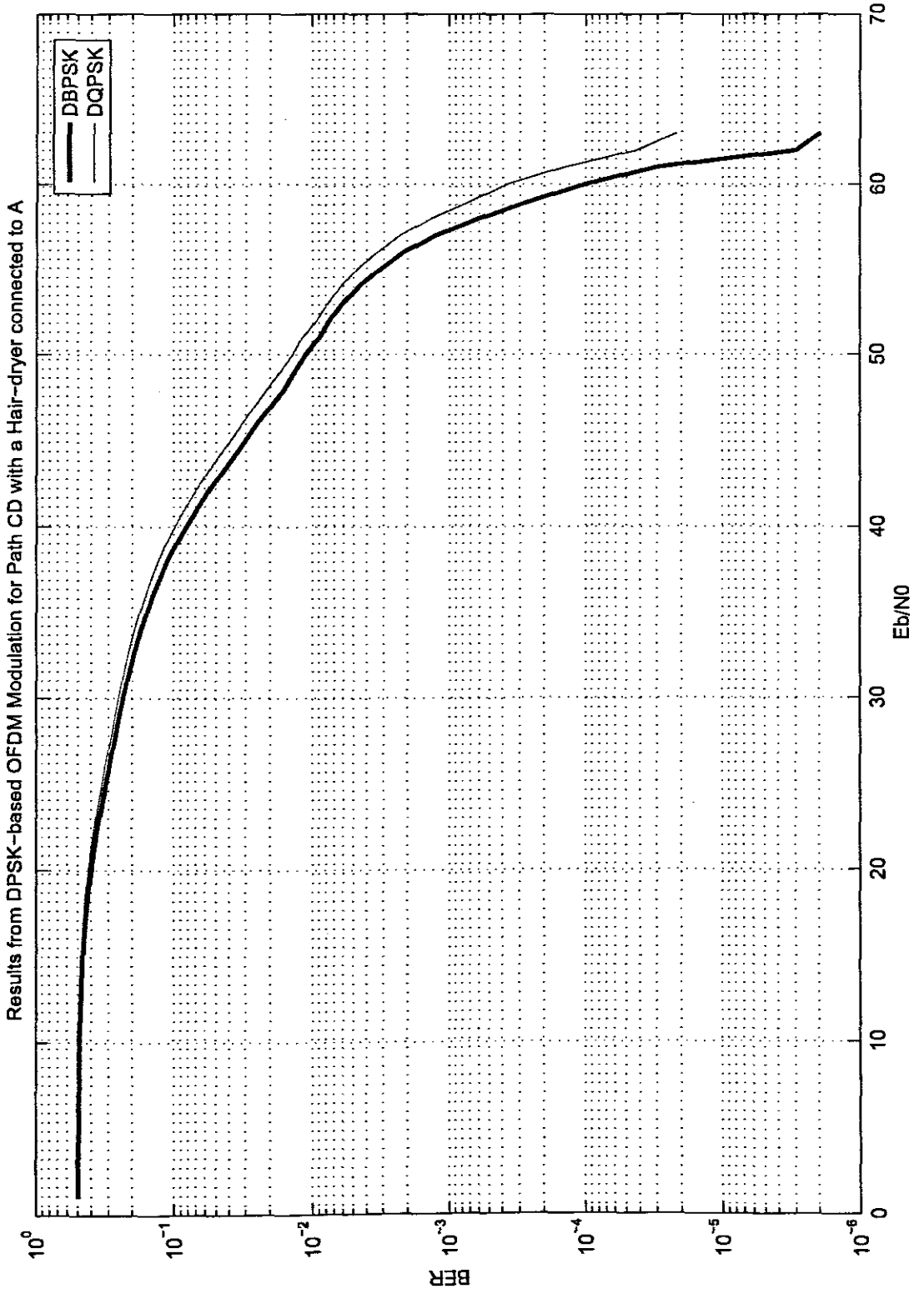

Figure 5.15: Results (DPSK) - Scenario 5

5.3.2.4 Scenario 4

As in the case of Scenario 2, OFDM-DBPSK and OFDM-DQPSK have similar responses. An average BER response for both OFDM-DBPSK and OFDM-DQPSK is the result of this scenario's simulation (Figure 5.14).

5.3.2.5 Scenario 5

In the final simulated scenario for the OFDM-DPSK simulations, have similar BER responses are shown (Figure 5.15), when compared to the same scenario for the OFDM-PSK based simulation (Figure 5.10).

5.3.3 QAM

Figures 5.16 to 5.20 represent the results for OFDM-QAM based simulations, for the five scenarios.

It should be noted that the erratic responses depicted in the OFDM-QAM BER responses, are due to implementation discrepencies which are introduced as a finite amount of bits was transmitted. In the case of the QAM BER simulations, fewer OFDM symbols were transmitted (as more bits are transmitted per OFDM symbol). This however leads to reduced resolution in the resultant BER plots.

5.3.3.1 Scenario 1

With the two QAM methods, from theory (Bateman 1999), (Harada & Prasad 2002), (Sklar 2001), it is expected that these methods will have a higher BER compared to the PSK and DPSK methods. This of course is a result of an increased probability of error, as the symbol constellation is higher.

In this scenario, the average difference between OFDM-8QAM and OFDM-16QAM is $\approx$ 2dB. Comparing OFDM-8QAM to OFDM-BPSK and OFDM-DBPSK, a difference of $\approx$ 3dB is evident.

When comparing OFDM-QPSK and OFDM-DQPSK to OFDM-16QAM, a difference of $\approx$ a 3dB is evident as well (Figures 5.6, 5.11, 5.16).

Although the QAM-methods might seem to be worse compared to the PSK and DPSK methods, it is important to note that the amount of bits transmitted when compared to the relatively small Eb/N0 differences, makes these techniques efficient in operation.

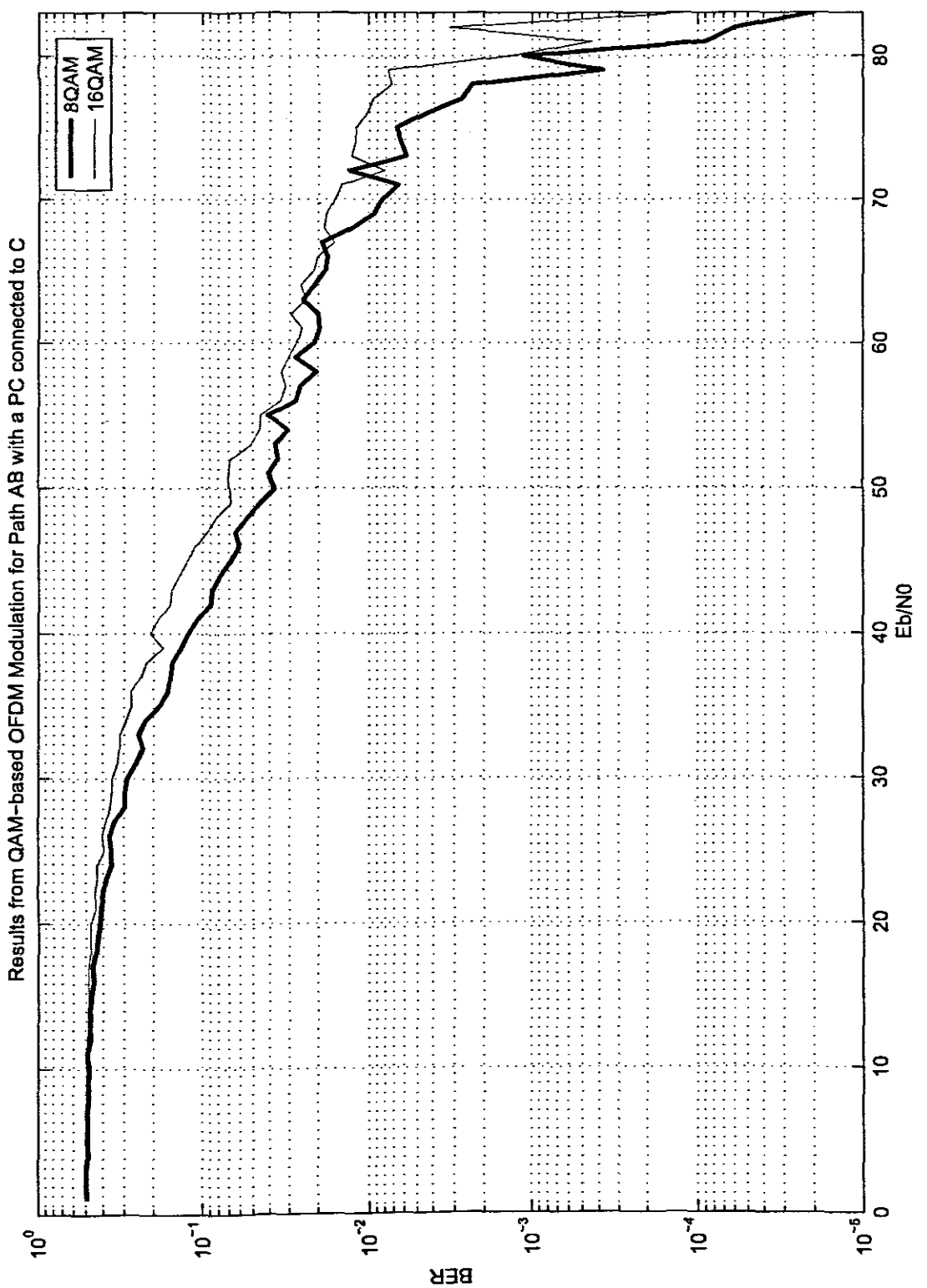

Figure 5.16: Results (QAM) - Scenario 1

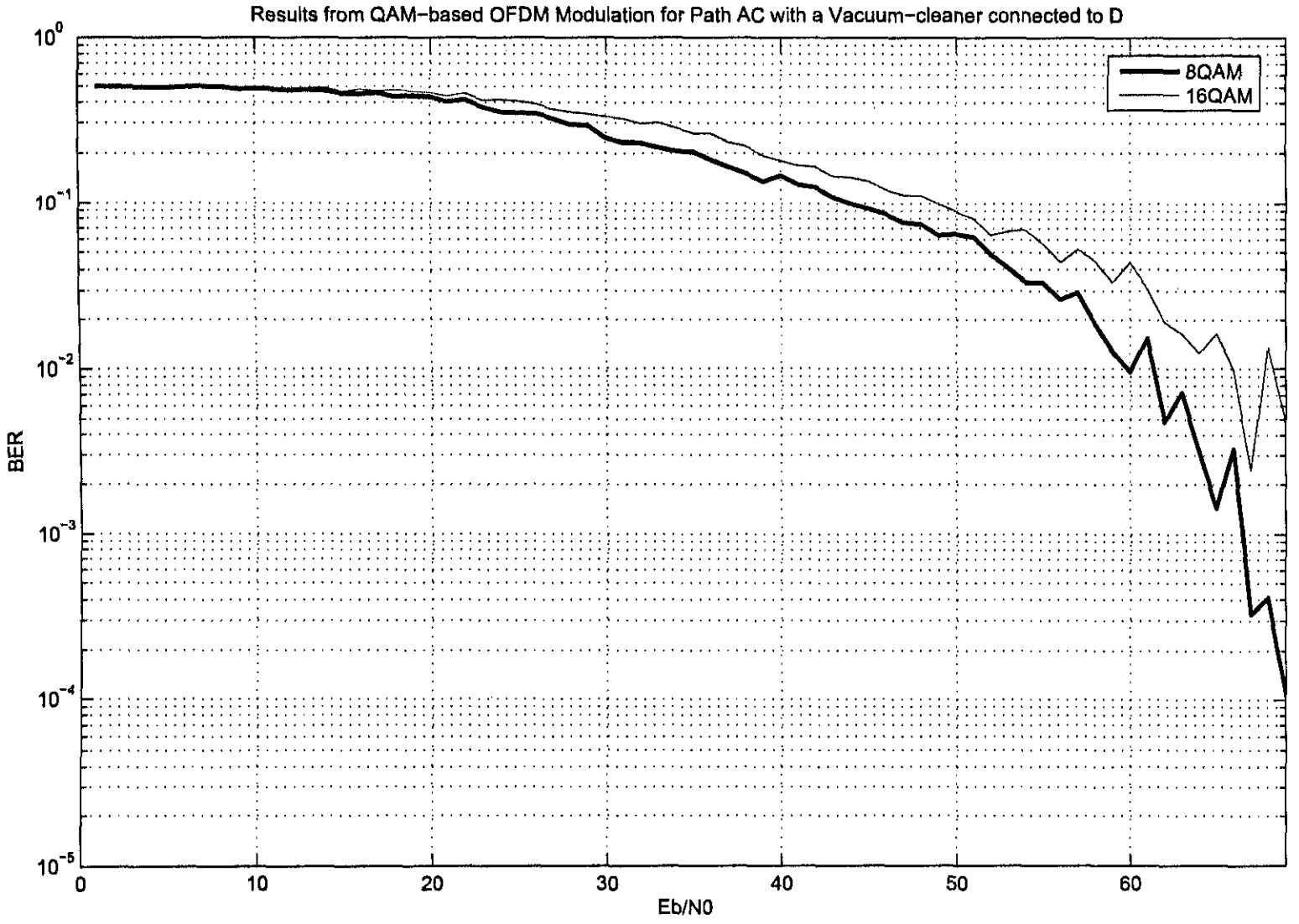

Figure 5.17: Results (QAM) - Scenario 2

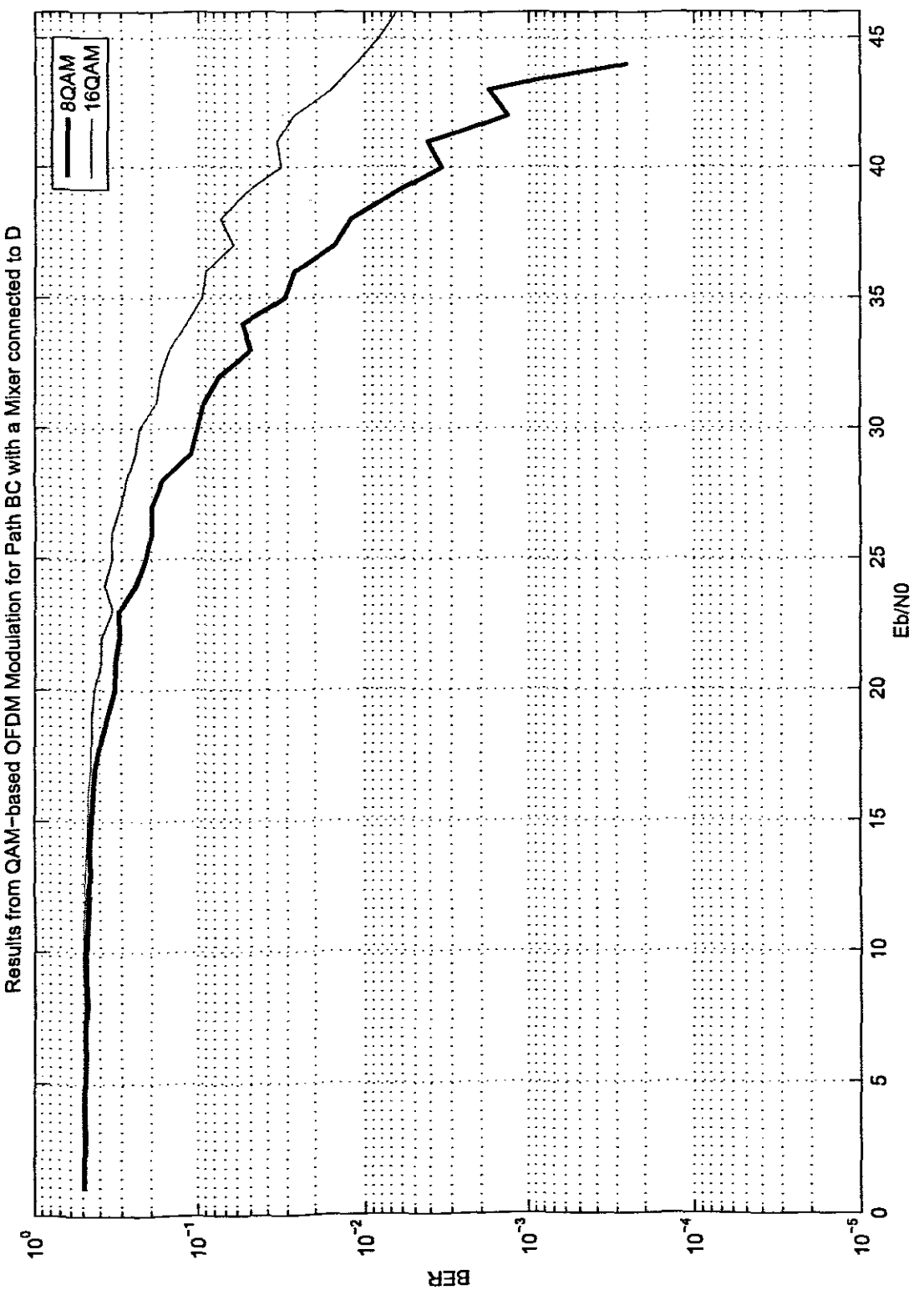

Figure 5.18: Results (QAM) - Scenario 3

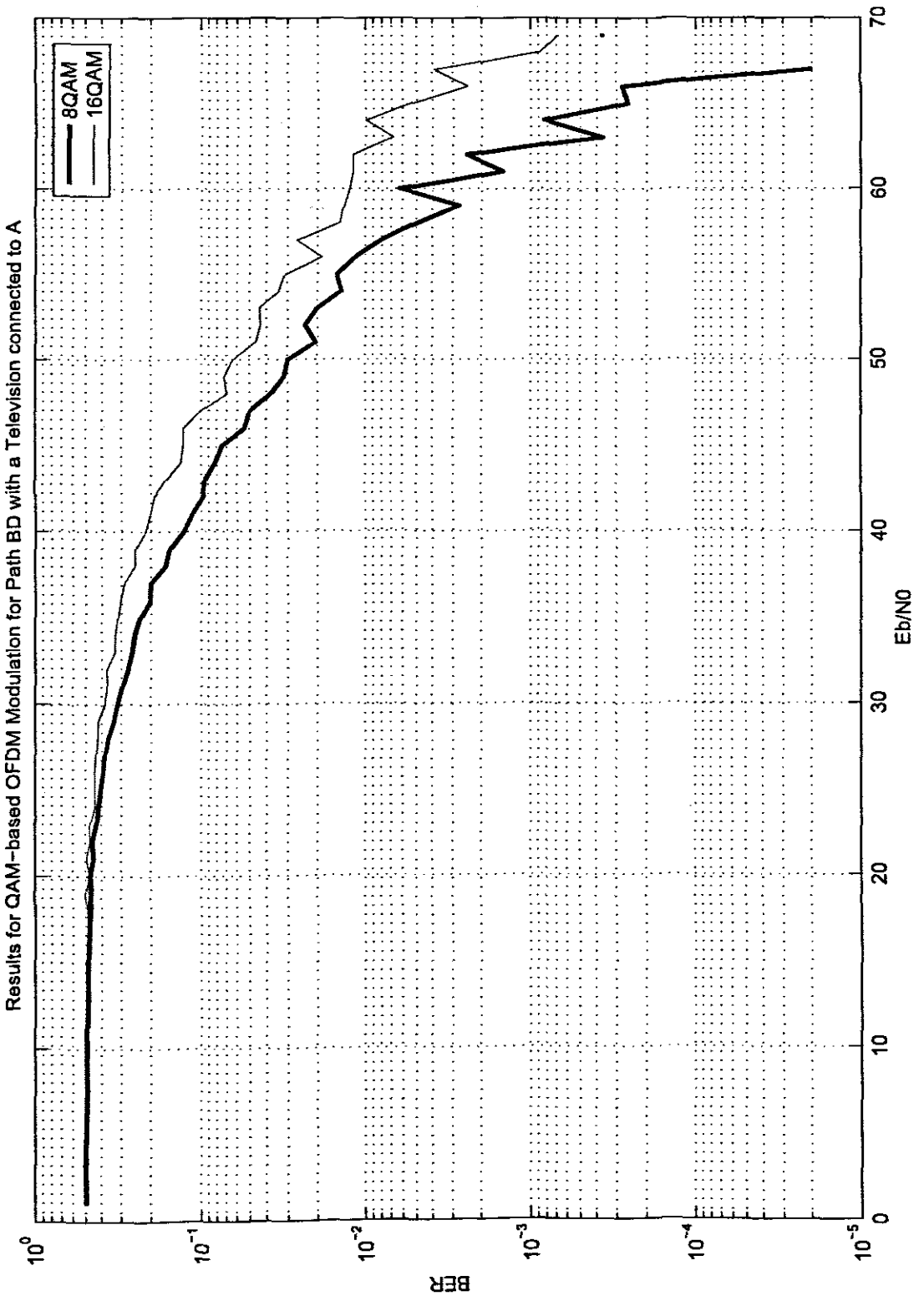

Figure 5.19: Results (QAM) - Scenario 4

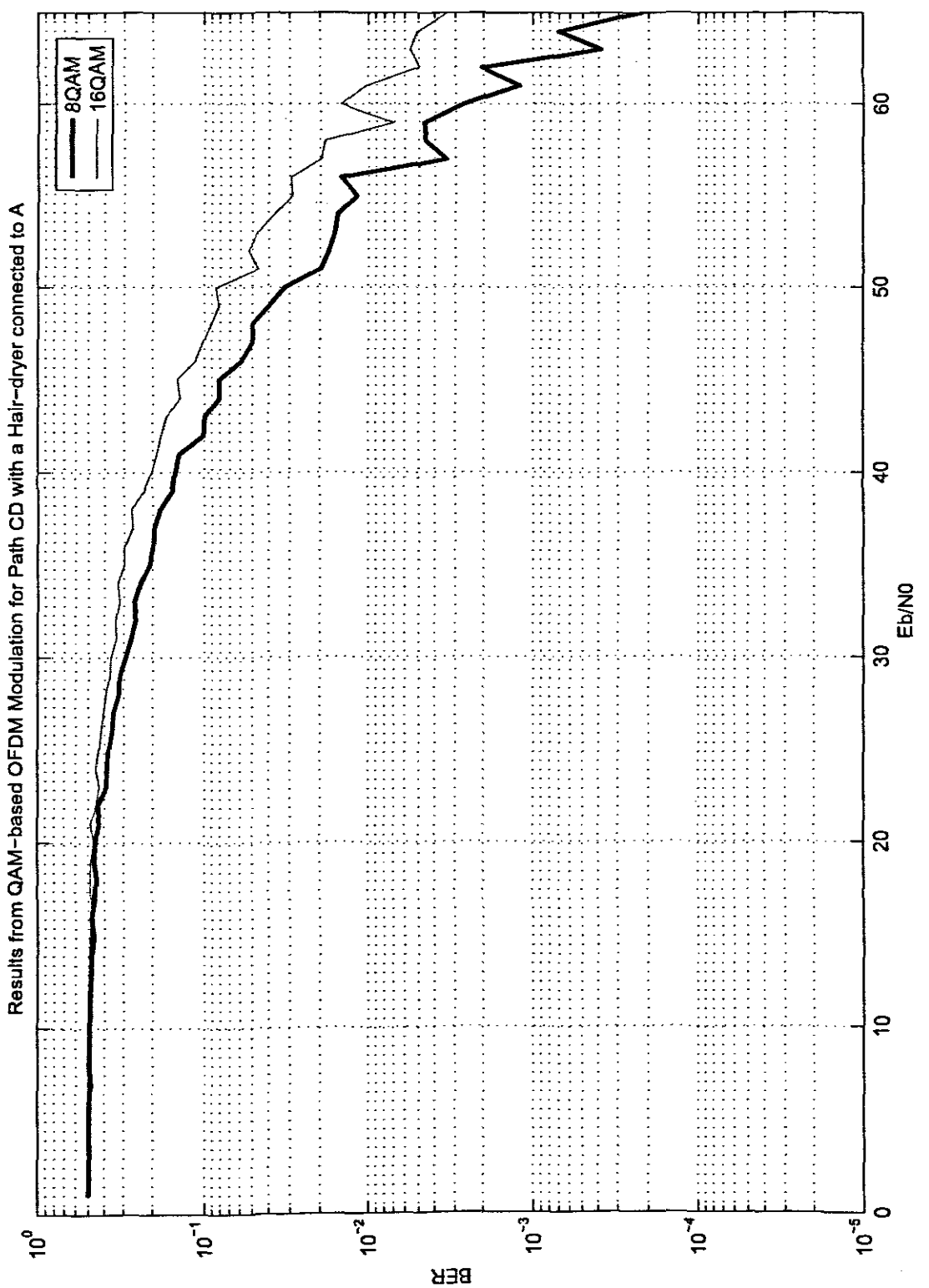

Figure 5.20: Results (QAM) - Scenario 5

5.3.3.2 Scenario 2

The second scenario results indicate (for this scenario):

- OFDM-8QAM has a better BER response than OFDM-16QAM
- OFDM-16QAM BER becomes worse as the Eb/N0 increases

When compared to OFDM-PSK and OFDM-DPSK, as expected, the BERs are higher. This can be explained when examining the Transfer function (Figure 5.2) plot, where three major attenuation dips are visible. Since the number of bits carried in each information symbol increases for QAM-based methods, so too does the probability of error increases as more bits are in error, especially on carriers near the attenuation dips.

5.3.3.3 Scenario 3

The third scenario, the Transfer function indicates an average attenuation of $\approx$ -10dB. This can then be assessed as the best case scenario, compared to the other four scenarios.

When examining the OFDM-8QAM and OFDM-16QAM BER responses (Figure 5.18), it is evident that the BER performance of OFDM-16QAM degrades with the increase in Eb/N0. There is $\approx$ 8dB difference between OFDM-BPSK and OFDM-DBPSK, compared to OFDM-8QAM as well as OFDM-QPSK, OFDM-DQPSK when compared to OFDM-16QAM.

5.3.3.4 Scenario 4

When examining the BER responses of both OFDM-PSK and OFDM-DPSK (Figures 5.9 and 5.14) of this scenario, compared to the results of OFDM-8QAM and OFDM-16QAM, again there is difference of $\approx$ 3dB in performance.

As has been the trend in previous scenarios, including this scenario, OFDM-8QAM has an advantage over OFDM-16QAM (as expected).

5.3.3.5 Scenario 5

In the final scenario, examination of the BER responses (Figure 5.20) indicates that OFDM-16QAM an increase in BER is to be expected with an increase in Eb/N0.

OFDM-8QAM BER response indicates a difference of ≈ 4-6dB, when compared to OFDM-PSK and OFDM-DPSK techniques in the same scenario. The OFDM-QAM BER responses depict degraded performance compared to the other OFDM techniques.

5.3.4 Comparative analysis and recommendations

In the previous sections, comparisons were made regarding BER performances amongst particular groups of modulation i.e. PSK, DPSK and QAM. This section will focus around the analysis of comparative BER results, shown in Figures 5.21 to 5.25.

When analysing the respective comparative BER plots, the following can be noted:

- *OFDM-DQPSK and OFDM-QPSK have identical responses in all of the given scenarios*
  As previously stated, from the BER results presented, it can be concluded that in most cases, coherent or non-coherent sub-modulation method have similar performances.

- *OFDM-BPSK has the best BER response in comparison with the other PSK, DPSK, QAM OFDM methods*
  When referring to theoretical probability of error, BPSK along with QPSK (both having identical probability of errors) are the best coherent modulation methods (Harada & Prasad 2002). It is thus expected that OFDM-BPSK would produce the best BER plot, as determined in (Harada & Prasad 2002) that overall OFDM probability of error would be equal to the sub-modulation's probability of error.

- *The OFDM-QAM techniques has the worst BER performances compared to the rest of the techniques*
  Performance of the OFDM-QAM techniques can be enhanced by applying a multi-tap equaliser (to improve distortion mitigation via channel estimation).

- *On average, a high Eb/NO is required for the effective and reliable transmission, through this particular channel*
  To reach an acceptable BER of 10^{-5}, with most of the scenarios, except Scenario 3, an average Eb/NO of $\pm$ 65dB. In terms of transmission, the average power of the transmitted signal,

needs to be quite high, in order to increase the probability of efficient and reliable data reception.

Given the last observation, it can also be concluded that in performance of uncoded OFDM Transmission, will not be able to present a viable solution, in terms of a transmission system, without the aid of an appropriate error detection / correction strategy.

5.3.4.1 Recommendations for a OFDM-PLC Communication system

Based on the results discussed thus far and on the comparative BER plots, the author recommends the use of either:

– *BPSK* or

– *DBPSK*

based on the good BER peformances of these two techniques, depicted in the comparative BER plots (Figures 5.21 to 5.25). Combined with appropriate error correction / detection strategies such as channel coding (Convolutional coding, BCH Coding, etc.) (Bateman 1999), (Sklar 2001) an optimised Home PLC OFDM Communication system can be realised.

This recommendation is based on specific criteria. In the case of BPSK or DBPSK, the results have shown that whether coherent or non-coherent modulation methods are used, in the case of the domestic power line channel, that attenuation is the strongest factor leading to the degradation of the transmitted signal (due to ad-hoc impedance variations on the power network).

And since the simulated throughput (42MBps) has been the same for all the OFDM variations, the comparison using BER, is sufficient and thus conclusions based on the BER plots are conclusive.

5.4 Conclusion

In this chapter, results for the five selected scenarios were presented and discussed. A comparative analysis of undertaken and the author's recommendations for a OFDM-PLC Communication system was given.

The final objective is thus reached and thus concludes the chapter.

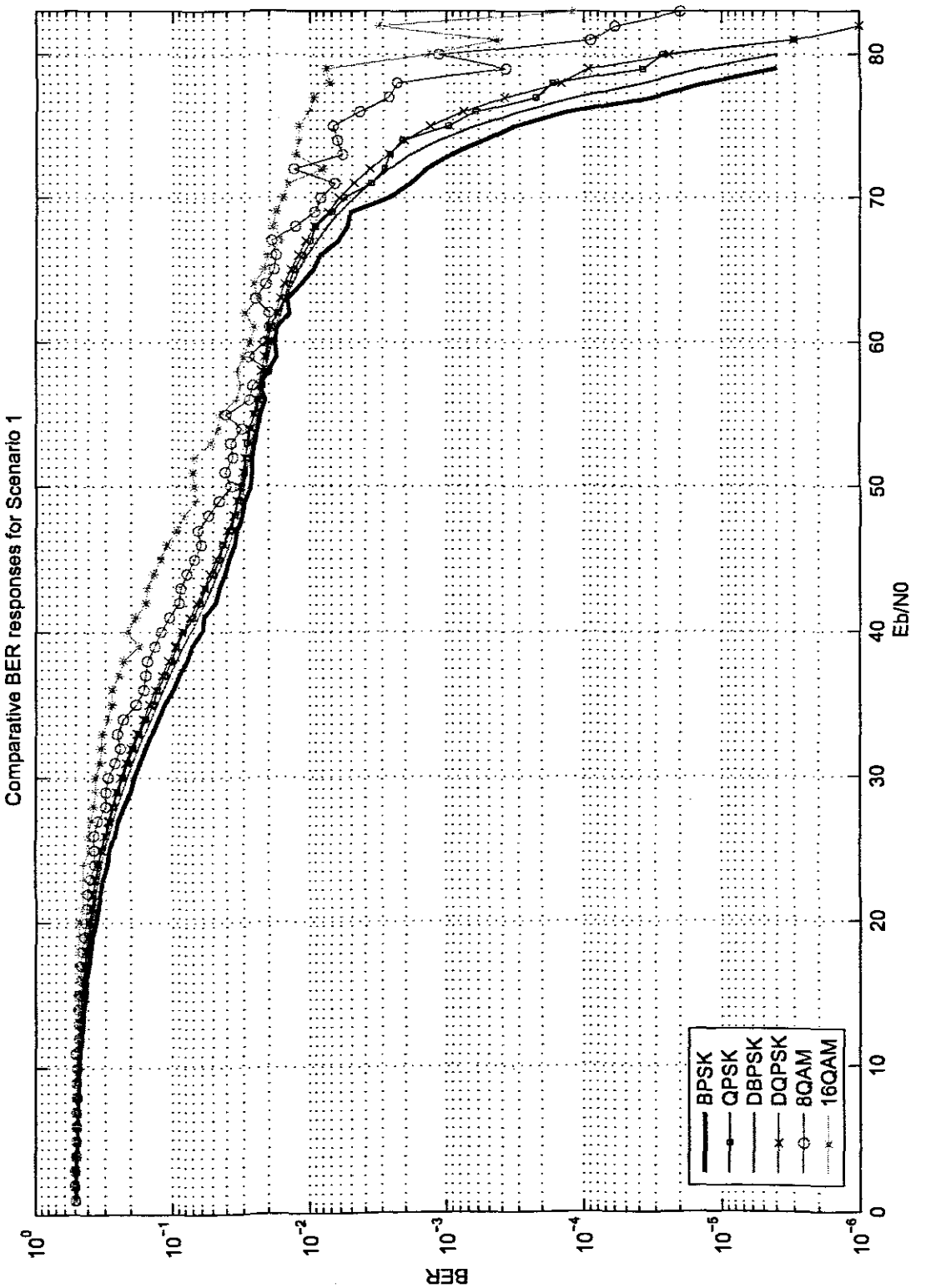

Figure 5.21: Scenario 1 - Comparative Results

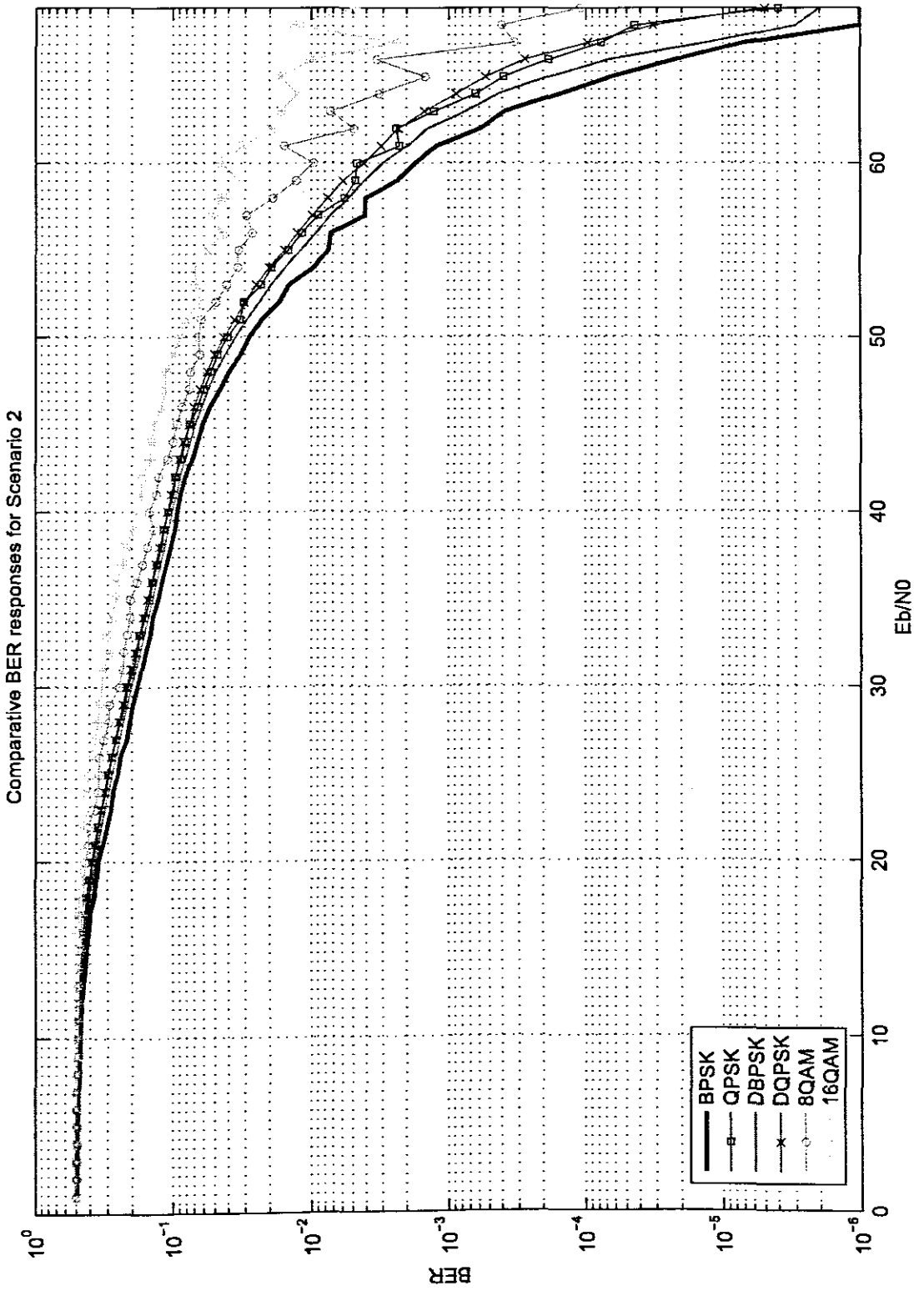

Figure 5.22: Scenario 2 - Comparative Results

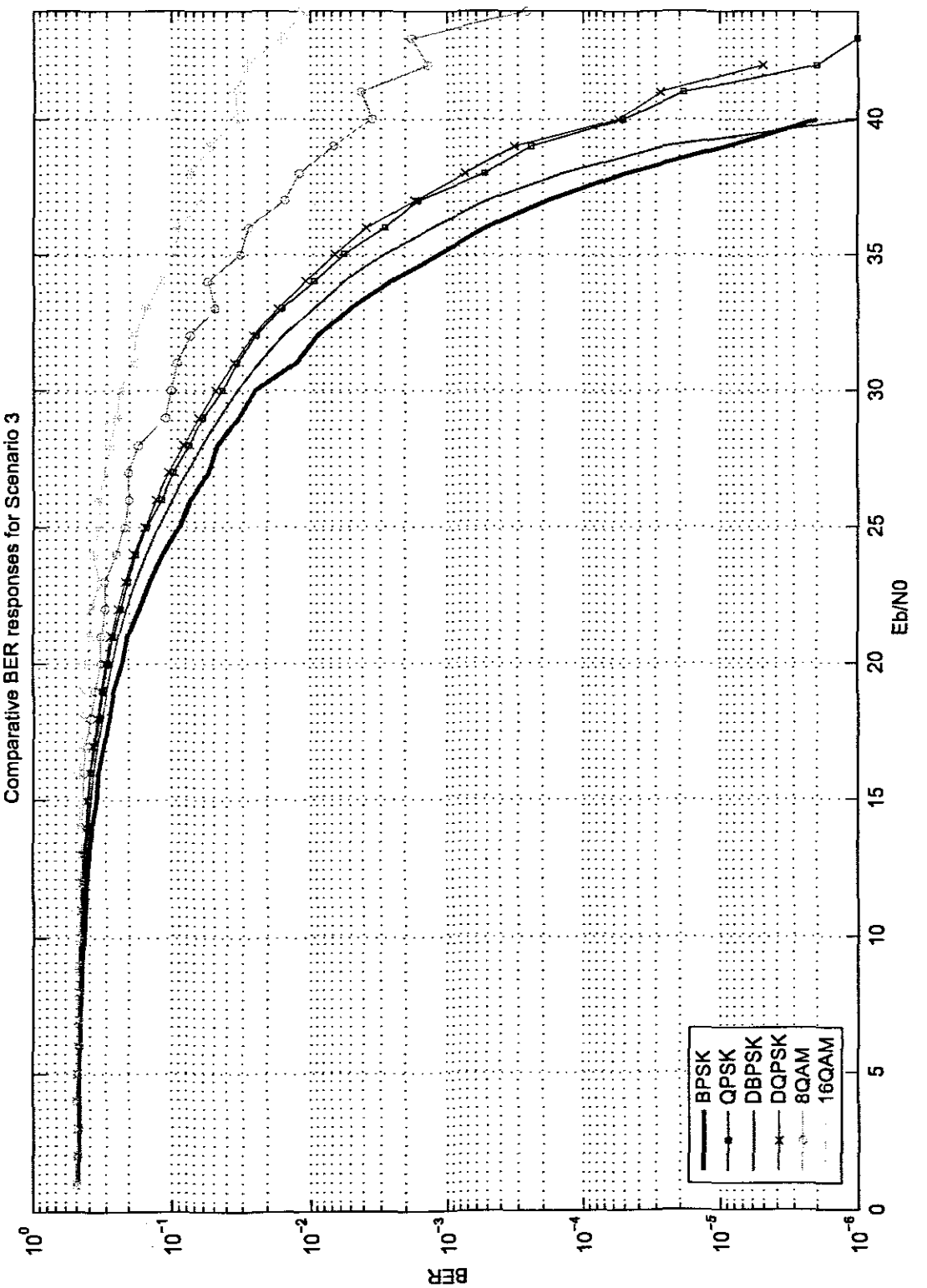

Figure 5.23: Scenario 3 - Comparative Results

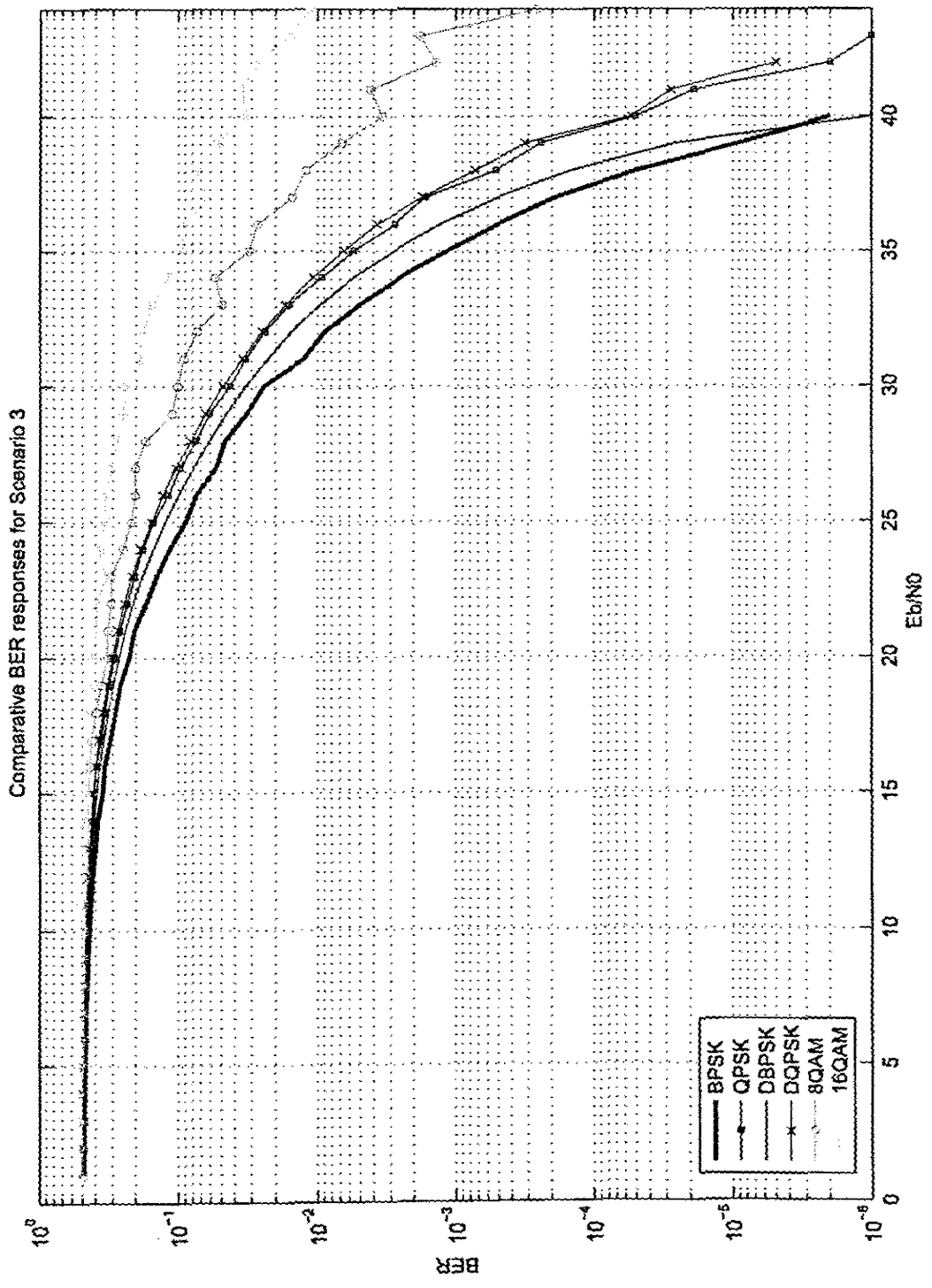

Figure 5.23: Scenario 3 - Comparative Results

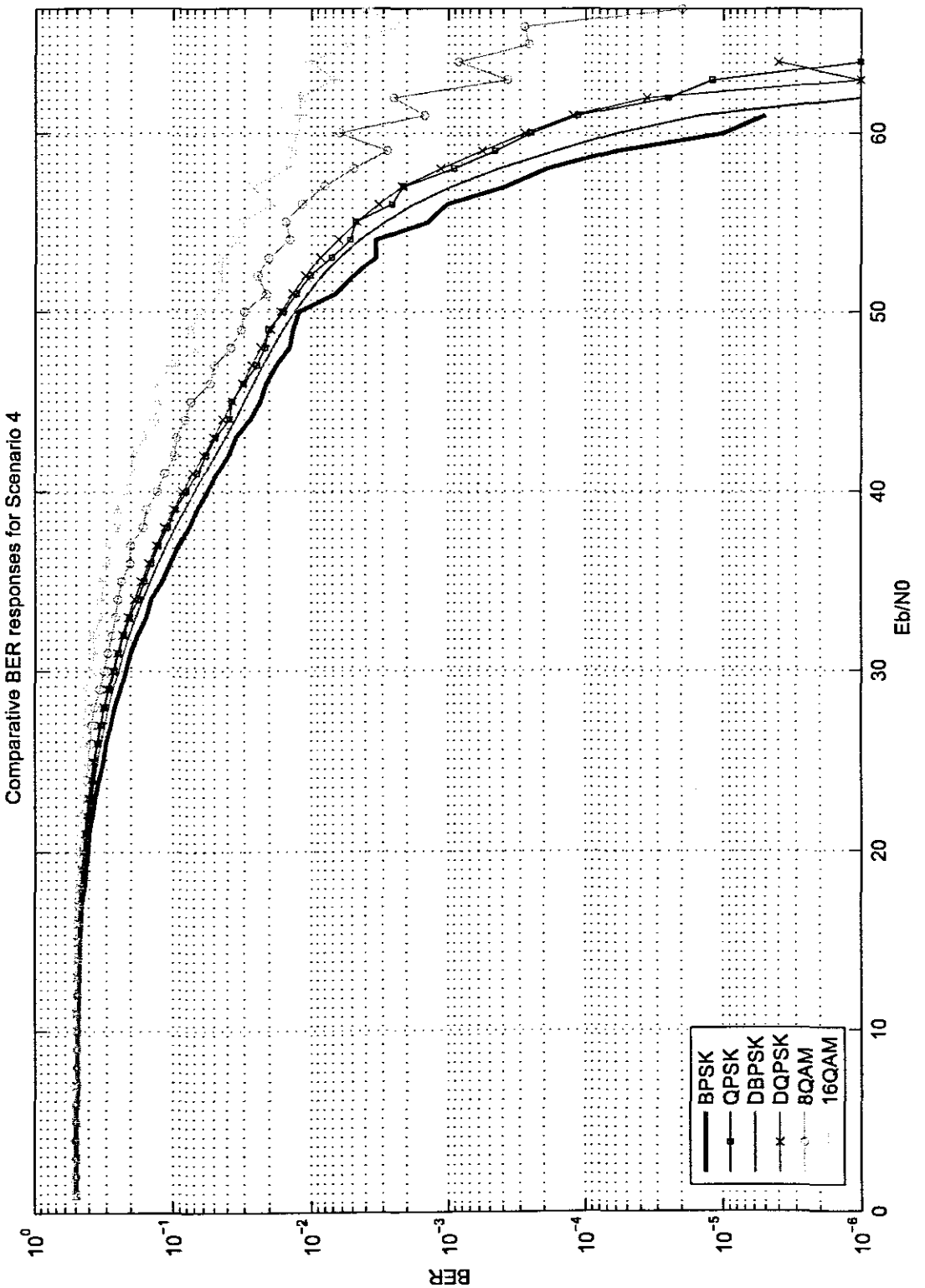

Figure 5.24: Scenario 4 - Comparative Results

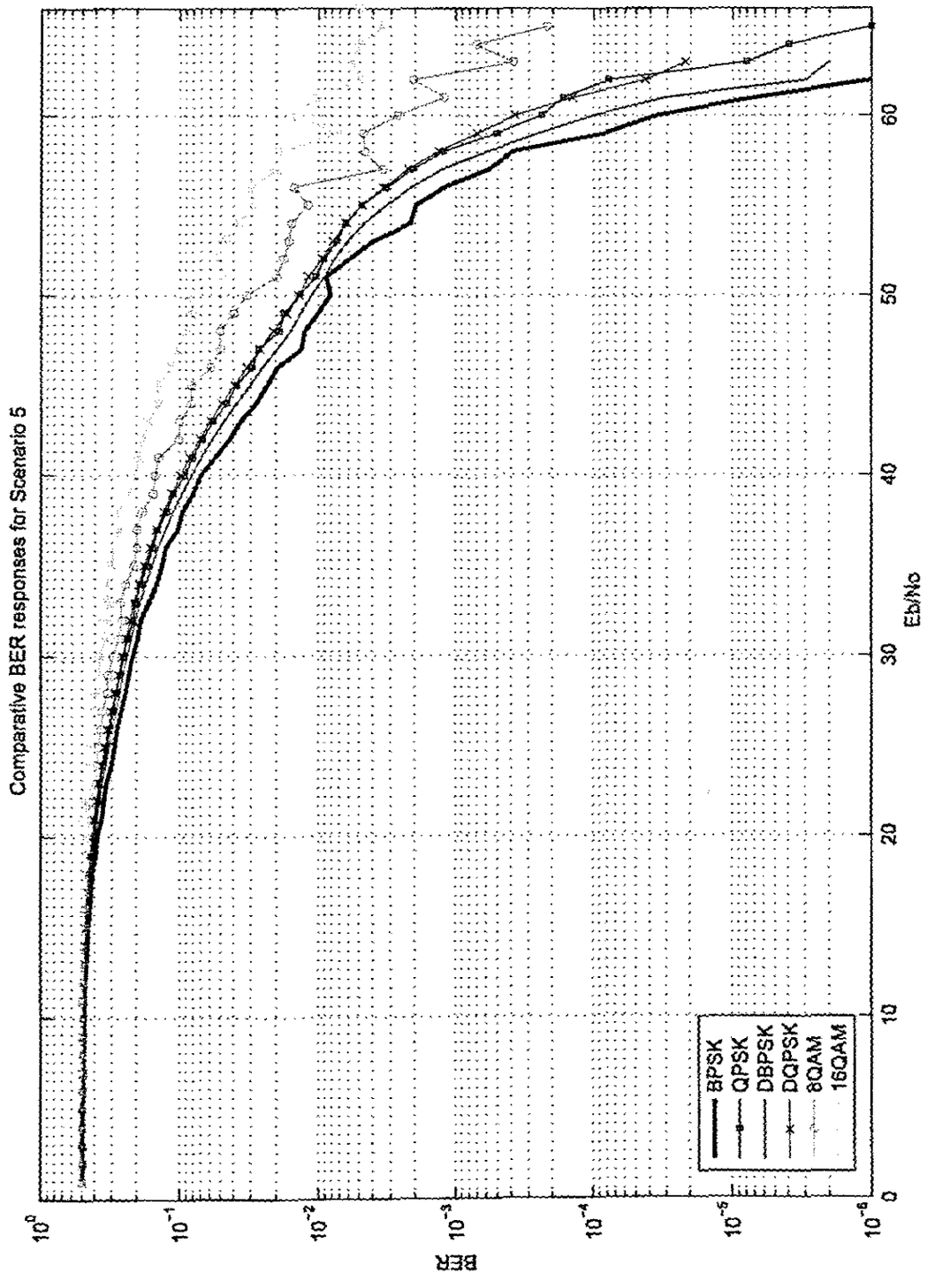

Figure 5.25: Scenario 5 - Comparative Results

Chapter 6

Conclusion

6.1 Overview and Achievements

The aim of this research project was to evaluate the performance of various sub-modulation techniques for an OFDM-based domestic power line modem. This has entailed the evaluation of OFDM modulation techniques (e.g. OFDM-BPSK, OFDM-QPSK, etc.) to determine an optimal specification for a domestic powerline modem.

The project started with research into Power Line Communication and Digital Modulation techniques, including multi-carrier transmission methods (Chapter 2). This provided the author with a better understanding of the domestic power line environment, as well as which communication strategies would be applicable in operating in this harsh environment.

An important step in fulfilling the aim of this research project, was the development of a SA domestic power line model. This has involved (Chapter 3):

- The construction of an experimental domestic power network for modeling purposes
- Measuring the characteristics of the power network (using a Network Analyser), with and without appliances connected to the experimental network
- Processing the measured results (S-Parameters) for all of the possible (84) scenarios to develop a domestic power line channel model in MATLAB

MATLAB was used to create the simulation environment for simulating the necessary scenarios for evaluation. Selected OFDM-based modulation algorithms were developed and implemented in MATLAB, and using the domestic power line model channel. A fully simulated, domestic PLC OFDM-based communication system was thus realised (Chapter 4).

Using the Simulation tool, an evaluation was conducted (Chapter 5) of 5 selected scenarios using various selected OFDM-base modulation schemes, e.g. OFDM-BPSK, OFDM-QPSK, etc. The evaluation consisted of a comparative analysis of the modulation schemes, by examining the respective BER plots for a given scenario.

The following was concluded from the results:

- OFDM-DQPSK and OFDM-QPSK have identical responses
- OFDM-BPSK has the best BER response in comparison with the other PSK, DPSK, QAM OFDM methods
- The OFDM-QAM techniques have the worst BER performances

Based on the simulations, the author recommends the use of either:

- BPSK or
- DBPSK

based OFDM communication system for use on the domestic power line network based on their respective BER responses. The author also recommends that an appropriate error correction / detection strategy, such as channel coding (Convolutional coding, BCH Coding, etc.), should be included.

In terms of research deliverables, a paper, titled *Transfer function approximation of an experimental domestic power network*, co-authored by the author and R. Van Zyl, was submitted

and accepted at the IEEE Africon 2004 (Wicomb & Van-Zyl 2004). Also a paper *Approximation methods for modeling an domestic power network*, has been submitted to JEDT (CPUT Research Journal).

6.2 Future Work

6.2.1 Simulation Software

Envisaged future work, in terms of Simulation software will involve developing additional features to the current MATLAB scripts to include:

- Channel Coding: Forward Error Correction (FEC) using either Convolutional Coding with Viterbi Decoding or Reed-Solomon Encoding and Decoding (Sklar 2001) to improve the system performance. This is depicted in Figure 6.1.
- Root raised-cosine filtering to be employed in the transmitter (Bateman 1999)
- Multi-tap equalisation implementation to be incorporated in the OFDM-QAM simulations
- Generation of an Eye-diagram for further performance analysis

6.2.2 Hardware Implementation

The realisation of a hardware equivalent of the simulated system, using DSP (Digital Signal Processing) technology, will aid in the determining the accuracy of the simulated system itself.

This stage would be a fundamental step if research in this particular subject is further undertaken by the author.

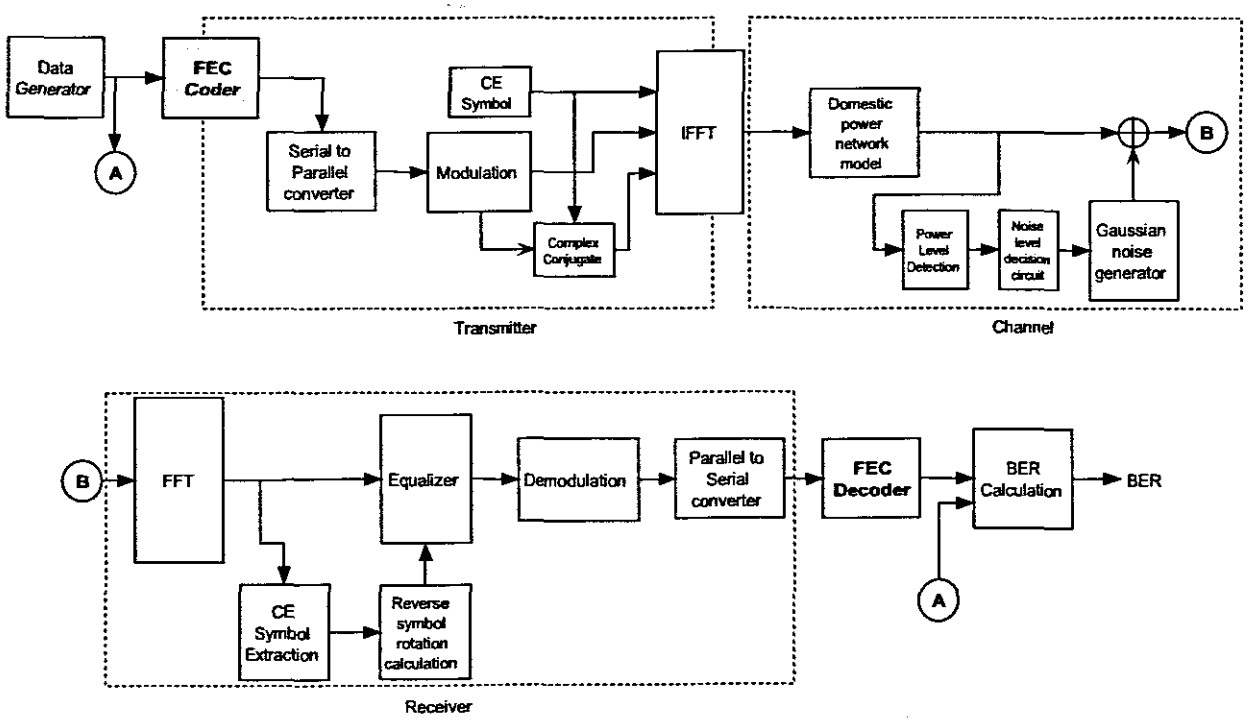

Figure 6.1: OFDM Simulation Diagram with FEC

LIST OF REFERENCES

Agilent-Technologies (2002). 'Measurement challenges for OFDM systems'. Tech. rep., Agilent Technologies.

D. Anastasiadou & T. Antonakopoulos (2002). 'An Experimental Setup for Characterizing the Residential Power Grid Variable Behaviour'. In *Proceedings of the 6th International Symposium on Power Lines Communications.*

V. B. Balakirsky & A. Han-Vinck (2005). 'Potential Limits on Power-Line Communication over Impulsive Noise Channels'.

T. Banwell & S. Galli (2001). 'A new approach to the modeling of the transfer function of the power line channel'. In *International Conference on Power Line Communications and Its Applications.* ISPLC, IEEE.

A. Bateman (1999). *Digital Communications - Design for the Real World.* Addison-Wesley.

E. Biglieri (2003). 'Coding and Modulation for a Horrible Channel'. *IEEE Communications Magazine* pp. 92–98.

J. Bingham (1990). 'Multicarrier Modulation for Data Transmission: An Idea whose time has come'. *IEEE Communications Magazine* pp. 5–14.

F. J. Cañete, et al. (2002). 'Broadband modelling of indoor power-line channels'. *IEEE Transactions on Consumer Electronics* **48**(1):175–183.

M. Chan & R. W. Donaldson (1989). 'Amplitude, Width and Interarrival Distributions for Noise Impulses on Intrabuilding Power Line Communication Networks'. *IEEE Transactions on Electromagnetic Compatibility* **31**(3):320–323.

L. Cimini (1985). 'Analysis and Simulation of a Digital Mobile Channel Using Orthogonal Frequency-Division Multiplexing'. *IEEE Transactions on Communications* **33**(7):665–675.

D. Clark (1998). 'Powerline Communications: Finally Ready for Prime Time ?'. *IEEE Internet Computing* **2**(1):10–11.

S. Coleri, et al. (2002a). 'Channel Estimation Techniques Based on Pilot Arrangement in OFDM systems'. *IEEE Transactions on Broadcasting* **48**(3):223–229.

S. Coleri, et al. (2002b). 'A Study of Channel Estimation in OFDM Systems'. In *Proceedings of IEEE 56th Vehicular Technology Conference*, pp. 894–898. IEEE, IEEE.

D. Cooper & T. Jeans (2002a). 'Narrowband, Low Data Rate Communications on the Low-Voltage Mains in the CENELEC Frequencies-Part I: Noise and Attenuation'. *IEEE Transactions on Power Delivery* **17**(3):718–723.

D. Cooper & T. Jeans (2002b). 'Narrowband, Low Data Rate Communications on the Low-Voltage Mains in the CENELEC Frequencies-Part II: Multiplicative Signal Fading and Efficient Modulation Schemes'. *IEEE Transactions on Power Delivery* **17**(3):724–729.

E. Cosby (2001). 'Orthogonal Frequency Division Multiplexing (OFDM): Tutorial and Analysis'. Tech. rep., Virginia Tech. - Northen Virginia Center.

L. Couch (1995). *Modern Communication Systems*. Prentice Hall.

B. G. D. Liu, E. Flint & Y. Kwark (1999). 'Wide Band AC Power line characterization'. *IEEE Transactions on Consumer Electronics* **45**(4):1087–1097.

V. Degardin & M. Lienard (2002). 'Interference on Multicarrier-based Power Line Communication systems'. In *Proceedings of the XXVIIth General Assembly of the International Union of Radio Science*.

K. Dostert (2001). *Powerline Communications*. Prentice Hall PTR, 1 edn.

K. Dostert & M. Zimmerman (2000). 'An analysis of the broadband noise scenario in powerline networks'. In *Proceedings of the 4th International Symposium on Powerline Communication and Its Applications*, pp. 131–138.

O. Edfors, et al. (1996). 'An introduction to Orthogonal Frequency Division multiplexing'. Research report, Luleå University of Technology.

H. Harada & R. Prasad (2002). *Simulation and Software Radio*. Universal Personal Communications Series. Artech House.

S. Haykin (1988). *Digital Communication*. John Wiley and Sons, third edn.

Homeplug-Alliance (2005). 'http://www.homeplug.org'.

M. Ingram (2000). 'OFDM Simulation using MATLAB'. Tech. rep., Smart Antenna Research Laboratory - Guillermo Acosta.

T. Keller, et al. (2001). 'Orthogonal Frequency Division Multiplex synchronization techniques for frequency-selective fading channels'. *IEEE Journal on selected areas in communications* **19**(6).

C. J. Kim & M. F. Chouikha (2002). 'Attenuation Characteristics of High Rate Home-Networking PLC signals'. *IEEE Transactions on Power Delivery* **17**(4):945–950.

C. N. Krishnan, et al. (2002). 'Power - Line as Access Medium - A Survey'. Tech. rep., MIT.

P. Langfeld & K. Dostert (2000). 'OFDM System synchronization for Powerline communications'. In *Proceedings of the 4th International Symposium on Powerline Communications*, pp. 15–22. ISPLC.

E. Lawrey & C. Kikkert (1999). 'Peak to Average Power Ratio Reduction of OFDM Signals using Peak Reduction Carriers'. In *Proceeding of the Fifth International Symposium on Signal Processing*, pp. 737–740, Brisbane Australia. Signal Processing Research Centre, QUT.

M. Lee, et al. (2003). 'HomePlug 1.0 powerline communication LANs - protocol description and performance results'. *International Journal of Communication systems* **16**:447–473.

Y.-J. Lin, et al. (2003). 'A Comparative performance study of wireless and power line networks'. *IEEE Communications Magazine* **41**(4).

L. Litwin & M. Puegel (2001). 'The principles of OFDM'. *RF Design (www.rfdesign.com)* pp. 32–48.

E. Liu, et al. (2004). 'Broadband characterization of indoor powerline channel'. In *8th International Symposium on Power-Line Communications and Its Applications (ISPLC)*. ISPLC, ISPLC.

D. Matic (1998). 'OFDM for Wireless Broadband'. In J.-P. Linnartz (ed.), *The Interactive Multimedia CDROM ISSN 1383-4231*. Wireless Communication.

A. Matov (2001). 'Measurements and Modelling of Power Line Channel at High Frequencies'. In *AIC 2001 Proceedings of the IASTED International Conference on Advanced Communications*, pp. 118–123.

N. Morrison (1994). *Introduction to Fourier Analysis*. Wiley and Sons.

National-Instruments (2004). 'S-Parameters'.

J. B. O'Neal (1986). 'The residential power circuit as a communication medium'. *IEEE Transactions on Consumer Electronics* **CE-32**(3):567–577.

D. Pozar (1998). *Microwave Engineering*. John Wiley and Sons, 2 edn.

D. Radford (1996). 'Spread-spectrum data leap through ac power wiring'. *IEEE Spectrum* **18**:48–43.

D. Raphaeli & E. Bassin (1999). 'A Comparison Between OFDM, Single Carrier, and Spread Spectrum for High Data Rate PLC'. International Symposium on Power-line Communications and its Applications.

B. Sklar (2001). *Digital Communications*, vol. 1. Prenitice Hall, 2 edn.

J. Smith (2003). 'Mathematics of the Discrete Fourier Transform'. Tech. rep., Centre for Computer Research in Music and Acoustics, Department of Music, Stanford University, http://www-ccrma.stanford.edu/ jos/mdft.

F. Stremler (1990). *Introduction to Communication Systems*. Addison-Welsey, third edn.

P. Sutterlin & W. Downey (1999). 'A Power Line Communication Tutorial - Challenges and Technologies'. Tech. rep., Echelon Corporation.

P. K. Van-Der-Gracht & R. W. Donaldson (1985). 'Communication using Psuedonoise Modulation on Electric Power Distribution Circuits'. *IEEE Transactions on Communications* **COM-33**(9):964–974.

L. Wicomb & R. Van-Zyl (2004). 'Transfer function approximation of an experimental domestic power network'. In *Proceedings of the IEEE Africon 2004*, p. 345. IEEE.

E. Yavuz, et al. (2002). 'Modelling of Power Lines for Digital Communications'. In ISPLC (ed.), *Proceedings of the 6th International Symposium on Power-line Communications and its Applications (ISPLC)*. ISPLC.

B. Sklar (2001). *Digital Communications*, vol. 1. Prenitice Hall, 2 edn.

J. Smith (2003). 'Mathematics of the Discrete Fourier Transform'. Tech. rep., Centre for Computer Research in Music and Acoustics, Department of Music, Stanford University, http://www-ccrma.stanford.edu/ jos/mdft.

F. Stremler (1990). *Introduction to Communication Systems*. Addison-Welsey, third edn.

P. Sutterlin & W. Downey (1999). 'A Power Line Communication Tutorial - Challenges and Technologies'. Tech. rep., Echelon Corporation.

P. K. Van-Der-Gracht & R. W. Donaldson (1985). 'Communication using Psuedonoise Modulation on Electric Power Distribution Circuits'. *IEEE Transactions on Communications* **COM-33**(9):964–974.

L. Wicomb & R. Van-Zyl (2004). 'Transfer function approximation of an experimental domestic power network'. In *Proceedings of the IEEE Africon 2004*, p. 345. IEEE.

E. Yavuz, et al. (2002). 'Modelling of Power Lines for Digital Communications'. In ISPLC (ed.), *Proceedings of the 6th International Symposium on Power-line Communications and its Applications (ISPLC)*. ISPLC.

Appendix A: Orthogonal functions in Digital Communication

A.1 Introduction

Digital Communication can be defined as the transmission of a relatively small number of distinct symbols. It is thus important that a receiver should be able to clearly distinguish between transmitted signals. Ensuring that the transmitted signals are orthogonal, the inner product of the various received signals can be computed. Those that produce a zero result can be eliminated and only one signal of interest will be non-zero and thus identification of that signal. Note that this uniqueness among all other orthogonal signals extends to communication theory as well.

A.2 Orthogonal Theory

The term orthogonal refers to two processes that are spatially orientated at right angles to each other. These processes can be in the form of vectors, matrices, functions, series, etc. More importantly, orthogonal processes have the unique property, that if one calculates the inner product of two processes, the result will be zero for arguments that are not equal and non-zero for arguments that are equal.

To examine the property of orthogonality, discussion on orthogonal vectors will begin.

A.2.1 Orthogonal Vectors

Lets consider two column vectors x and y. Let the dimension for vector x be $Mx1$ and for the vector y be $Nx1$. From matrix theory (N. Morrison, 1994), the inner product of the vectors x and y is defined as $x^{*T}y$ where x^{*T} denotes the transpose of the complex conjugate of vector x.

An inner product function can be described as an operation on two vectors that produces a scalar value. If the **inner product** of vectors x and y are zero, then the two vectors are said to be **orthogonal** (N. Morrison, et al).

Other notations for the inner product are denoted as:

$$x \perp y \longleftrightarrow \langle x, y \rangle = 0 \tag{A.1}$$

where the Inner Product is defined as (J. Smith 2003):

$$\langle x, y \rangle = \sum_{n=0}^{N-1} x(n)\overline{y(n)} \tag{A.2}$$

Example A demonstrates the process of verifying whether two vectors are orthogonal, both mathematically and graphically.

Example A

Let vectors x and y be defined as $x = [1, 1]$ and $y = [1, -1]$

For simplicity, these vectors are real, which means the complex conjugate does not apply:

The inner product of these two vectors equates to (J. Smith 2003):

$$\langle x,y \rangle = \sum_{n=0}^{N-1} x(n)\overline{y(n)}\langle x, y \rangle = x(0) \cdot \overline{y(0)} + x(1) \cdot \overline{y(1)} = 1 \cdot \overline{1} + 1 \cdot \overline{-1}\langle x, y \rangle = 0 \tag{A.3}$$

Thus proving orthogonality between vectors x and y.

The following diagram can graphically represent this:

As can be seen in the figure above, the lines intersect at right angles and are therefore perpendicular, graphically illustrating orthogonality.

Any vector of *finite length* may be *expressed* as a sum of its components along n *mutually orthogonal* vectors provided these vectors form a complete set of perpendicular co-ordinates (F.G.

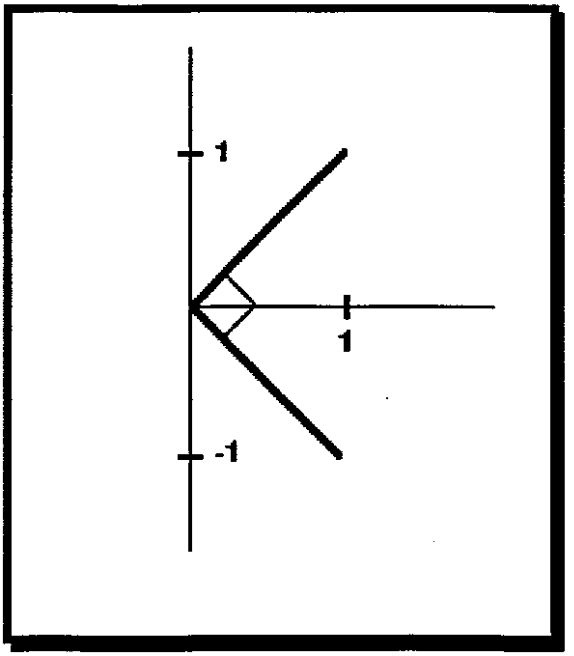

Figure A.1: Vectors x and y

Stremler 1990).

Example B

Consider the vector $\boldsymbol{S}$ with a finite length of 3. Vector $\boldsymbol{S}$ can be expressed as sum of three vectors i.e. $\boldsymbol{S} = \{u, v, x\}$ where vectors u, v, x are mutually orthogonal:

$$u \perp v, v \perp x, u \perp x$$

Vectors u, v, x thus form a complete set of orthogonal functions. The *set of orthogonal functions* are called *basis functions*. u, v, x are therefore the basis functions of $\boldsymbol{S}$.

A.3 Orthogonal Functions

Orthogonal functions represent any particular function be it vector, matrices, complex exponentials, etc. where the functions in the set are mutually orthogonal.

If we consider a set of functions (real or complex):

$$\boldsymbol{S} = \{\phi_1(t), \phi_2(t), \phi_3(t), ..., \phi_n(t)\}$$

over the time interval $(0, T)$ where (F. G. Stremler, 1990):

$$\int_0^T \phi_n(t)\phi_m^*(t)\,\mathrm{d}x = \begin{cases} 0 & when \quad n \neq m \\ K_n & when \quad n = m \end{cases} \tag{A.4}$$

The functions form an orthogonal set since all the functions are mutually orthogonal. The functions are thus referred to as **basis functions**.

If

$$K_n = \int_0^T \mid \phi_n(t) \mid^2 \mathrm{d}x = 1 \ for \ all \ n \tag{A.5}$$

then the above set of basis functions (ϕ_n) are said to be *"normalised"*. The set is then termed as an **orthonormal** set, meaning it is both **orthogonal** and **normalised** (F. G. Stremler, 1990).

Often in signal processing it is required to expand a given function f(t), as a linear combination of orthonormal functions $\phi_n(t)$ (F. G. Stremler 1990, S. Haykin 1988). This can be expressed as:

$$f(t) = \sum_{n=1}^{N} f_n \phi_n(t) \tag{A.6}$$

where

$$f_n = \int_0^T f(t)\phi_n(t) \tag{A.7}$$

Equations A.6 and A.7 will prove useful to the analysis of a Digital communication system. **Equation A.6** represents the **Theorem** for an **Orthogonal Series**. The coefficients (f_n) can be derived through the following proof of Equation A.7:

Proof of Equation A.7

Multiplying Equation A.6 throughout by one of the **orthonormal functions**, $\phi_m(t)$ (which is part of the orthogonal basis vectors) and integrating term by term the following is obtained:

$$\int_0^T f(t)\phi_m(t) = \sum_{m=1}^{N} f_n \int_0^T \phi_n(t)\phi_m(t)\,\mathrm{d}x$$

which, on using Equation A.1 and A.2 reduces to:

$$\int_0^T f(t)\phi_m(t) = f_m \int_0^T \phi_m(t)^2\,\mathrm{d}x$$

or

$$\int_0^T f(t)\phi_m(t) = f_m K_n = f_m$$

(since $K_n = 1$ for orthonormal functions)

This verifies that for the orthonormal function $\phi_m(t)$, the corresponding coefficient is f_m thus proving that Equation A.7 can be used for obtaining the appropriate coefficients f_m.

Orthonormal functions can also be extended to the definition of a Fourier series, where orthonormal functions are used to describe and input function as a linear combination of complex exponentials (F.G. Stremler 1990).

As mentioned in the introduction, the relevance of orthogonal and orthonormal functions in Digital Communication will be discussed. This will follow in the subsequent section.

A.4 Orthogonal functions in Digital Communication

In Digital Communication, there exist a finite number *(N)* of symbols, which can be transmitted. These symbols can be represented by the set $M_i = \{M_1; M_2, ..., M_n\}$. In the transmission stage, these symbols are multiplied by a basis function ϕ_i, then summed together to form the transmitted signal **S(t)**.

Using Equation A.6 function **S(t)** can be represented as the following:

$$S(t) = \sum_{n=1}^{N} M_n \phi_n(t) \tag{A.8}$$

This operation can thus be defined as modulation where symbols are mixed with basis function to the transmitted signal. This is depicted in **Figure A.2**.

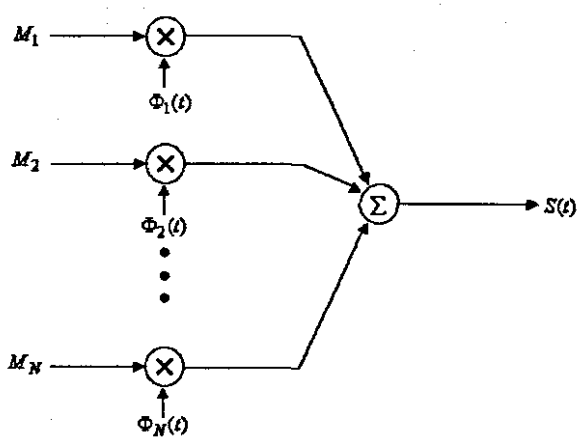

Figure A.2: Scheme for generating S(t)

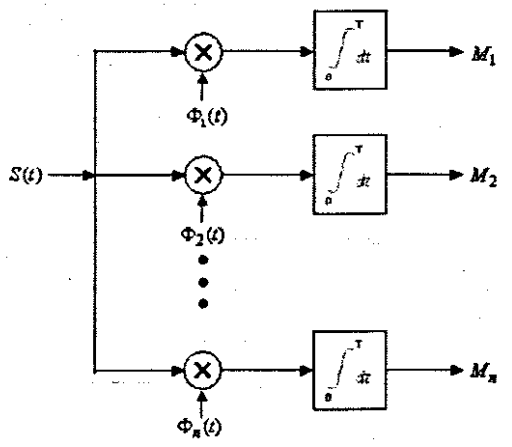

Figure A.3: Correlator Receiver

Inversely, if the symbols (M_n) need to be retrieved from the transmitted signal **S(t), Equation A.2** can be used to determine the symbols. This operation forms the part of the detection stage in a receiver. Looking at the equation below, the operation can be compared to a correlator receiver for time interval (0,T).

$$M_n = \int_0^T S(t)\phi_n(t) \tag{A.9}$$

A.4.1 Orthogonal functions in Quadrature Amplitude Modulation

A modulation system that uses these principles in the transmission and detection of symbols in Quadrature Amplitude Modulation (QAM). QAM can be defined as:

$$S(t) = \sum_{n=1}^{N} M_n\phi_n(t) = I(t)Cos(2\pi ft) + Q(t)Sin(2\pi ft) \tag{A.10}$$

In QAM, the two basis functions are used to carry symbol information:

$$\phi_n(t) = \{Sin(2\pi ft + 90^o); Sin(2\pi ft)\} \tag{A.11}$$

where the symbols are combinations of I and Q levels (M_n) as shown in Figure A.4.

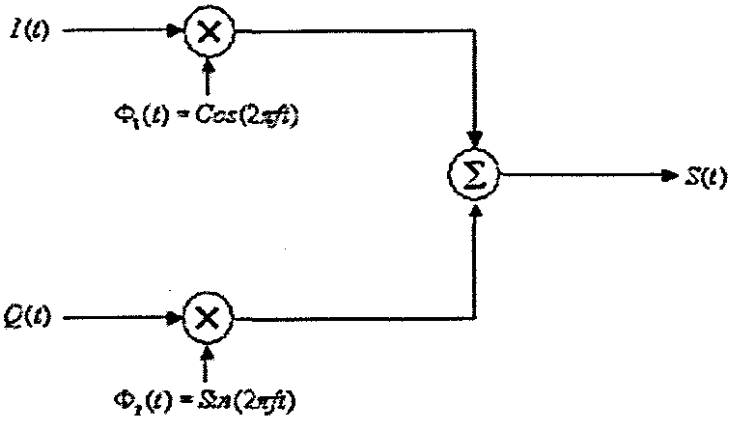

Figure A.4: QAM Modulator

It is therefore possible to use the Correlator Receiver depicted in Figure A.3 for the detection of a QAM Symbol (Figure A.5).

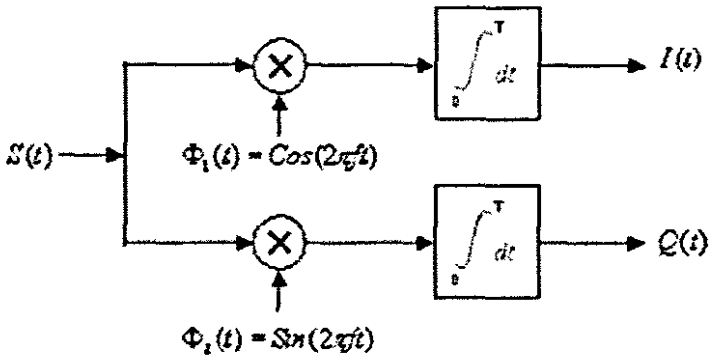

Figure A.5: QAM Correlator Receiver

Appendix B: GUI Development

The development of a graphical user interface (GUI) was necessitated by the need to provide a user-friendly, graphical front-end for the simulation. Since there are only a few simulation parameters which can be set, a GUI ensures that all these parameters are passed to the developed MATLAB functions for simulation.

The objectives for developing a GUI are thus:

- Providing a user-friendly graphical interface to the MATLAB functions for the various simulation options,
- Providing a graphical display of the *domestic power network transfer functions* of the simulated scenarios, including the display of *BER* plots from simulated scenarios.

B.0.1 GUI Development in MATLAB

Constructing the GUI in MATLAB requires the use of GUIDE. GUIDE allows for rapid development of the GUI front-end as well as the generation of the MATLAB script code, which controls the behavior of the various objects within the GUI e.g. buttons, axes, etc.

An object will generate an event (a button is pressed), which will then start the call to a function within the MATLAB script code of the GUI. The developer thus has to add the script code for each function, so that all the object events are processed correctly and that the GUI responds to a user's request. A screen-shot of the GUIDE environment is given in Figure B.1.

For this particular implementation, the GUI has been designed to provide the following functionality:

- Plotting of Transfer functions for various scenarios (example depicted in Figure B.2)
- Capturing of simulation parameters for a selected simulation scenario
- Displaying the results of a simulation (BER plots)

Figure B.3 displays the first screen which the user is presented with, where the experimental network is displayed to provide a graphical view of a simulation scenario. The user is then able to select a particular noise source on the domestic network graphic and manipulate simulation parameters.

Once the user depresses the Simulate button, the process of BER determination starts. The result is a BER plot (an example given in Figure B.4) which is utilized for analysis purposes. The process of creating the BER plot is discussed in the forthcoming section.

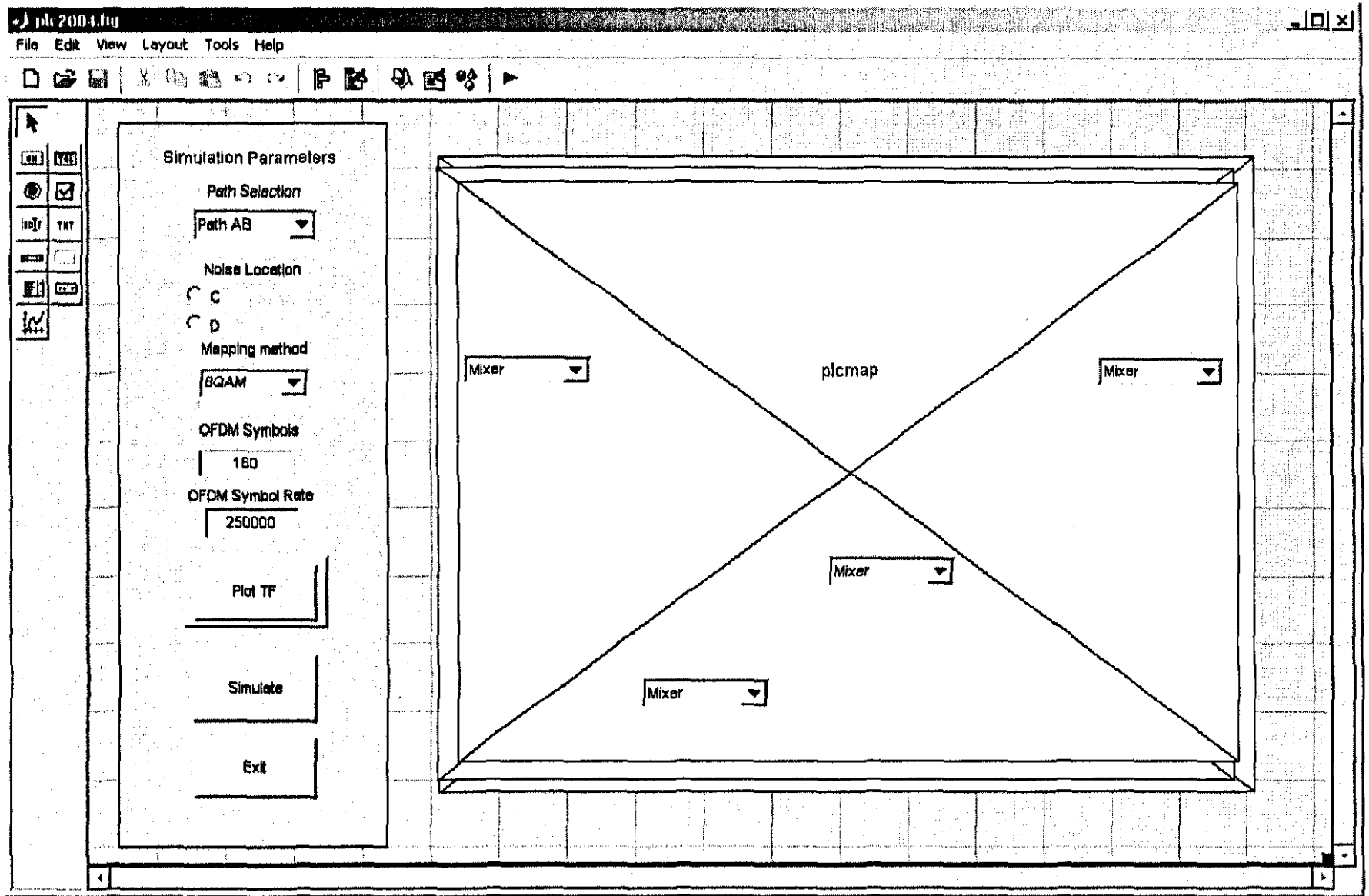

Figure B.1: Screen-shot of the GUIDE Environment used for GUI Development

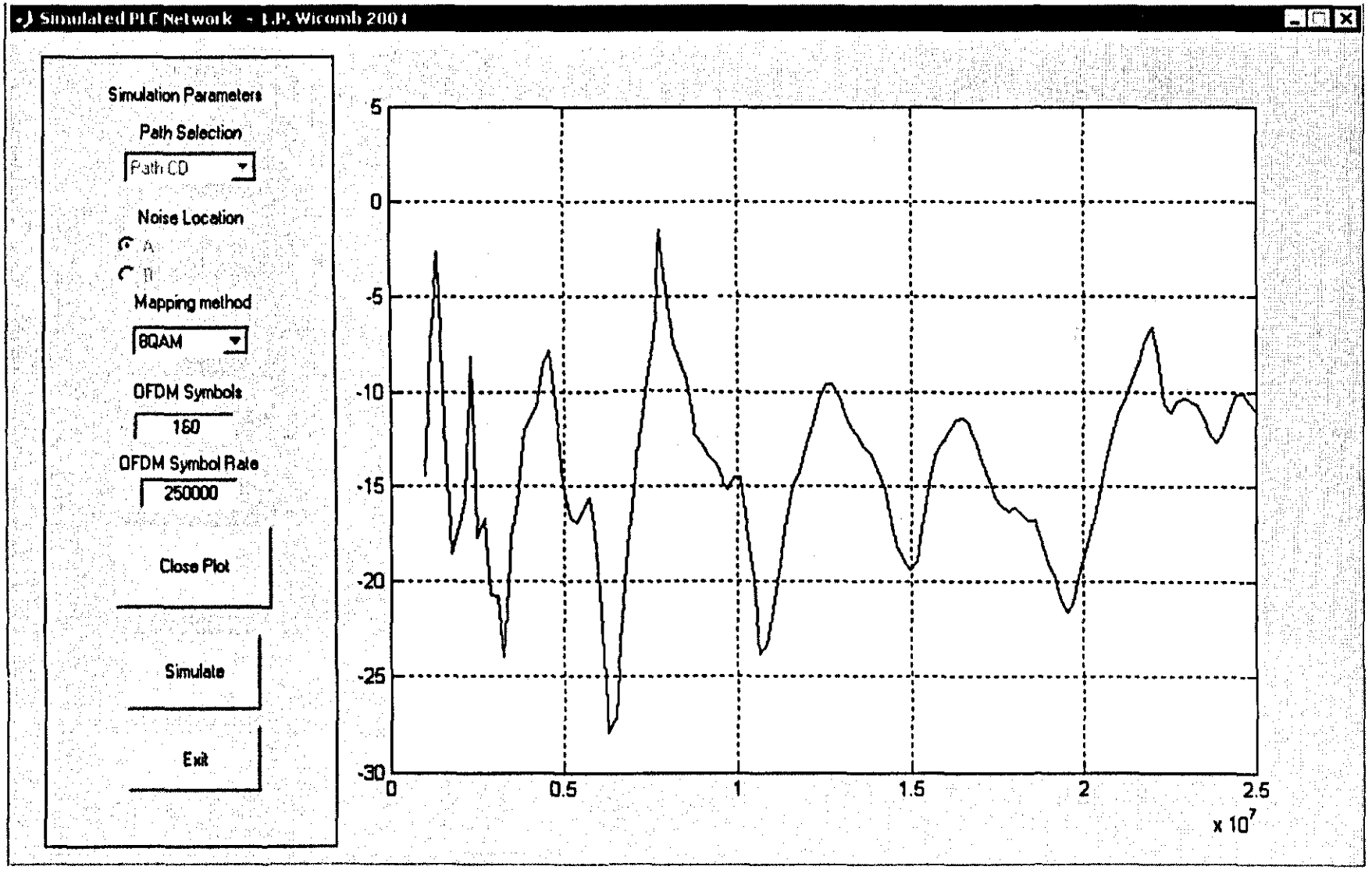

Figure B.2: An example of a TF plot displayed on the GUI

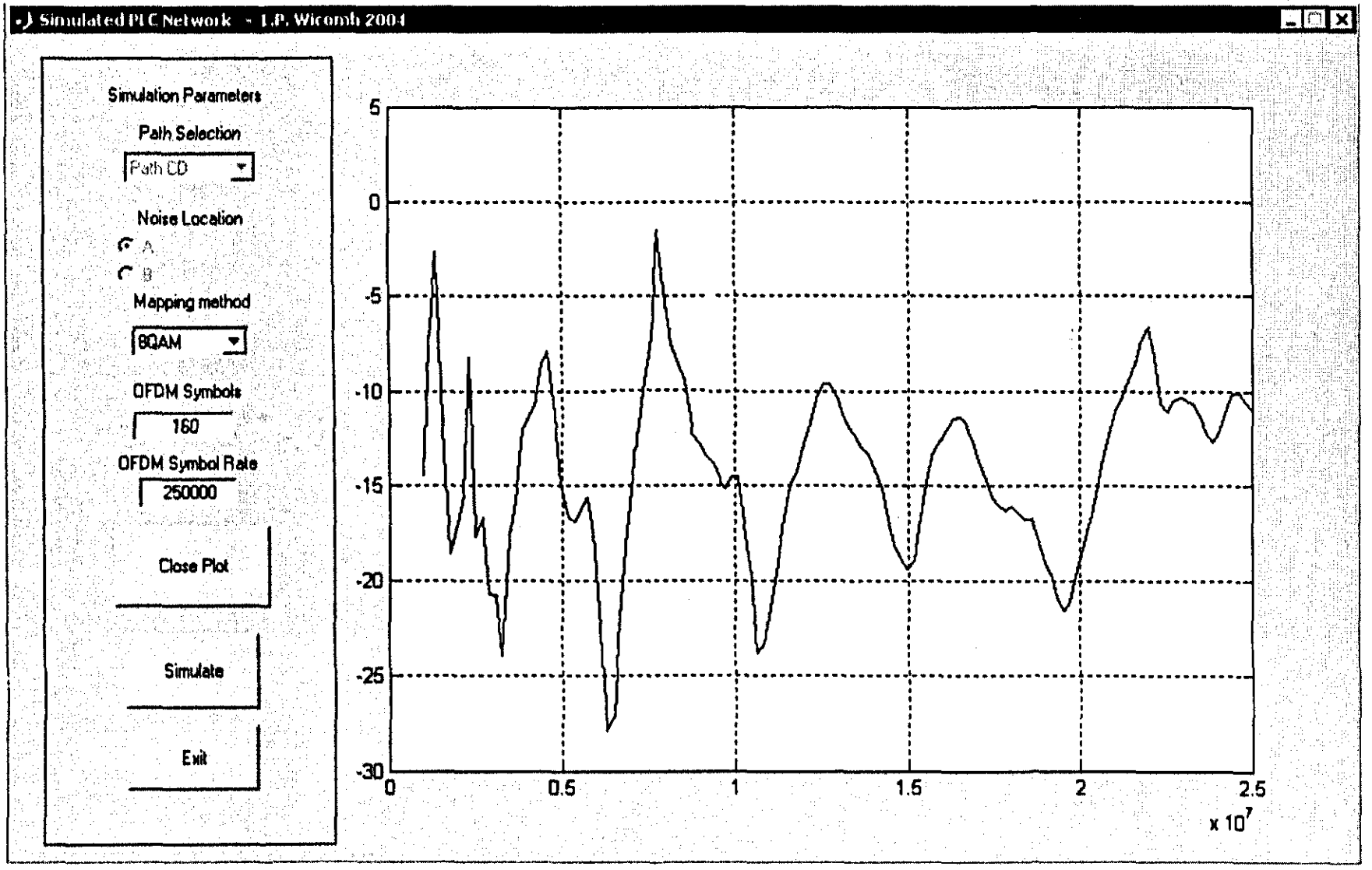

Figure B.2: An example of a TF plot displayed on the GUI

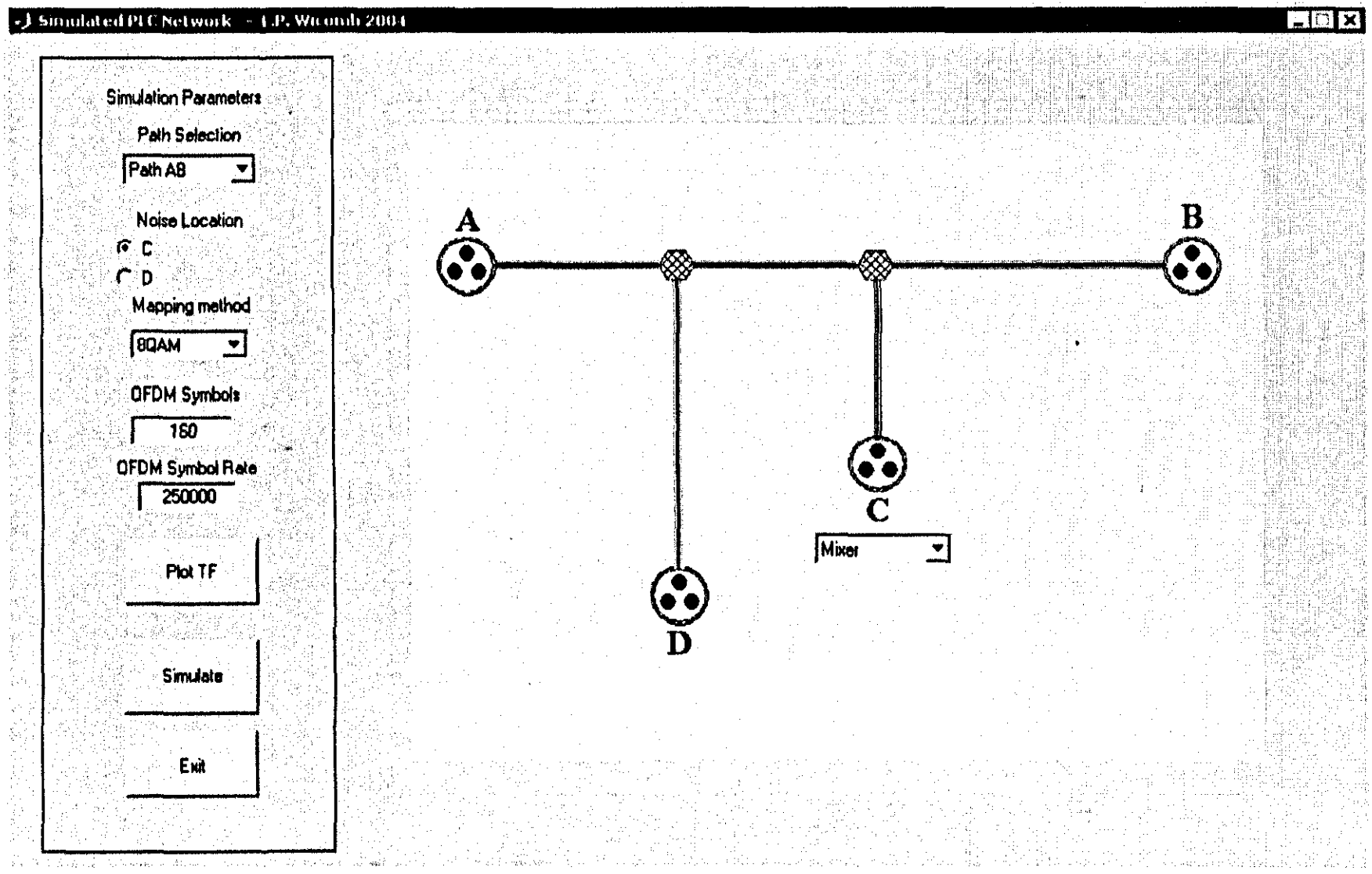

Figure B.3: Screen-shot of the initial user screen when the GUI is launched

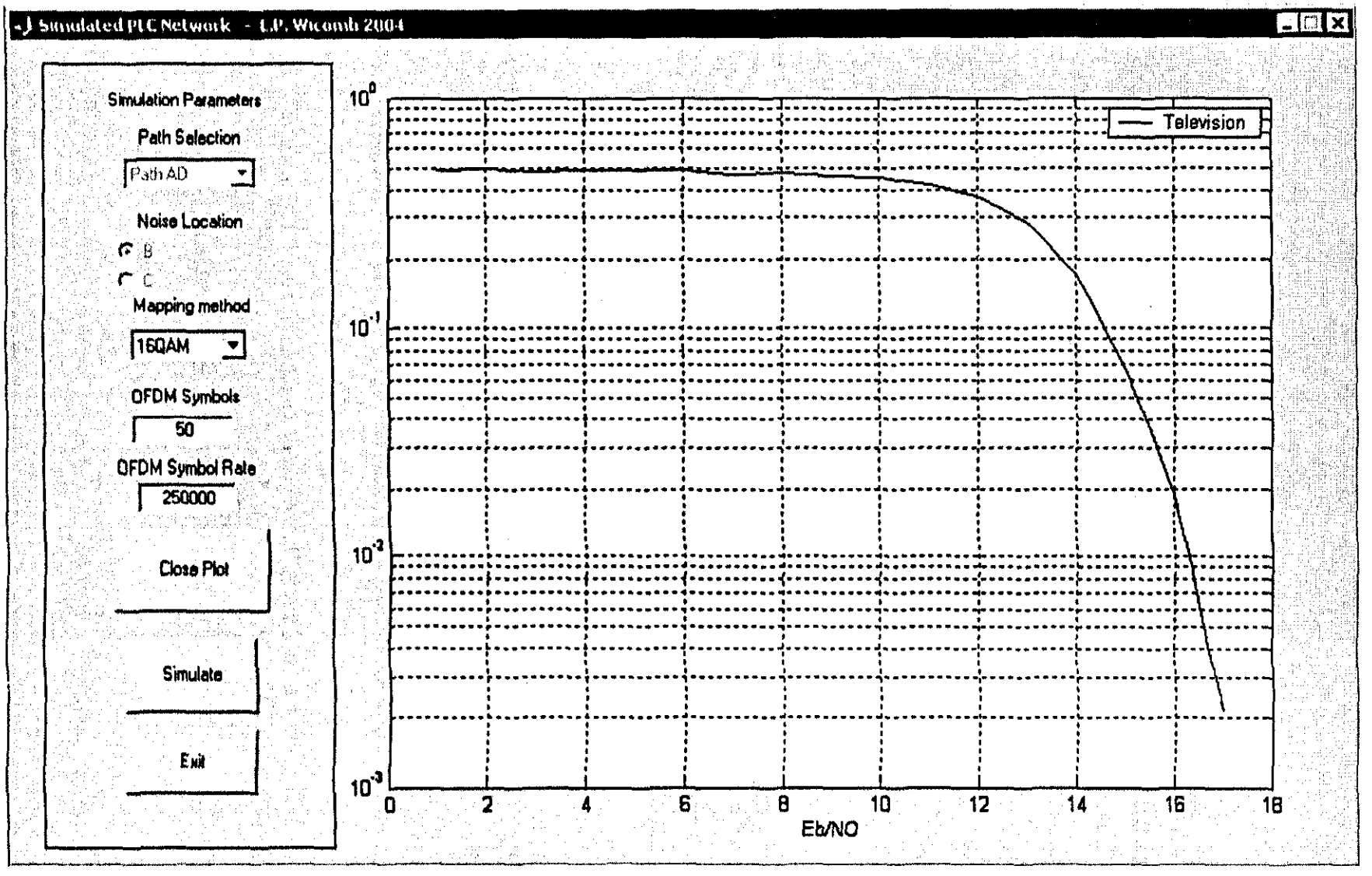

Figure B.4: An example of a BER plot given after a simulated scenario

B.2 BER Calculation and Plotting

The BER plot is the output of the simulation system. The BER plot (as mentioned earlier) of individual simulation scenarios will be imperative in the analysis and understanding of the OFDM system's performance.

This section will discuss how a BER plot is obtained, using the developed simulation components.

For each specific digital modulation method a MATLAB function was created, which incorporates the BER determination algorithm. The respective functions will return the simulated BER response for the simulation scenario.

Using the GUI, the first step in the BER calculation is selecting the appropriate path (e.g. path_ab, pathac, etc.) for a given simulation scenario. The transfer function files are stored in this sub-folder (within the MATLAB work directory).

Once the folder is selected, the appropriate transfer function file loaded for the simulation. Simulation begins at an Eb/N0 of 0 and the process is reiterated until and Eb/N0 of less than 100.

The core simulation process is then run for a specific amount of loops to obtain an average BER for that specific Eb/N0. As mentioned before, this process is reiterated for each specific Eb/N0, until a set of average BER values is obtained so that a BER graph can be plotted.

This entire process is depicted in the flowchart (Figure B.5).

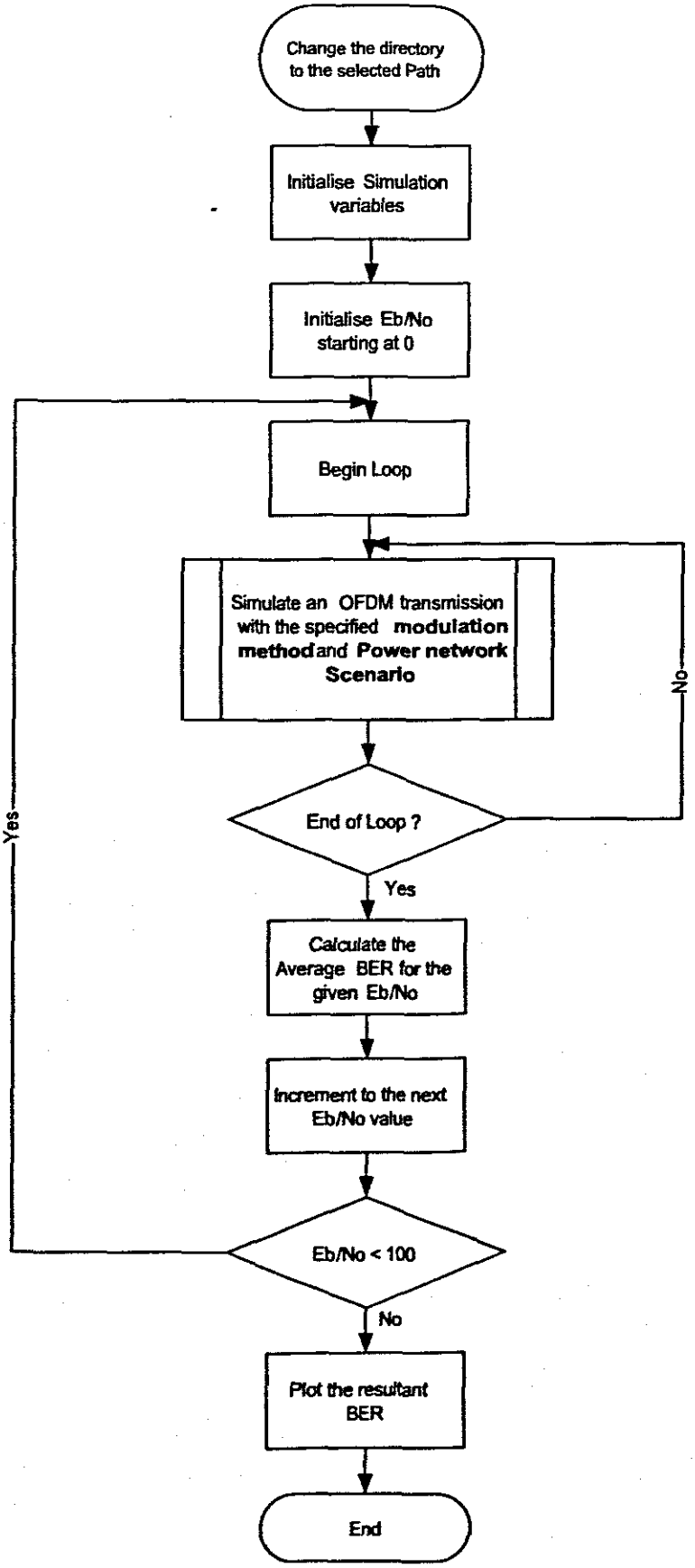

Figure B.5: Flowchart for BER Calculation

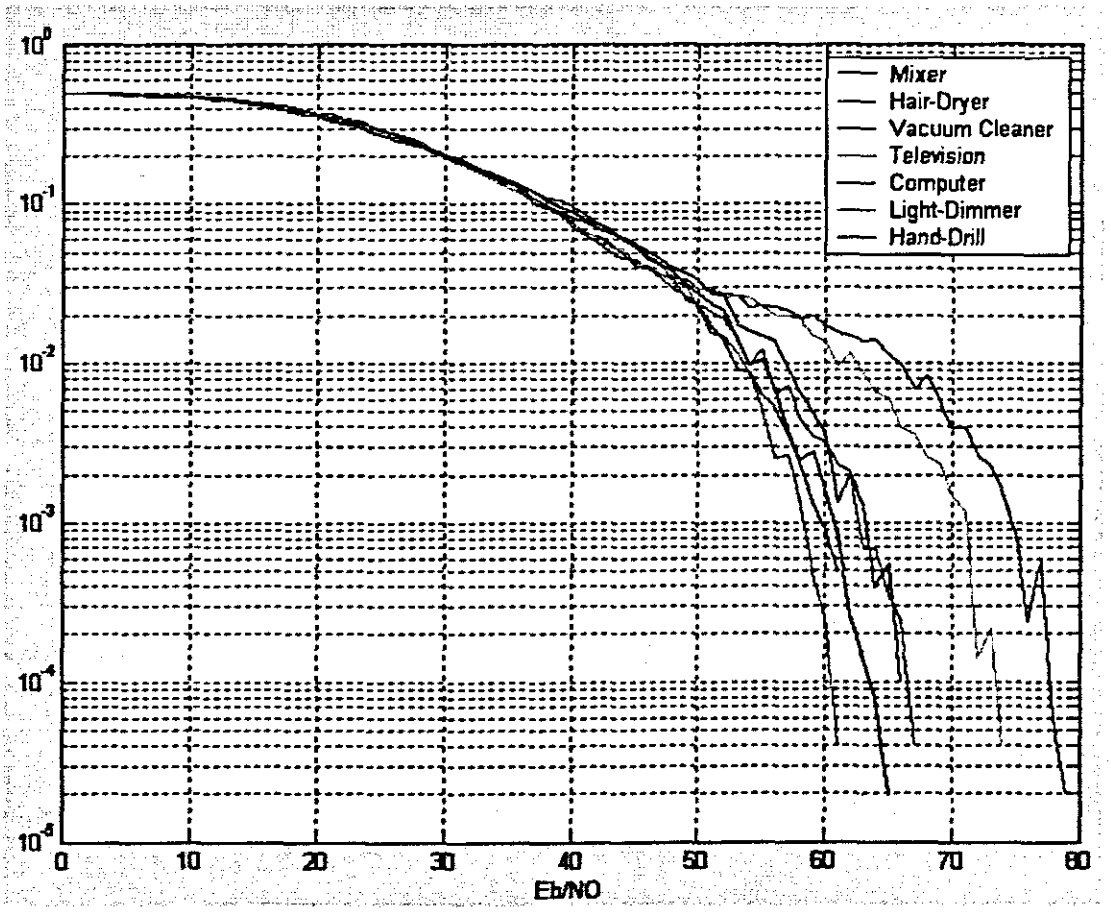

Figure B.6: Multiple BER Plots for a given scenario

Appendix C: MATLAB scripts for Domestic Power Network Modeling

C.1 MATLAB Script - *s2t.m*

```
% Script to Calculate the Transfer Matrix Parameters
% from a measured set of S-Parameters

% L.P. Wicomb 2004
% Cape Peninsula University of Technology

% Requires:
% The S-parameters to be loaded into the workspace

% Close all windows and clear the previous S-parameters in MATLAB
close all
clear S11 S22 S12 S21

% Define the Sampling Frequency
Fs = 50e+6;

% Convert the measured S-Parameters to Complex S-Parameters
for k = 1:1:length(freq)

    [x11,y11] = pol2cart(deg2rad(s11phase(k)),10^(s11mag(k)/10));
    [x12,y12] = pol2cart(deg2rad(s12phase(k)),10^(s12mag(k)/10));
    [x21,y21] = pol2cart(deg2rad(s21phase(k)),10^(s21mag(k)/10));
    [x22,y22] = pol2cart(deg2rad(s22phase(k)),10^(s22mag(k)/10));

    S11(k) = complex(x11,y11);
```

```
    S12(k) = complex(x12,y12);
    S21(k) = complex(x21,y21);
    S22(k) = complex(x22,y22);

end

% Define the Characteristic Impedance
Zo = 50;

% Convert the Complex S-Parameters to ABCD Parameters
for k =1:1:length(freq)
    A(k) = ((1+S11(k))*(1-S22(k))+(S12(k)*S21(k)))/(2*S21(k));
    B(k) = Zo * (((1+S11(k))*(1-S22(k))-(S12(k)*S21(k)))/(2*S21(k)));
    C(k) = (1/Zo) * ((1-S11(k))*(1-S22(k))-(S12(k)*S21(k))) / (2*S21(k));
    D(k) = ( ((1-S11(k))*(1+S22(k))) + (S12(k)*(S21(k))) ) / (2*S21(k));
end

% Convert the ABCD Matrix to the equivalent Inverse
for k =1:1:length(freq)
    T = [A(k) B(k); C(k) D(k)];
    Ti = inv(T);
    Ai(k) = Ti(1);
    Bi(k) = Ti(3);
    Ci(k) = Ti(2);
    Di(k) = Ti(4);
end
```

C.2 MATLAB Script - *tmath.m*

```
% Script to Calculate the Transfer function from
% a set of measured T-parameters.

% L.P. Wicomb 2004
% Cape Peninsula University of Technology

% Import the ABCD-Parameters for the Couplers
load tcpl1.mat
load tcpl2.mat

% Calculate for each Discrete Frequency Point
for k =1:1:length(freq)

    T1 = [Ai(k) Bi(k);Ci(k) Di(k)];
    T2 = [A1i(k) B1i(k);C1i(k) D1i(k)];
    T_total = [A(k) B(k);C(k) D(k)];

    % Matrix multiplication to determine the overall response
    % (in terms of ABCD-parameters)
    T_channel = T1*T_total*T2;

    Ach(k) = T_channel(1);
    Bch(k) = T_channel(3);
    Cch(k) = T_channel(2);
    Dch(k) = T_channel(3);

    % Impedance of the Network Analyser
    ZL = 50;
```

```
    % Calculate the Transfer function for the system
    TF(k) = ZL/(ZL*Ach(k)+Bch(k));
end
```

Appendix D: MATLAB script for the experimental power line model function

```
% Home Power line Model function

% L.P. Wicomb 2004
% Cape Peninsula University of Technology

% Experimental Channel Distortion Function
function signal_out = pwrchan(signal_in ,scenario ,nd)

% Load the Channel characteristics
filename = strcat(scenario ,'.mat');
load(filename);

% Construct the TF
tf_distort = [tfchan conj(tfchan(128:-1:1))];
size(tf_distort);
%tf_distort = reshape(tf_distort ,256,1);
signal_out = [];
k = 172;

for p = 1:1:nd

    % Covert the Input Signal into Frequency Domain Information
    signal_freq = fft(signal_in(k+1:1:k+256),256);
    k = k + 428;

    % Multiply the Input signal by the Channel Transfer Function
    distort_freq = signal_freq.* tf_distort;
```

```
    % Convert the Distorted Signal back to Time Domain Information
    signal_out1 = real(ifft(distort_freq));
    signal_out = [signal_out signal_out1(85:256) signal_out1];
end
```

Appendix E: MATLAB scripts for OFDM-PLC Simulation

E.1 MATLAB Script for OFDM-BPSK Simulation - *ofdmbpsk.m*

```
% Simulation program to realize OFDM transmission system
% Orginally Programmed by T. Yamamura and H. Harada
% Program 4-8
% ofdmce.m

% OFDM-BPSK Simulation - ofdmbpsk.m
% Adapted by L.P. Wicomb for M.Tech Project
% Cape Peninsula University of Technology
% September 2005

function ber = ofdmbpsk(nd, sr, scenario)

%********************** preparation part ****************************
para=84;        % Number of parallel channel to transmit (points)
fftlen=256;     % FFT length
noc=84;         % Number of carriers
knd=1;          % Number of known channel estimation (CE) OFDM symbol
ml=1;           % Modulation level : BPSK
br=sr.*ml;      % Bit rate per carrier
gilen=172;      % Length of guard interval (points)


%************************** main loop part ****************************
nloop=10; % Number of simulation loops
% Sweep the Eb/N0 value between 0 and 100
for index = 1:1:100
```

```
ebn0 = index;
noe = 0;     % Number of error data
nod = 0;     % Number of transmitted data
eop = 0;     % Number of error packet
nop = 0;     % Number of transmitted packet

%************************** transmitter ******************************
for iii=1:nloop

seridata=rand(1,para*nd*ml)>0.5;
paradata=reshape(seridata,para,nd);

%----------------BPSK modulation----------------
ich = paradata.*2-1;
qch = zeros(para,nd);

% Normalisation
kmod=1/sqrt(2);
ich=ich.*kmod;

% CE data generation
kndata0=2.*(rand(1,84)>0.5)-1;
ceich=kndata0; % CE:BPSK
ceqch=zeros(1,84);

ich2=[ceich.' ich]; % I-channel transmission data
qch2=[ceqch.' qch]; % Q-channel transmission data

%----------------IFFT----------------
```

```
x=ich2+qch2.*i;

for f = 1:nd+1
x1(:,f) = [zeros(22,1); x(:,f); zeros(45,1); conj(x(noc:-1:1,f)); zeros(21,1)
end

y=ifft(x1);
ich3=real(y);

%----------Guard interval insertion----------
fftlen2=fftlen+gilen;
[ich4]= giins(ich3,fftlen,gilen,nd+1);

%----------Attenuation Calculation----------
spow=sum(ich4.^2)/nd./para;
attn=0.5*spow*sr/br*10.^(-ebn0/10);
attn=sqrt(attn);

%***************************** Receiver ******************************

%----------AWGN addition----------
ich5 = comb(pwrchan(ich4,scenario,nd+1),attn);

%----------Guard interval removal----------
[ich6]= girem(ich5,fftlen2,gilen,nd+1);

%---------- FFT ----------
rx=ich6;
ry=fft(rx);
ich7=real(ry(23:106,:));
```

```
qch7=imag(ry(23:106,:));

% preparation known CE data
ce=1;
ice0=ich2(:,ce);
qce0=qch2(:,ce);

% taking CE data out of received data
ice1=ich7(:,ce);
qce1=qch7(:,ce);

% calculating reverse rotation
iv=real((1./(ice1.^2+qce1.^2)).*(ice0+i.*qce0).*(ice1-i.*qce1));
qv=imag((1./(ice1.^2+qce1.^2)).*(ice0+i.*qce0).*(ice1-i.*qce1));

ieqv1=[];
qeqv1=[];

% matrix for reverse rotation
for u = 1:1:nd+1
        ieqv1=[ieqv1 iv];
        qeqv1=[qeqv1 qv];
end

% reverse rotation
icompen=real((ich7+i.*qch7).*(ieqv1+i.*qeqv1));
qcompen=imag((ich7+i.*qch7).*(ieqv1+i.*qeqv1));
ich7=icompen;
qch7=qcompen;
```

```
%----------CE symbol removal----------
ich8=ich7(:,knd+1:nd+1);
qch8=qch7(:,knd+1:nd+1);

%----------demodulation----------
ich10=ich8./kmod;
qch10=qch8./kmod;
demodata = ich8 > 0;

%---------- error calculation ----------
demodata1=reshape(demodata,1,para*nd*ml);
noe2=sum(abs(demodata1-seridata));
nod2=length(seridata);

% Calculating PER
        if noe2~=0
                eop=eop+1;
        else
                eop=eop;
        end

eop;
nop=nop+1;

% Calculating BER
noe=noe+noe2;
nod=nod+nod2;
end

% BER and PER outputs
```

```
per(index)=eop/nop;
ber(index)=noe/nod;

end
```

E.2 MATLAB Script for OFDM-QPSK Simulation - *ofdmqpsk.m*

```
% Simulation program to realize OFDM transmission system
% Orginally Programmed by T. Yamamura and H. Harada
% Program 4-8
% ofdmce.m

% OFDM-QPSK Simulation - ofdmqpsk.m
% Adapted by L.P. Wicomb for M.Tech Project
% Cape Peninsula University of Technology
% September 2005

function ber = ofdmqpsk(nd, sr, scenario)

%********************** preparation part ****************************

para=84;        % Number of parallel channel to transmit (points)
fftlen=256;     % FFT length
noc=84;         % Number of carriers
knd=1;          % Number of known channel estimation (CE) OFDM symbol
ml=2;           % Modulation level : QPSK
br=sr.*ml;      % Bit rate per carrier
gilen=172;      % Length of guard interval (points)

%************************** main loop part ****************************
nloop=10; % Number of simulation loops

% Sweep the Eb/N0 value between 0 and 100
for index = 1:1:100
```

```
ebn0 = index;
noe = 0;     % Number of error data
nod = 0;     % Number of transmitted data
eop = 0;     % Number of error packet
nop = 0;     % Number of transmitted packet

%************************** transmitter ******************************
for iii=1:nloop

seridata=rand(1,para*nd*ml)>0.5;
paradata=reshape(seridata,para,nd*ml); %size(51 * nd*ml)

%---------------ml modulation---------------
% QPSK Modulation
[ich,qch]=qpskmod(paradata,para,nd,ml);

% Normalisation stage
kmod=1/sqrt(2);
ich=ich.*kmod;
qch=qch.*kmod;

% CE data generation
kndata0=2.*(rand(1,84)>0.5)-1;
ceich=kndata0; % CE:BPSK
ceqch=zeros(1,84);

ich2=[ceich.' ich]; % I-channel transmission data
qch2=[ceqch.' qch]; % Q-channel transmission data

%-------------------IFFT -------------------
```

```
x=ich2+qch2.*i;
for f = 1:nd+1
x1(:,f) = [zeros(22,1); x(:,f); zeros(45,1); conj(x(noc:-1:1,f)); zeros(21,1)
end

y=ifft(x1);
ich3=real(y);

%---------- Guard interval insertion ----------
fftlen2=fftlen+gilen;
[ich4]= giins(ich3,fftlen,gilen,nd+1);

%---------- Attenuation Calculation ----------
spow=sum(ich4.^2)/nd./para;
attn=0.5*spow*sr/br*10.^(-ebn0/10);
attn=sqrt(attn);

%**************************** Receiver ********************************

%---------- AWGN addition ----------
ich5 = comb(pwrchan(ich4,scenario,nd+1),attn);

%---------- Guard interval removal ----------
[ich6]= girem(ich5,fftlen2,gilen,nd+1);

%---------- FFT ----------
rx=ich6;
ry=fft(rx);
ich7=real(ry(23:106,:));
qch7=imag(ry(23:106,:));
```

```
% preparation known CE data
ce=1;
ice0=ich2(:,ce);
qce0=qch2(:,ce);

% taking CE data out of received data
ice1=ich7(:,ce);
qce1=qch7(:,ce);

% calculating reverse rotation
iv=real((1./(ice1.^2+qce1.^2)).*(ice0+i.*qce0).*(ice1-i.*qce1));
qv=imag((1./(ice1.^2+qce1.^2)).*(ice0+i.*qce0).*(ice1-i.*qce1));

ieqv1=[];
qeqv1=[];

% matrix for reverse rotation
        for u = 1:1:nd+1
                ieqv1=[ieqv1 iv];
                qeqv1=[qeqv1 qv];
        end

% reverse rotation
icompen=real((ich7+i.*qch7).*(ieqv1+i.*qeqv1));
qcompen=imag((ich7+i.*qch7).*(ieqv1+i.*qeqv1));
ich7=icompen;
qch7=qcompen;

%----------CE symbol removal----------
```

```
ich8=ich7(:,knd+1:nd+1);
qch8=qch7(:,knd+1:nd+1);

%------------------ demodulation ------------------
ich10=ich8./kmod;
qch10=qch8./kmod;
demodata]=qpskdemod(ich10,qch10,para,nd,ml);

%------------------ error calculation ------------------
demodata1=reshape(demodata,1,para*nd*ml);
noe2=sum(abs(demodata1-seridata));
nod2=length(seridata);

% Calculating PER
        if noe2~=0
                eop=eop+1;
        else
                eop=eop;
        end

eop;
nop=nop+1;

% Calculating BER
noe=noe+noe2;
nod=nod+nod2;

end
```

```
% BER and PER Outputs
per(index+1)=eop/nop;
ber(index+1)=noe/nod;

end
```

E.3 MATLAB Script for OFDM-DBPSK Simulation - *ofdmdbpsk.m*

```
% Simulation program to realize OFDM transmission system
% Orginally Programmed by T. Yamamura and H. Harada
% Program 4-8
% ofdmce.m

% OFDM-DBPSK Simulation - ofdmdbpsk.m
% Adapted by L.P. Wicomb for M.Tech Project
% Cape Peninsula University of Technology
% September 2005

function ber = ofdmdbpsk(nd, sr, scenario)

%********************** preparation part ****************************

para=84;        % Number of parallel channel to transmit (points)
fftlen=256;     % FFT length
noc=84;         % Number of carriers
knd=1;          % Number of known channel estimation (CE) OFDM symbol
ml=1;           % Modulation level : DBPSK
br=sr.*ml;      % Bit rate per carrier
gilen=172;      % Length of guard interval (points)

%************************** main loop part ****************************

nloop=10; % Number of simulation loops

% Sweep the Eb/N0 value between 0 and 100
for index = 1:1:100
```

```
ebn0 = index;
noe = 0;     % Number of error data
nod = 0;     % Number of transmitted data
eop = 0;     % Number of error packet
nop = 0;     % Number of transmitted packet

%************************** transmitter ********************************
for iii=1:nloop

seridata=rand(1,para*nd*ml)>0.5;
paradata=reshape(seridata,para,nd);

%--------------------DBPSK modulation--------------------
[ich,qch]=dbpskmod(paradata,para,nd);

% Normalisation
kmod=1/sqrt(2);
ich=ich.*kmod;

% CE data generation
kndata0=2.*(rand(1,84)>0.5)-1;
ceich=kndata0; % CE:BPSK
ceqch=zeros(1,84);

ich2=[ceich.' ich]; % I-channel transmission data
qch2=[ceqch.' qch]; % Q-channel transmission data

%--------------------IFFT --------------------
x=ich2+qch2.*i;
```

```
% preparation known CE data
ce=1;
ice0=ich2(:,ce);
qce0=qch2(:,ce);

% taking CE data out of received data
ice1=ich7(:,ce);
qce1=qch7(:,ce);

% calculating reverse rotation
iv=real((1./(ice1.^2+qce1.^2)).*(ice0+i.*qce0).*(ice1-i.*qce1));
qv=imag((1./(ice1.^2+qce1.^2)).*(ice0+i.*qce0).*(ice1-i.*qce1));

ieqv1=[];
qeqv1=[];

% matrix for reverse rotation
        for u = 1:1:nd+1
                ieqv1=[ieqv1 iv];
                qeqv1=[qeqv1 qv];
        end

% reverse rotation
icompen=real((ich7+i.*qch7).*(ieqv1+i.*qeqv1));
qcompen=imag((ich7+i.*qch7).*(ieqv1+i.*qeqv1));
ich7=icompen;
qch7=qcompen;

%----------CE symbol removal----------
```

```
ich8=ich7(:,knd+1:nd+1);
qch8=qch7(:,knd+1:nd+1);

%------------------- demodulation -----------------
ich10=ich8./kmod;
qch10=qch8./kmod;

[demodata] = dbpskdemod(ich10,qch10,para);

%------------- error calculation ------------
demodata1=reshape(demodata,1,para*nd*ml);
noe2=sum(abs(demodata1-seridata));
nod2=length(seridata);


% Calculating PER
        if noe2~=0
                eop=eop+1;
        else
                eop=eop;
        end

eop;
nop=nop+1;

% Calculating BER
noe=noe+noe2;
nod=nod+nod2;

end
```

```
% BER and PER outputs
per(index)=eop/nop;
ber(index)=noe/nod;

end
```

E.4 MATLAB Script for OFDM-DQPSK Simulation - *ofdmdqpsk.m*

```
% Simulation program to realize OFDM transmission system
% Orginally Programmed by T.Yamamura and H.Harada
% Program 4-8
% ofdmce.m

% OFDM-DQPSK Simulation - ofdmdqpsk.m
% Adapted by L.P. Wicomb for M.Tech Project
% Cape Peninsula University of Technology
% September 2005

function ber = ofdmdqpsk(nd, sr, scenario)

%********************** preparation part ****************************

para=84;        % Number of parallel channel to transmit (points)
fftlen=256;     % FFT length
noc=84;         % Number of carriers
knd=1;          % Number of known channel estimation (CE) OFDM symbol
ml=2;           % Modulation level : DQPSK
br=sr.*ml;      % Bit rate per carrier
gilen=172;      % Length of guard interval (points)

%************************** main loop part ***************************

nloop=10; % Number of simulation loops

% Sweep the Eb/N0 value between 0 and 100
for index = 1:1:100
```

```
ebn0 = index;
noe = 0;     % Number of error data
nod = 0;     % Number of transmitted data
eop = 0;     % Number of error packet
nop = 0;     % Number of transmitted packet

%************************** transmitter ******************************
for iii=1:nloop

seridata=rand(1,para*nd*ml)>0.5;
paradata=reshape(seridata,para,nd*ml); %size(51 * nd*ml)

%----------------DQPSK modulation----------------
[ich,qch]=dqpskmod(paradata,para,nd);
kmod=1/sqrt(2);
ich=ich.*kmod;
qch=qch.*kmod;

% CE data generation
kndata0=2.*(rand(1,84)>0.5)-1;
ceich=kndata0; % CE:BPSK
ceqch=zeros(1,84);

ich2=[ceich.' ich]; % I-channel transmission data
qch2=[ceqch.' qch]; % Q-channel transmission data

%-------------------IFFT -------------------
x=ich2+qch2.*i;
```

```
for f = 1:nd+1
x1(:,f) = [zeros(22,1); x(:,f); zeros(45,1); conj(x(noc:-1:1,f)); zeros(21,1)
end

y=ifft(x1);
ich3=real(y);

%----------Guard interval insertion----------
fftlen2=fftlen+gilen;
[ich4]= giins(ich3,fftlen,gilen,nd+1);

%----------Attenuation Calculation----------
spow=sum(ich4.^2)/nd./para;
attn=0.5*spow*sr/br*10.^(-ebn0/10);
attn=sqrt(attn);

%***************************** Receiver ******************************

%----------AWGN addition----------
ich5 = comb(pwrchan(ich4,scenario,nd+1),attn);

%----------Guard interval removal----------
[ich6]= girem(ich5,fftlen2,gilen,nd+1);

%---------- FFT ----------
rx=ich6;
ry=fft(rx);
ich7=real(ry(23:106,:));
qch7=imag(ry(23:106,:));
```

```
% preparation known CE data
ce=1;
ice0=ich2(:,ce);
qce0=qch2(:,ce);

% taking CE data out of received data
ice1=ich7(:,ce);
qce1=qch7(:,ce);

% calculating reverse rotation
iv=real((1./(ice1.^2+qce1.^2)).*(ice0+i.*qce0).*(ice1-i.*qce1));
qv=imag((1./(ice1.^2+qce1.^2)).*(ice0+i.*qce0).*(ice1-i.*qce1));

ieqv1=[];
qeqv1=[];

% matrix for reverse rotation
        for u = 1:1:nd+1
                ieqv1=[ieqv1 iv];
                qeqv1=[qeqv1 qv];
        end

% reverse rotation
icompen=real((ich7+i.*qch7).*(ieqv1+i.*qeqv1));
qcompen=imag((ich7+i.*qch7).*(ieqv1+i.*qeqv1));
ich7=icompen;
qch7=qcompen;

%----------CE symbol removal----------
ich8=ich7(:,knd+1:nd+1);
```

```
qch8=qch7(:,knd+1:nd+1);

%————————————demoduration————————————
ich10=ich8./kmod;
qch10=qch8./kmod;
[demodata]=dqpskdemod(ich10,qch10,para);

%————————————error calculation————————————
demodata1=reshape(demodata,1,para*nd*ml);
noe2=sum(abs(demodata1-seridata));
nod2=length(seridata);

% Calculating PER
        if noe2~=0
                eop=eop+1;
        else
                eop=eop;
        end
eop;
nop=nop+1;

% Calculating BER
noe=noe+noe2;
nod=nod+nod2;

end

% BER and PER outputs
per(index)=eop/nop;
ber(index)=noe/nod;
```

E.5 MATLAB Script for OFDM-8QAM Simulation - *ofdm8qam.m*

```
% Simulation program to realize OFDM transmission system
% Orginally Programmed by T. Yamamura and H. Harada
% Program 4-8
% ofdmce.m

% OFDM-8QAM Simulation - ofdm8qam.m
% Adapted by L.P. Wicomb for M.Tech Project
% Cape Peninsula University of Technology
% September 2005

function ber = ofdm8qam(nd, sr, scenario)

%********************** preparation part ****************************

para=84;        % Number of parallel channel to transmit (points)
fftlen=256;     % FFT length
noc=84;         % Number of carriers
knd=1;          % Number of known channel estimation (CE) OFDM symbol
ml=3;           % Modulation level : 8 QAM
br=sr.*ml;      % Bit rate per carrier
gilen=172;      % Length of guard interval (points)

%************************** main loop part ****************************

nloop=1; % Number of simulation loops

% Sweep the Eb/N0 value between 0 and 100
for index = 1:1:100
```

```
ebn0 = index;
noe = 0;     % Number of error data
nod = 0;     % Number of transmitted data
eop = 0;     % Number of error packet
nop = 0;     % Number of transmitted packet

%************************** transmitter ******************************
for iii=1:nloop

seridata=rand(1,para*nd*ml)>0.5;
paradata=reshape(seridata,para,nd*ml); %size(51 * nd*ml)

%-------------------8QAM modulation-------------------
[ich,qch]=qam8mod(paradata,para,nd);
kmod=1/sqrt(2);
ich=ich.*kmod;
qch=qch.*kmod;

% CE data generation
kndata0=2.*(rand(1,84)>0.5)-1;
ceich=kndata0; % CE:BPSK
ceqch=zeros(1,84);

ich2=[ceich.' ich]; % I-channel transmission data
qch2=[ceqch.' qch]; % Q-channel transmission data

%-------------------IFFT -------------------
x=ich2+qch2.*i;
```

```
for f = 1:nd+1
x1(:,f) = [zeros(22,1); x(:,f); zeros(45,1); conj(x(noc:-1:1,f)); zeros(21,1)
end

y=ifft(x1);
ich3=real(y);

%---------- Guard interval insertion ----------
fftlen2=fftlen+gilen;
[ich4]= giins(ich3,fftlen,gilen,nd+1);

%---------- Attenuation Calculation ----------
spow=sum(ich4.^2)/nd./para;
attn=0.5*spow*sr/br*10.^(-ebn0/10);
attn=sqrt(attn);

%**************************** Receiver ******************************

%---------- AWGN addition ----------
ich5 = comb(pwrchan(ich4,scenario,nd+1),attn);

%---------- Guard interval removal ----------
[ich6]= girem(ich5,fftlen2,gilen,nd+1);

%---------- FFT ----------
rx=ich6;
ry=fft(rx);
ich7=real(ry(23:106,:));
qch7=imag(ry(23:106,:));
```

```
for f = 1:nd+1
x1(:,f) = [zeros(22,1); x(:,f); zeros(45,1); conj(x(noc:-1:1,f)); zeros(21,1)
end

y=ifft(x1);
ich3=real(y);

%----------Guard interval insertion----------
fftlen2=fftlen+gilen;
[ich4]= giins(ich3,fftlen,gilen,nd+1);

%----------Attenuation Calculation----------
spow=sum(ich4.^2)/nd./para;
attn=0.5*spow*sr/br*10.^(-ebn0/10);
attn=sqrt(attn);

%**************************** Receiver ******************************

%----------AWGN addition----------
ich5 = comb(pwrchan(ich4,scenario,nd+1),attn);

%----------Guard interval removal----------
[ich6]= girem(ich5,fftlen2,gilen,nd+1);

%---------- FFT ----------
rx=ich6;
ry=fft(rx);
ich7=real(ry(23:106,:));
qch7=imag(ry(23:106,:));
```

```
% preparation known CE data
ce=1;
ice0=ich2(:,ce);
qce0=qch2(:,ce);

% taking CE data out of received data
ice1=ich7(:,ce);
qce1=qch7(:,ce);

% calculating reverse rotation
iv=real((1./(ice1.^2+qce1.^2)).*(ice0+i.*qce0).*(ice1-i.*qce1));
qv=imag((1./(ice1.^2+qce1.^2)).*(ice0+i.*qce0).*(ice1-i.*qce1));

ieqv1=[];
qeqv1=[];

% matrix for reverse rotation
        for u = 1:1:nd+1
                ieqv1=[ieqv1 iv];
                qeqv1=[qeqv1 qv];
        end

% reverse rotation
icompen=real((ich7+i.*qch7).*(ieqv1+i.*qeqv1));
qcompen=imag((ich7+i.*qch7).*(ieqv1+i.*qeqv1));
ich7=icompen;
qch7=qcompen;

%----------CE symbol removal----------
ich8=ich7(:,knd+1:nd+1);
```

```
qch8=qch7(:,knd+1:nd+1);

%------------------demodulation------------------
ich10=ich8./kmod;
qch10=qch8./kmod;
[demodata]=qam8demod(ich10,qch10,para,nd,ml);

%-------------- error calculation --------------
demodata1=reshape(demodata,1,para*nd*ml);
noe2=sum(abs(demodata1-seridata));
nod2=length(seridata);

% Calculating PER
        if noe2~=0
                eop=eop+1;
        else
                eop=eop;
        end
eop;
nop=nop+1;

% Calculating BER
noe=noe+noe2;
nod=nod+nod2;

end

% BER and PER outputs
per(index)=eop/nop;
ber(index)=noe/nod;
```

20

end

E.6 MATLAB Script for OFDM-16QAM Simulation - *ofdm16qam.m*

```
% Simulation program to realize OFDM transmission system
% Orginally Programmed by T. Yamamura and H. Harada
% Program 4-8
% ofdmce.m

% OFDM-16QAM Simulation -- ofdm16qam.m
% Adapted by L.P. Wicomb for M.Tech Project
% Cape Peninsula University of Technology
% September 2005

function ber = ofdm16qam(nd, sr, scenario)

%********************** preparation part ****************************

para=84;        % Number of parallel channel to transmit (points)
fftlen=256;     % FFT length
noc=84;         % Number of carriers
knd=1;          % Number of known channel estimation (CE) OFDM symbol
ml=4;           % Modulation level : 16 QAM
br=sr.*ml;      % Bit rate per carrier
gilen=172;      % Length of guard interval (points)

%************************** main loop part ***************************

nloop=1; % Number of simulation loops

% Sweep the Eb/N0 value between 0 and 100
for index = 1:1:100
```

```
ebn0 = index;
noe = 0;     % Number of error data
nod = 0;     % Number of transmitted data
eop = 0;     % Number of error packet
nop = 0;     % Number of transmitted packet

%************************** transmitter ******************************
for iii=1:nloop

seridata=rand(1,para*nd*ml)>0.5;
paradata=reshape(seridata,para,nd*ml);

%---------------16QAM modulation---------------
for uu = 1:1:para
[ich(uu,:), qch(uu,:)]=qam16mod(paradata(uu,:),1,nd,ml);
end

% CE data generation
kndata0=2.*(rand(1,84)>0.5)-1;
ceich=kndata0; % CE:BPSK
ceqch=zeros(1,84);

ich2=[ceich.' ich]; % I-channel transmission data
qch2=[ceqch.' qch]; % Q-channel transmission data

%---------------IFFT ---------------
x=ich2+qch2.*i;
for f = 1:nd+1
x1(:,f) = [zeros(22,1); x(:,f); zeros(45,1); conj(x(noc:-1:1,f)); zeros(21,1)
```

```
end

y=ifft(x1);
ich3=real(y);

%----------Guard interval insertion----------
fftlen2=fftlen+gilen;
[ich4]= giins(ich3,fftlen,gilen,nd+1);

%----------Attenuation Calculation----------
spow=sum(ich4.^2)/nd./para;
attn=0.5*spow*sr/br*10.^(-ebn0/10);
attn=sqrt(attn);

%*************************** Receiver ******************************

%----------AWGN addition----------
ich5 = comb(pwrchan(ich4,scenario,nd+1),attn);

%----------Guard interval removal----------
[ich6]= girem(ich5,fftlen2,gilen,nd+1);

%---------- FFT ----------
rx=ich6;
ry=fft(rx);
ich7=real(ry(23:106,:));
qch7=imag(ry(23:106,:));

% preparation known CE data
ce=1;
```

```
ice0=ich2(:,ce);
qce0=qch2(:,ce);

% taking CE data out of received data
ice1=ich7(:,ce);
qce1=qch7(:,ce);

% calculating reverse rotation
iv=real((1./(ice1.^2+qce1.^2)).*(ice0+i.*qce0).*(ice1-i.*qce1));
qv=imag((1./(ice1.^2+qce1.^2)).*(ice0+i.*qce0).*(ice1-i.*qce1));

ieqv1=[];
qeqv1=[];

% matrix for reverse rotation
        for u = 1:1:nd+1
                ieqv1=[ieqv1 iv];
                qeqv1=[qeqv1 qv];
        end

% reverse rotation
icompen=real((ich7+i.*qch7).*(ieqv1+i.*qeqv1));
qcompen=imag((ich7+i.*qch7).*(ieqv1+i.*qeqv1));
ich7=icompen;
qch7=qcompen;

%----------CE symbol removal----------
ich8=ich7(:,knd+1:nd+1);
qch8=qch7(:,knd+1:nd+1);
```

```
%------------------ demodulation ------------------
ich10=ich8;
qch10=qch8;

for uu2 = 1:1:para
demodata(uu2,:)=qam16demod(ich10(uu2,:),qch10(uu2,:),1,nd,ml);
end

%------------------ error calculation ------------------
demodata1=reshape(demodata,1,para*nd*ml);
noe2=sum(abs(demodata1-seridata));
nod2=length(seridata);

% Calculating PER
        if noe2~=0
                eop=eop+1;
        else
                eop=eop;
        end
eop;
nop=nop+1;

% Calculating BER
noe=noe+noe2;
nod=nod+nod2;

end

% BER and PER outputs
per(index)=eop/nop;
```

```
ber(index)=noe/nod;

end
```

Appendix F: MATLAB scripts for PSK, DPSK and QAM modulation and demodulation

F.1 MATLAB Script for BSPK Modulation - *bpskmod.m*

```
% Function to perform BPSK modulation using the
% MATLAB PSK modulation function
% bpskmod.m

% L.P. Wicomb
% Cape Peninsula University of Technology
% September 2005%

function [ich , qch]=bpskmod(paradata ,para ,nd,ml)
c = 0;
dematrix = zeros(para ,nd);

for k = 1:nd
    dematrix(:,k) = bi2de(paradata(:,c));
    c = c+1;
end

bpskmatrix = pskmod(dematrix ,2);
ich = round(real(bpskmatrix));
qch = round(imag(bpskmatrix));
end
```

F.2 MATLAB Script for BSPK Demodulation - *bpskdemod.m*

```
% Function to perform BPSK demodulation using the
% MATLAB PSK demodulation function
% bpskdemod.m

% L.P. Wicomb
% Cape Peninsula University of Technology
% September 2005

function [binmatrix]=bpskdemod(ich,qch,para,nd,ml)
c = 0;
demomatrix1 = zeros(para,nd);

for k = 1:1:nd
    demomatrix1(:,k) = ich(:,k) + i.*qch(:,k);
end

for k = 1:1:nd
    for g = 1:1:84
        demomatrix(g,k) = pskdemod(demomatrix1(g,k),2);
    end
end

binmatrix = [];
a = 1;

for y = 1:1:nd
    for h = 1:1:84
        binmatrix(h,a) = out2bin(demomatrix(h,y)+1,:);
```

```
    end
    a = a+1;
end
```

F.3 MATLAB Script for QSPK Modulation - *qpskmod.m*

```
% Function to perform QPSK modulation using the
% MATLAB PSK modulation function
% qpskmod.m

% L.P. Wicomb
% Cape Peninsula University of Technology
% September 2005

function [ich , qch]=qpskmod(paradata ,para ,nd,ml)
c = 0;
dematrix = zeros(para ,nd);

for k = 1:nd
    dematrix(:,k) = bi2de(paradata(:,(c+1):(c+2)));
    c = c+2;
end

qpskmatrix = pskmod(dematrix ,4);
ich = round(real(qpskmatrix));
qch = round(imag(qpskmatrix));

end
```

F.4 MATLAB Script for QSPK Demodulation - *qpskdemod.m*

```
% Function to perform QPSK demodulation using the
% MATLAB PSK demodulation function
% qpskdemod.m

% L.P. Wicomb
% Cape Peninsula University of Technology
% September 2005

function [binmatrix]=qpskdemod(ich,qch,para,nd,ml)
c = 0;
out2bin = [0 0; 1 0; 0 1; 1 1];
demomatrix1 = zeros(para,nd);

for k = 1:1:nd
    demomatrix1(:,k) = ich(:,k) + i.*qch(:,k);
end

for k = 1:1:nd
    for g = 1:1:84
        demomatrix(g,k) = pskdemod(demomatrix1(g,k),4);
    end
end

binmatrix = [];
a = 1;

for y = 1:1:nd
    for h = 1:1:84
```

```
        binmatrix(h,a:a+1) = out2bin(demomatrix(h,y)+1,:);
    end
    a = a+2;
end
```

F.5 MATLAB Script for DBSPK Modulation - *dbpskmod.m*

```
% Function to perform DBPSK modulation using the
% MATLAB DPSK modulation function
% dbpskmod.m

% L.P. Wicomb
% Cape Peninsula University of Technology
% September 2005%

function [nd, ich , qch]=dbpskmod(paradata ,para ,nd)
c = 1;

% Define the Symbol Matrix for DBPSK Modulation (First Symbol in error -> nd+
dematrix = zeros(para ,nd+1);

% Conversion from Binary to Decimal Data for DBPSK Modulation
for k = 2:1:nd+1
    dematrix(:,k) = paradata(:,c);
    c = c+1;
end

% Perform DBPSK Modulation
for j = 1:1:para
    dbpskmatrix(j ,:) = dpskmod(dematrix(j ,:) ,2);
end

% Output real and imaginary values for symbol transmission
ich = real(dbpskmatrix);
qch = imag(dbpskmatrix);
```

```
nd = nd+1;
end
```

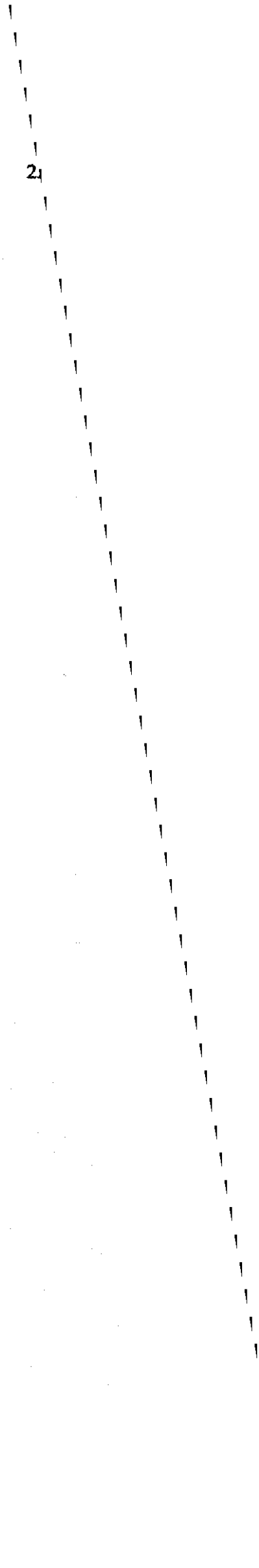

F.6 MATLAB Script for DBPSK Demodulation - *dbpskdemod.m*

```
% Function to perform DBPSK demodulation using the
% MATLAB DPSK demodulation function
% dbpskdemod.m

% L.P. Wicomb
% Cape Peninsula University of Technology
% September 2005

function [nd, binmatrix]=dbpskdemod(ich,qch,para)

% Determine the size of the incoming Data
[x,y] = size(ich);
c = 0;

% Define the Output Binary Lookup Table
out2bin = [0; 1];

% Conversion to complex information
for k = 1:1:y
    demomatrix1(:,k) = ich(:,k) + i.*qch(:,k);
end

% Perform the DBPSK Demodulation
for g = 1:1:para
    demomatrix(g,:) = dpskdemod(demomatrix1(g,:),2);
end

% Define the Output Binary Matrix
```

```
binmatrix = [];
a = 1;

% Calculate the output Binary Matrix based on the Lookup table
for yl = 2:1:y
    for h = 1:1:para
        binmatrix(h,a) = out2bin(demomatrix(h,yl)+1,:);
    end
    a = a+1;
end
nd = y-1;
```

```
binmatrix = [];
a = 1;

% Calculate the output Binary Matrix based on the Lookup table
for y1 = 2:1:y
    for h = 1:1:para
        binmatrix(h,a) = out2bin(demomatrix(h,y1)+1,:);
    end
    a = a+1;
end
nd = y-1;
```

F.7 MATLAB Script for DQSPK Modulation - *dqpskmod.m*

```
% Function to perform DQPSK modulation using the
% MATLAB DPSK modulation function
% dqpskmod.m

% L.P. Wicomb
% Cape Peninsula University of Technology
% September 2005

function [nd, ich , qch]=dqpskmod(paradata ,para ,nd)
c = 0;

% Define the Symbol Matrix for DQPSK Modulation (First Symbol in error -> nd+
dematrix = zeros(para ,nd+1);

% Conversion from Binary to Decimal Data for DQPSK Modulation
for k = 2:1:nd+1
    dematrix(:,k) = bi2de(paradata(:,(c+1):(c+2)));
    c = c+2;
end

% Perform DQPSK Modulation
for j = 1:1:para
    qpskmatrix(j ,:) = dpskmod(dematrix(j ,:) ,4);
end

% Output real and imaginary values for symbol transmission
ich = real(qpskmatrix);
qch = imag(qpskmatrix);
```

```
nd = nd+1;

end
```

F.8 MATLAB Script for DQSPK Demodulation - *dqpskdemod.m*

```
% Function to perform DQPSK demodulation using the
% MATLAB DPSK demodulation function
% dqpskdemod.m

% L.P. Wicomb
% Cape Peninsula University of Technology
% September 2005

function [nd, binmatrix]=dqpskdemod(ich,qch,para)

% Determine the size of the incoming Data
[x,y] = size(ich);
c = 0;

% Define the Output Binary Lookup Table
out2bin = [0 0; 1 0; 0 1; 1 1];

% Conversion to complex information
for k = 1:1:y
    demomatrix1(:,k) = ich(:,k) + i.*qch(:,k);
end

% Perform the DQPSK Demodulation
for g = 1:1:para
    demomatrix(g,:) = dpskdemod(demomatrix1(g,:),4);
end

% Define the Output Binary Matrix
```

```
binmatrix = [];
a = 1;

% Calculate the output Binary Matrix based on the Lookup table
for y1 = 2:1:y
    for h = 1:1:para
        binmatrix(h,a:a+1) = out2bin(demomatrix(h,y1)+1,:);
    end
    a = a+2;
end

nd = y-1;
```

F.9 MATLAB Script for 8QAM Modulation - *qam8mod.m*

```
% Function to perform 8QAM modulation using the
% MATLAB QAM modulation function
% qam8mod.m

% L.P. Wicomb
% Cape Peninsula University of Technology
% September 2005

function [ich , qch]=qam8mod(paradata ,para ,nd ,ml)
c = 0;

dematrix = zeros(para ,nd);

for k = 1:nd
    dematrix(:,k) = bi2de(paradata(:,(c+1):(c+3)));
    c = c+3;
end
qpskmatrix = qammod(dematrix ,8);
ich = round(real(qpskmatrix));
qch = round(imag(qpskmatrix));

end
```

F.10 MATLAB Script for 8QAM Demodulation - *qam8demod.m*

```
% Function to perform 8QAM demodulation using the
% MATLAB QAM demodulation function
% qam8demod.m

% L.P. Wicomb
% Cape Peninsula University of Technology
% September 2005

function [binmatrix]=qam8demod(ich,qch,para,nd,ml)
c = 0;
out2bin = [0 0 0; 1 0 0; 0 1 0; 1 1 0; 0 0 1; 1 0 1; 0 1 1; 1 1 1];
demomatrix1 = zeros(para,nd);

for k = 1:1:nd
    demomatrix1(:,k) = ich(:,k) + i.*qch(:,k);
end

for k = 1:1:nd
    for g = 1:1:para
        demomatrix(g,k) = qamdemod(demomatrix1(g,k),8);
    end
end

binmatrix = [];
a = 1;

for y = 1:1:nd
    for h = 1:1:para
```

```
        binmatrix(h,a:a+2) = out2bin(demomatrix(h,y)+1,:);
    end
    a = a+3;
end
```

F.11 MATLAB Script for 16QAM Modulation - *qam16mod.m*

```
% Function to perform 16QAM modulation using the
% MATLAB QAM modulation function
% qam16mod.m

% L.P. Wicomb
% Cape Peninsula University of Technology
% September 2005

function [ich , qch]=qam16mod(paradata ,para ,nd,ml)
c = 0;

dematrix = zeros(para ,nd);

for k = 1:nd
    dematrix(:,k) = bi2de(paradata(:,(c+1):(c+4)));
    c = c+4;
end

qpskmatrix = qammod(dematrix ,16);
ich = round(real(qpskmatrix));
qch = round(imag(qpskmatrix));

end
```

F.12 MATLAB Script for 16QAM Demodulation - *qam16demod.m*

```
% Function to perform 16QAM demodulation using the
% MATLAB QAM demodulation function
% qam16demod.m

% L.P. Wicomb
% Cape Peninsula University of Technology
% September 2005

function [binmatrix]=qam16demod(ich,qch,para,nd,ml)
c = 0;

out2bin = [0 0 0 0; 1 0 0 0; 0 1 0 0; 1 1 0 0; 0 0 1 0; 1 0 1 0;
0 1 1 0; 1 1 1 0; 0 0 0 1; 1 0 0 1; 0 1 0 1; 1 1 0 1; 0 0 1 1;
1 0 1 1; 0 1 1 1; 1 1 1 1];

demomatrix1 = zeros(para,nd);

for k = 1:1:nd
    demomatrix1(:,k) = ich(:,k) + i.*qch(:,k);
end

for k = 1:1:nd
    for g = 1:1:para
        demomatrix(g,k) = qamdemod(demomatrix1(g,k),16);
    end
end

binmatrix = [];
```

```
a = 1;

for y = 1:1:nd
    for h = 1:1:para
        binmatrix(h,a:a+3) = out2bin(demomatrix(h,y)+1,:);
    end
    a = a+4;
end
```

Appendix G: Miscellaneous MATLAB scripts used in the OFDM simulation scripts

The following listed MATLAB scripts are taken from (Harada & Prasad 2002) and were utilised in the OFDM simulations listed in this dissertation.

G.1 MATLAB Script for generating AWGN - *comb.m*

```
% Program 2-4
% comb.m
%
% Generate additive white gausian noise
%
% Programmed by H. Harada
%
function iout = comb (idata , attn)

%****************** variables ***************************
% idata : input Ich data
% qdata : input Qch data
% iout    output Ich data
% qout    output Qch data
% attn : attenuation level caused by Eb/No or C/N
%*********************************************************

iout = randn(1,length(idata)).* attn;
iout = iout+idata(1:length(idata));

% ************************end of file ************************************
```

G.2 MATLAB Script for inserting the Guard Interval - *giins.m*

```
% Function 4-3
% giins.m
%
% Function to insert guard interval into transmission signal
%
% Programmed by T. Yamamura and H. Harada
%

function [iout]= giins(idata,fftlen,gilen,nd);

%****************** variables ***************************
% idata     : Input Ich data
% qdata     : Input Qch data
% iout      : Output Ich data
% qout      : Output Qch data
% fftlen    : Length of FFT (points)
% gilen     : Length of guard interval (points)
%*************************************************************

idata1=reshape(idata,fftlen,nd);
idata2=[idata1(fftlen-gilen+1:fftlen,:); idata1];
iout=reshape(idata2,1,(fftlen+gilen)*nd);

%******************** end of file ***************************
```